Argonne National Laboratory
9700 S. Cass Avenue
Argonne, IL 60439

Monitoring and Mitigation of Sustained Localized Pitting Corrosion

Submitted to:

Nancy C. Comstock
U.S. Department of Energy (DOE)
National Petroleum Technology Office

By:

YuPo J. Lin, Edward J. St.Martin, and James R. Frank
Argonne National Laboratory
Argonne, IL 60439

January 2003

The submitted manuscript has been created by the University of Chicago as Operator of Argonne National Laboratory ("Argonne") under Contract No. W-31-109-Eng-38 with the U.S. Department of Energy. The U.S. Government retains for itself, and others acting on behalf, a paid-up, nonexclusive, irrevocable worldwide license and said article to reproduce, prepare derivative works, distribute copies to the public, and perform publicly and display publicly, by or on behalf of the Government.

Executive Summary

The purposes of this project are to (1) minimize the environmental discharge of hydrocarbons and treatment chemicals due to failures resulting from sustained localized pitting corrosion, (2) reduce the use of toxic treatment chemicals used by field operators to prevent those failures, and (3) identify treatment approaches that reduce the use of toxic chemicals. The approach in this project has been to develop an on-line, real-time method to monitor sustained localized pitting so that treatment chemicals (e.g., biocides and chemical inhibitors) can be applied only when needed. In addition, field operators need to know whether pitting corrosion is due to microbiologically influenced corrosion or other chemical corrosion mechanisms so that they can appropriately apply either biocides or corrosion inhibitors only if needed using minimal treatment applications. Argonne National Laboratory (ANL) has been developing an instrument that can be used by field operators to allow them to make such decisions in real-time while minimizing toxic discharges and treatment chemical use. This instrument has also been used as a tool to evaluate less toxic treatment approaches.

Many unexpected failures in pipelines and storage vessels can be traced to sustained localized pitting (SLP) corrosion. Detecting such pitting is often difficult because standard corrosion probes can only measure generalized corrosion, not the localized corrosion that can drill holes into metal. Argonne used both laboratory and field experiments to design a corrosion probe that detects rapid SPL corrosion by taking electrochemical noise measurements. Argonne researchers have reexamined electrochemical noise (ECN) analysis of localized corrosion by using hardware, signal collection, and signal processing designs that are different from those used in conventional ECN analysis techniques. The new data acquisition system was designed to identify and monitor the progress of SLP by analyzing the power spectral density (PSD) of the trend of the corrosion potential noise level (PNL). The results of the PSD analysis consistently demonstrated that the trends of PNL contain information that can be used to differentiate between SLP corrosion and general corrosion mechanisms. The degree of linear slope in the low-frequency portion of the PSD analysis was correlated with the SLP corrosion process. Laboratory metal coupons, as well as commercial corrosion probes, were tested to ensure the reproducibility and consistency of the results. Argonne evaluated the on-line monitoring capability of this new ECN analysis method in a bench-scale flow-loop system, which simulated microbially influenced corrosion (MIC) activity. The ECN analysis results demonstrated that this in-situ corrosion monitoring system could effectively identify SLP corrosion associated with MIC, compared to a more uniform general corrosion mechanism. A reduction in SLP activity could be clearly detected by the ECN monitoring system when a corrosion inhibitor was added into one of the test loops during the corrosion testing. On the basis of the results obtained from laboratory experiments and field tests, Argonne integrated a user-friendly ECN analysis system, designed for on-line and continuously monitoring of corrosion activity that can automatically report the onset of SLP corrosion.

The occurrence of SLP corrosion on the surface of the metal electrodes of the ECN probes and the metal coupons is difficult to predict and reproduce in the laboratory as well as in the field. A method to increase the probability that SLP will occur on the electrodes is required. Therefore, in addition to developing the ECN analysis system, ANL also designed a new electrode to increase the sensitivity (or reproducibility) of the ECN probe to SLP corrosion attack

and also to be able to measure the general corrosion rate via ECN analysis system. The new design is to modify the surface morphology of the working electrodes in the conventional three-electrode EN probe. We have found that the counter intuitive approach of using a smooth, polished surface does favor pitting corrosion attack. Reducing surface roughness of a metal will increase its general corrosion resistance. The reduction of metal surface roughness will therefore increase the tendency for localized corrosion attack. In addition, a reproducible method to force the general corrosion on one electrode of an ECN probe may make it possible to also accurately measure the general corrosion rate using the electrochemical current noise measurements.

The combination of on-line ECN analysis system, the new ECN probe design and the laboratory flow loop testing facility provides the advantage for evaluating the effectiveness of inhibitor treatments. We can reproducibly control the test conditions and deliberately induce pitting corrosion. This reduced the test period to a few weeks as compared to the months that would be required for a field test. This was demonstrated in two industrial collaboration tasks. The first task was that one of the industrial partners needed to urgently resolve the failures of pipelines and storage facility caused by MIC in one of their oil refinery sites near coast. A chemical was considered to be used in the facility to prevent the MIC cause of SLP corrosion inhibitor. It was determined, within a short period of time using the ECN analysis system, that control the concentration of the specific corrosion inhibitor is extremely important when used in the refinery facility to prevent the rapid increase of corrosion rates of the treated facility. Another task was to evaluate the performance of biocide to stop MIC. The results indicated that the particular biocide could retard the biofilm built up. However, it also would cause more severe SLP corrosion attack in the treated testing loop.

The on-line ECN analysis system was field tested in a natural gas storage facility in southern California. The ECN analysis system was demonstrated to be able to detect the SLP corrosion on the monitored facilities. The slopes of PSDPNL were correlated very well with the maximum pitting rate measured by the microscope.

With the successful demonstration of on-line ECN analysis system in the laboratory as well as on the field, a major chemical supplier and service company for corrosion control is very interested to commercialize ANL's ECN analysis system for their clients. Evaluation of the ECN technology in their laboratory and, maybe, further in the field was planned with their own expense.

1. Development of Electrochemical Noise (ECN) Sensor for Sustained Localized Pitting Corrosion Detection in Laboratory

Introduction

Corrosion of pipelines and storage facilities is a significant problem for the oil and gas industry. The most destructive form of corrosion is SLP corrosion, in which the metal or alloy is perforated rapidly. Although several methods to measure general corrosion rates are available, reliable on-line methods to predict when — and where — SLP will occur are not available. A preliminary evaluation indicated that electrochemical noise analysis could be an effective method to analyze SLP corrosion [1].

ECN analysis is a nondestructive, in-situ method of monitoring natural corrosion processes. Using ECN analysis, researchers measure the endogenous electrochemical corrosion current and potential fluctuations simultaneously. Because natural corrosion processes are chaotic, signal processing of the recorded current and potential noise is very critical in interpreting the data collected. To characterize the corrosion mechanism, Argonne used different signal processing algorithms to interpret the ECN analysis data. Several characteristic evaluations of the time-series noise signal, such as potential and current noise levels, noise resistance [2,3,4,5], and pitting index [6], were proposed to describe the corrosion mechanism. These data and methods alone did not allow researchers to effectively identify the different corrosion mechanisms [7]. However, when spectral analysis of the chaotic electrochemical noise was also applied, researchers found that it was a powerful signal processing technique that could be used to characterize the noise data in a frequency domain [8,9]. In this technique, the slope of the power spectral density (PSD) versus frequency of the transformed signal is believed to relate to the corrosion mechanism [10,11,12,13]. Most of the results presented in the references demonstrated a correlation between the corrosion process and the slope of the PSD under controlled constant potential or current laboratory studies. However, very few literature citations discussed the application of this technique in a natural corrosion process in which the potential or current is not controlled. Coupling the PSD analysis technique with ECN analysis would be an important step in developing a practical tool for monitoring SLP for industrial applications.

The main challenge was to differentiate SLP from uniform corrosion. The uniform corrosion process discussed here includes general corrosion and the development of a very large number of uniformly distributed small corrosion pits. SLP, as its name implies, refers to the few pits or group of pits that dominate the corrosion process and force a very fast metal loss on a small portion of the surface area. As discussed in Reference 13, uniform corrosion appears to be a stochastic process; localized pitting corrosion appears to be a deterministic process. In most natural corrosion systems, SLP occurs together with uniform corrosion. They can be seen in the potential noise PSD analysis as a plateau in the high-frequency portion of the spectrum for the stochastic process and as a slope in the low-frequency portion of the spectrum for the deterministic process [13]. Therefore, the low-frequency portion of the potential noise PSD could be used to characterize the pitting corrosion process. Conventional ECN analysis techniques have been used with some success in detecting the pitting corrosion process. However, it was not clear from these studies whether conventional ECN analysis could effectively differentiate the rapid growth of corroded pits in a small area (i.e., SLP) from the

uniformly distributed pitting over the entire area. Inspecting a much lower frequency range of the potential noise PSD spectrum (e.g., beyond 10^{-3} Hz) may be necessary to differentiate dominating SLP from uniformly distributed pitting. However, in this low-frequency range, some artifacts, such as flicker noise, could limit the application of conventional ECN analysis.

Argonne has developed a new approach to signal collection for electrochemical noise measurements. The new method can effectively detect the SLP process and avoid the artifacts. Instead of collecting the original corrosion current and potential noise signal, Argonne collects the current and potential noise level (CNL and PNL). The CNL and PNL values are collected by calculating (in-situ) the mean-square-error (MSE) of a few hundred noise-signal data points. These data points are recorded continuously during one electrochemical noise measurement. In Argonne's new method, the data collected reflect the trend of amplitude change of the current and potential noise caused by corrosion during any test period. Therefore, in theory, researchers can collect the new form of signal data at much lower frequencies (e.g., 10^{-6} or lower), allowing them to avoid the signal drift (or any interference from other sources) caused by using a very low recording (i.e., sampling) rate. Also, Argonne did not find any artifacts, such as flicker noise effect, from the instruments or environment during the CNL and PNL measurements. This new approach, in principle, should improve the resolution of PSD analysis in the low-frequency range and allow analysis of any deterministic process recorded by the noise signal. The effectiveness of this new technique in detecting SLP was demonstrated by conducting well-controlled laboratory experiments and a field test in a natural gas pipeline. The laboratory experiments were carried out in flow-loop systems that were built to simulate corrosion in a gas pipeline. With the flow-loop system, Argonne could also design reproducible experiments under controlled conditions to examine various corrosion mechanisms and the effects of chemical treatments.

1.1 Apparatus of ECN Measurement System

Probes

Electrochemical noise measurements were taken by simultaneously recording the current noise and potential noise with a three-electrode probe. The working and counter electrodes were shorted together and connected through a zero-resistance amperometer (ZRA) to monitor the corrosion current flow. The third electrode was used as a reference electrode to measure the corrosion potential of the shorted electrode pair through a high-impedance voltmeter. A personal computer with a plug-in potentiostat[(1)] served as the ZRA and voltmeter.

Two types of electrochemical probes were used. The type I probe included a standard calomel electrode (SCE) as the reference electrode and a carbon steel coupon (C1018)[(2)] as the working electrode. The counter electrode was either the same material as the working electrode or a stainless-steel (S.S. 316) electrode. The stainless-steel counter electrode is nobler than the carbon steel coupon. Therefore, the working electrode (i.e., the carbon steel coupon) was forced into a galvanic corrosion. The type II probe was a commercial probe[(3)] that consisted of three round-end cylindrical electrodes. Again, carbon steel (C1018) was used both in the working and in the counter electrodes. A stainless-steel (S.S. 304) electrode was used as the reference.

Before each experiment, the new method coupon and electrode specimens were cleaned in an acid cleaning solution and rinsed with deionized water. After rinsing, the specimen was cleaned by sonication in water. The cleaned specimen was dipped into acetone and then dried in an oven to remove the water. Electrochemical noise and weight loss were measured in each experiment.

Flow-Loop System

Four independent flow loops (A, B, C, and D) with separate simulated produced-water solutions, fluid reservoirs, and pumps were used. Each flow loop was 4 in. in diameter and 6 ft long with separate flow-control and gas-purging systems. The superficial velocity was approximately 0.04 cm/s (0.016 in/s). Each loop held eight 3”x1/2” metal coupons. The simulated produced-water fluid was circulated through each loop. Two commercial ECN probes (i.e., type II) were inserted into each of the four loops, for a total of eight probes (see Figure 1).

To evaluate the performance of the new ENA technique in detecting SLP caused by MIC, several nutrients and salts (such as chloride and sulfate) were added to accelerate the MIC in the flow-loop system. Ethanol was injected into each test loop to trigger pitting corrosion because ethanol was rapidly converted by sulfate-reducing bacteria to acetic acid and hydrogen sulfide. This step resulted in a localized low-pH region that accelerated the sustained pitting corrosion under the biofilm.

Data Acquisition

The current and potential fluctuations of corroding samples were read during a short period (e.g., 4–30 s) with consecutive 400–600 measurements (i.e., sampling rate of 0.01 s–0.05 s). The MSE of these consecutive data points was calculated, and the results were recorded in a data file. The measurement/calculation was repeated at every time interval (e.g., at 10–120 s) for a long period (e.g., 20–120 h). Thus, the data recorded represent the potential and current noise levels. The results were analyzed by fast Fourier transform to obtain the PSD of potential and current noise levels. The linear slope of the low-frequency portion of the PSD (called the α value) was calculated by linear fitting by using the least-square method.

1.2 Characterization and Analysis of ECN for Corrosion Detection

Corrosion Process Evaluation in a Laboratory Electrochemical Cell

Researchers have demonstrated some success in using the conventional ENA technique to detect the initiation of pitting corrosion, but the technique is subject to interference in the analysis of the PSD in low-frequency ranges. Although detecting the initiation of pitting corrosion in a process environment is important, the ultimate goal is to monitor the sustained growth of pits in a localized area. Pits caused by corrosion can cover the entire or a large portion of the area of the material, or pits can form in only a very limited area. On the basis of total weight loss from a metal surface, the former is no different than the latter. However, SLP is obviously of more concern because of its tendency to cause a hole in the material. The uniform corrosion rate can be measured by using many different methods. The challenge is to detect the

severity of SLP in a background of uniform corrosion. The new ENA technique is capable of extracting the sustained corrosion signal from the mixture of uniform corrosion and pitting corrosion processes.

Figures 2(a) and (b) show the PSD of conventional ENA of SLP and uniform corrosion on metal coupons. The potential PSD in both cases shows a very similar value of slope (i.e., $1/f^{-\alpha}$, $\alpha = 37$) with the linear portion of each line, both bending at a frequency of around 0.1 Hz. On the basis of Figure 1, it appears that the conventional PSD of potential (PSDP) cannot be used to distinguish between SLP and uniform corrosion. This result was expected because of the difficulties caused by the interference generated in the low-frequency range of the PSD analysis. However, using the new ENA data acquisition procedure, Figures 2 (c) and (d) show a clear difference in the PSDs of measured potential noise level (PSDPNL). The slope (i.e., the $-\alpha$) of the PSDPNL of the coupon with uniform corrosion is –11, while that of the coupon with SLP is -39. The α value thus shows a significant difference between uniform corrosion and SLP.

The correlation of SLP corrosion with the PSDPNL is demonstrated for metal coupons in Figures 3 and 4. When SLP is in progress, the PSDPNL changes dramatically. Unlike uniform corrosion, which is represented by the stochastic process, once SLP occurs, the PSDPNL reveals a deterministic process. This process can be seen in Figure 3(a), which shows a carbon steel coupon with deep pits. Because the coupon was immersed in pure water with air purge only, a passivation film of iron hydroxide covered most of the coupon surface area. However, traces of chloride or other ions exist in the water and aid in the formation of pits. The PSDPNL (Figure 3[b]) shows a α value of 40 in the low-frequency portion, which indicates a deterministic process. Depending on the total number and depth of the pits that are forming, the α value for the PSDPNL could vary from 0 to 40, which reflects the domination of the SLP corrosion formation, compared with uniform corrosion. When the α value is between 10 and 30, the metal surface is under an intermediate corrosion process attack. In this regime, the pits were either relatively shallow, or many shallow pits were merging to form a group of pits that extended over a large portion of the total surface area. An example of uniform corrosion caused by shallow and uniformly distributed pits is shown in Figure 4. In this case, the coupon was immersed in deionized water for 68 h. The final α value of the PSDPNL is 15; the surface morphology shows that shallow pits have formed on the coupon surface. This apparently indicates a less-dominating deterministic process of small pit formation, compared with the stochastic process of uniform corrosion. A comparison between the coupon in Figure 3 and the coupon in Figure 4 supports the hypothesis of a competition between a deterministic and a stochastic process more clearly. The operating conditions for coupons in Figure 3 and Figure 4 were the same. However, the coupon shown in Figure 3 has much deeper pits than the coupon in Figure 4. The total number of pits on the coupon in Figure 4 is greater than that on the coupon in Figure 3 (the total pit number ratio $\approx$ 50/5). The aggressiveness of SLP corrosion (i.e., the domination of the deterministic process over the stochastic process) shown in Figure 3 makes its α value near 40. The overall corrosion rate for the coupon in Figure 3 is one order of magnitude smaller than that for the coupon in Figure 4 (i.e., 1.08×10^{-2} mg/h vs. 1.78×10^{-1} mg/h from the weight loss measurement). These results are also evidence for the domination of SLP over uniform corrosion.

Evaluation of Corrosion Process Using Flow-Loop System

The new ENA system was used to monitor MIC by using simulated produced-water fluid in a flow-loop system.

To evaluate the performance of the new ENA technique in detecting SLP, several chemicals were added to accelerate MIC pitting. Ethanol was injected into each loop to introduce acetic acid production and trigger pitting corrosion during the test period. Figure 5 shows the slope profile (5a) of PSDPNL and the morphology on the tip of the probe (5b). As discussed above, the slope indicates that uniform corrosion was dominating the corrosion process. This finding was confirmed by the morphology on the tip shown in Figure 5(b).

Figure 6(a) shows the change in slopes in PSDPNL during the test period from a separate probe in a different loop. From the change in profile of the PSDPNL slopes, it is clear that uniform corrosion and pitting corrosion can alternate and dominate the corrosion process. The injection of ethanol was also able to trigger SLP, which is indicated by a decrease in the slope. Analysis of the change in profile of slope in the tested probes revealed that six out of the eight probes developed SLP. These results were confirmed by weight loss and morphology analysis of the probes after the test period. Figure 6(b) shows the morphology of the localized pitting corrosion attack on an electrode surface. Similar statistical correlation between maximum pitting rate or the total corrosion rate and several other parameters derived from the signal processing of the prescreened ENA data were attempted. None of them appeared to have a significant linear correlation constant.

Another experiment was performed in the flow loops to monitor the in-situ effectiveness of corrosion inhibitors in the test system. During the test period, corrosion inhibitor was added to loop D, while ethanol was added to both loops D and B. Figure 7 shows the change in the profile of the slope of PSDPNL in loops B and D. As expected, the PSDPNL slope of the probe in loop D changed immediately upon addition of the treatment chemical from an SLP signal to a uniform corrosion signal (i.e., larger than -10). On the other hand, the probe in loop B continued to show SLP signal. Therefore, it appears that the new ENA method can be used as an in-situ process monitor for corrosion control.

On the basis of these findings, an on-line ENA system was designed that could continuously measure, monitor, and report the SLP corrosion activities automatically. This new remote-controlled ENA system can update corrosion activities every few minutes, and no attendant is needed. Therefore, this device can detect the onset of SLP corrosion in the early stages and provide early warning of unexpected material failure.

Summary

Argonne has developed a new data-collection and analysis approach for ENA to monitor SLP. The new PSD analysis technique, with an appropriate ENA sensor, was used to distinguish SLP from generalized corrosion mechanisms on a metal surface in an aqueous system. When the metal was under a SLP attack, the PSDPNL curve appeared as a linear decline in the low-frequency portion with a slope equal to -40 dB/decrease (α = 40). The linear decline in the

low-frequency range is believed to be caused by the dominating process of localized pitting corrosion on the entire surface. Under the hypothesis of stochastic/deterministic competition during the SLP process (13), the corrosion mechanism changed to a deterministic process from a more general stochastic process. When only uniform corrosion occurs, the PSDPNL was maintained at a near-constant level throughout the entire frequency range (i.e., the α value is close to zero) because (according to the hypothesis) the general corrosion mechanism is a stochastic process. Therefore, its PSDPNL is independent of the frequency. If the uniform and SLP equally dominate on the metal surface, a slope between -10 and -30 (db/decade) is observed. The departure of α value from the 40-db/decade levels may occur for two reasons. First, the large increase in the number of pitting sites on the coupon surface would diminish the deterministic signal created by the SLP process as it started to shift into a more random signal. The second reason is opposite to the first — if the localized pitting sites were very few and small, their weak potential noise signal would be influenced more strongly by the random signal from the background general corrosion signal that predominates.

A flow-loop system was used to test the ENA corrosion-monitoring system. The ENA probes were evaluated by using simulated produced water in a flow-loop system with nutrients added to activate the MIC processes. As demonstrated previously by using small corrosion cells under stagnant conditions, the linear slope of PSDPNL is also capable of detecting the SLP in a flow-loop system. The ENA probes were able to detect the onset of pitting corrosion and record the change in corrosion when treatment chemicals were added.

2. Improvements of ECN Analysis System

2.1 New Electrode Design for ECN Problems

Introduction

The occurrence of localized sustained pitting corrosion on the surface of the metal electrodes of the ECN probes and the metal coupons is difficult to predict and reproduce in the laboratory as well as in the field. Therefore, a method to increase the probability that sustained localized pitting will occur on the electrodes is required. In addition, a reproducible method to force the general corrosion on one electrode of an ECN probe may make it possible to also accurately measure the general corrosion rate using the electrochemical current noise measurements.

ANL was granted a U.S. patent [15] for a new electrode design to increase the sensitivity (or reproducibility) of the EN probe to sustained localized pitting corrosion attack and also to be able to measure the general corrosion rate via ECN analysis system. The new design is to modify the surface morphology of the working electrodes in the conventional three-electrode EN probe. Other researchers have tried to increase the occurrence of pitting corrosion attack on the electrodes by using pre-pitted electrodes with the thought that these small pits would favor the continued attack at these selected sites. This did not work and we have found that the counter intuitive approach of using a smooth polished surface does favor pitting corrosion attack. Reducing surface roughness of a metal will increase its general corrosion resistance. The reduction of metal surface roughness will therefore increase the tendency for localized corrosion attack.

If one of the shorted working electrodes in the EN probe has less roughness than the other one, this will result in preferential general metal corrosion on the working electrode with higher surface roughness. The stronger the metal corrosion preference for one electrode, the better correlations between the measured noise current and the general corrosion rate of the metal.

Thus, the smooth electrodes corrosion potential can be used to measure pitting corrosion attack while the rough electrodes corrosion current can be used to measure general corrosion. Experimental results of laboratory development of the new ECN electrode design are described in the followings.

Experimental Results

The new electrode design of ECN probe contained one surface modified electrode (SME) and one non-surface modified electrode (NSME) and one reference electrode. Four different sets ECN probes with SME that were prepared by using a series of alumina polishing slurry. These surfaces of SME were polished down to 600 grite, 1 μm, 0.3 μm and 0.05 μm roughness, respectively. These ECN probes were inserted into two flow loops with 1% NaCl solution.

Table 1 lists the final corrosion rate measurements and the corrosion mechanisms inspected by microscope. The ECN probe with 0.3 μm roughness of SME showed a severe sustained localized pitting corrosion attack but minor uniform corrosion. The ECN analysis showed (Figure 8) that the 0.3 mm SME is more sensible to the localized pitting corrosion attack. Figure 9 shows 95% correlation of the average anodic current recorded by the ECN measurement and the uniform corrosion rates measured by weight-loss method.

To reproduce the results found for the new electrode design of ECN probe, two sets of experiments, runs ECN34 and ECN35 were carried out to demonstrate the increase of sensitivity to sustained localized pitting (SLP) corrosion on electrochemical noise (ECN) probes by using surface modified electrodes (SME) in a chemical corrosion environment (1.0 % NaCl solution). A total of four flow loops were used in runs ECN34 and ECN35. Each loop included one original ECN probe and one newly designed ECN probe. The new ECN probe consists of one SME and one non-surface-modified electrode (NSME). The original ECN probe includes two NSMEs. All of the four SMEs developed severe localized pitting corrosion (see tables 2 and 3). The maximum pitting corrosion rate (measured by using an optical microscope) on these SMEs was at least 2.5 times higher than the general or uniform corrosion rate (measured by weight loss). One of the SME showed 30 times higher localized pitting corrosion than the general corrosion rate (13.9 mpy vs. 0.42 mpy). None of the NSMEs developed significant localized pitting corrosion. Only uniform pitting corrosion, where small pits are uniformly seen all over the electrodes surface, was observed. The uniform pitting corrosion rates in these NSMEs were much smaller than their general corrosion rates. It was also demonstrated that the general corrosion rates of the NSMEs in the new ECN probes were linearly proportional to the total noise current. The linear correlation constant was as high as 95.6%. No such correlation was found using the original ECN probes. Thus, these probes can be used to measure the general corrosion rate directly from the total noise current measurements.

Experiment ECN 36 was carried out to demonstrate the new ECN electrode design in a microbially influenced corrosion (MIC) environment. The ECN probes were placed in a simulated produced water solution in the flow loop test system. The solution was inoculated with sulfate reducing bacteria and acid produce bacteria that are responsible for initiating microbially influenced corrosion. Two flow loops were used. Each loop included one original ECN probe and one newly designed ECN probe. The new ECN probe consists of one SME and one non-surface-modified electrode (NSME). The original ECN probe includes two NSMEs. The experiment lasted more than 1,200 hours. The two SMEs developed severe localized pitting corrosion (see table 4). The maximum pitting corrosion rate (measured by using an optical microscope) on these SMEs was 4 to 7 times higher than the general or uniform corrosion rate (measured by weight loss). None of the NSMEs developed significant localized pitting corrosion. Only uniform pitting corrosion, where small pits are uniformly seen all over the electrodes surface, was observed. The uniform pitting corrosion rates in these NSMEs were much smaller than their general corrosion rates. The correlation between current noise and the uniform corrosion rate was as high as 99% (Figure 10).

2.2 Automatic Electrochemical Noise Measurement and Data Interpretation System

For a continued monitored and quick detection response for the corrosion system activities, the original ECN analysis system of “batch” noise measurements and “manual expertise” data interpretation was re-packaged. A new user-friendly software package for automatic electrochemical noise measurement and data interpretation and corrosion monitoring was developed. Combined with a multiplexer and desktop computer, the system can monitor up to 8 ECN probes and interpret the signals from each individual probe. The prototype software was written using an industrial standard data acquisition-programming platform, Labview®, from National Instrument Inc. The corrosion status of the on-line monitored equipment is updated continuously and can be displayed every 5 to 10 minutes. The information that is currently displayed includes the corrosion mechanism (i.e., sustained localized vs. uniform corrosion), the corrosion current, and estimated uniform corrosion rate. It also includes the information obtained from high-order statistical analysis of the electrochemical noise signals (e.g., the Kurtosis and Skewness values). Additional statistical analysis capabilities of the on-line measured signals can be easily implemented. The automatic ECN analysis system allows truly on-line monitor of the corrosion activities and can provide a tool for corrosion control. Figure 11 shows the display of the continuous ECN measurement and automatic interpretation system for corrosion detection.

3. APPLICATION OF ECN ANALYSIS SYSTEM

Evaluation of Corrosion Inhibitor

With the on-line ECN analysis system, ANL's flow loop testing facility for corrosion control was used very effectively to evaluate the corrosion inhibitors that may prevent the sustained localized corrosion attack caused by MIC. The accelerated localized pitting corrosion environments created in the flow loop system shorten the testing period and the on-line assessment of the corrosion offset from the ECN analysis provide a quick and accurate evaluation of the corrosion control strategy, such as the selection of the chemicals for corrosion inhibitor. It saved millions of dollar for the industries. Described below are two cases for the application of on-line ECN to evaluate the corrosion inhibitors.

CASE 1. Evaluation of the Effect of Inhibitor on to Control the Microbially Influenced Corrosion in a Oil Refinery

One of the industrial partners has the urgent to resolve the failures of pipelines and storage facility caused by MIC in one of their oil refinery sites near coast. A chemical was considered to be used in the facility to prevent the MIC cause of sustained localized corrosion inhibitor. ANL was called to demonstrate our on-line ECN analysis system to help to evaluate the inhibitor.

Introduction

A series of four test loops were run at Argonne to simulate corrosion at the field site. Although the actual field conditions cannot be fully reproduced, the lab units used the same microbial population, metal coupons and approximate salts composition as the field site. The advantage of the lab units for evaluating the effectiveness of inhibitor treatments is that we can reproducibly control the test conditions and deliberately induce pitting corrosion. This reduced the test period to a few weeks as compared to the months that would be required for a field test.

Simulated firewater and produced water solutions were prepared and inoculated with mixed cultures of bacteria obtained from the field metal corrosion sites (i.e., sulfate reducers and other acid-producing bacteria). These test solution were re-circulated independently in four 10-liter flow loops (A-B-C-D) to simulate pipeline conditions. The produced water samples in loops A and B failed to become colonized. After growth of a biofilm had been established in the firewater loops C and D, ethanol was injected into each loop to accelerate microbially influenced corrosion (MIC). Ethanol can be rapidly converted to acetic acid by sulfate reducing bacteria (SRB) that are present in biofilms on the metal surfaces. Two electrochemical noise probes and 8 metal coupons were installed in each loop. An initial experiment using a single dose of inhibitor indicated that there was an effect on corrosion but that the effect quickly dissipated. A second longer-term treatment experiment was planned. After 2,200 hours of exposure, the analysis of ECN signals and the microscopic inspection of the coupons demonstrated that the metal samples in both loops had developed localized sustained pitting corrosion. Fresh metal coupons were added into both loops and 40 ppm of Inhibitor was added into loop D. Loop C served as an untreated control. The inhibitor concentration was measured at regular intervals and additional amounts of Inhibitor were added to loop D to maintain the Inhibitor concentration at

approximately 40 ppm. The electrochemical noise signals from the ECN probe and the microbial population counts of SRB in the fluid were monitored during a 668-hour testing period. The remaining coupons were examined for bacterial colonization on the coupon surfaces by fluorescence microscopy and then analyzed for general and pitting corrosion.

Experimental Methods

Flow Loop System and the Installed Components

Four flow loops were used for these tests. Each loop had an independent flow recirculation system. They were constructed from PVC pipe that was 40 in. long and 4 in. in diameter. The superficial velocity was approximately 0.04 cm/s (0.016 in/s). Each loop held 8 3”x1/2” metal coupons and 2 electrochemical noise (ECN) probes. Each ECN probe contains 3 round-end rod electrodes. The material used in 2 of the electrodes was carbon steel (c1018). The third electrode used as the reference electrode was stainless steel (S.S. 316). The 8 coupons used in the loop were all carbon steel. Four of the 8 coupons were obtained from the metal sampling company. The other 4 coupons were manufactured from the pipeline material, which were shipped from the field (i.e., the hemis and fire water system). Simulated produced and firewater solutions were prepared and inoculated with 1 liter of mixed cultures of bacteria obtained from metal corrosion sites (i.e., sulfate reducers and other acid-producing bacteria). Ten liters of the test solutions were re-circulated independently in the flow loops. Ethanol was injected into each loop to accelerate microbially influenced corrosion (MIC) by its rapid conversion to acetic acid by sulfate reducing bacteria (SRB) contained in biofilms on the metal surfaces. After 2,200 hours of exposure, the analysis of ECN signals and the microscopic inspection of the coupons demonstrated that the metal samples in loop C and D had developed localized sustained pitting corrosion. Additional fresh metal coupon sets (1 c1018 and 1 field metal) were added into loop C and D and 40 ppm of Inhibitor was added into loop D. Loop C served as an untreated control. At the beginning of the Inhibitor evaluation period, there were total 5 coupons in each loop (2 c1018 and 3 field coupons). The Inhibitor concentration was measured at regular intervals and additional amounts of Inhibitor were added to loop D to maintain the Inhibitor concentration at approximately 40 ppm. The electrochemical noise signals from the ECN probe and the microbial population counts of SRB in the fluid were monitored during a 668-hour testing period. The remaining coupons were examined for bacterial colonization on the coupon surfaces by fluorescence microscopy and then analyzed for general or pitting corrosion.

Analysis of Metal Samples

During the test, the metal coupons were pulled out at different time intervals to inspect for microbial colonization, morphology of the corrosion on the metal, and weight loss. The metal coupons to be inspected for the microbial colonization were first rinsed with a pH buffer and then stained with FTIC (fluorescein isothiocyanate). The stained coupons were inspected with an optical microscope (Olympus, BX60) with a wide band filter (type MWU) using a reflected light source (Halogen lamp). The number of colonies on the metal surface was estimated under 1,000 X magnification in a 100μm by 100μm square area. The acid producing and sulfate reducing bacterial population was measured by using a series dilution vials. The

liquid samples were diluted directly in MIC test kit vials. The coupon surface samples were obtained by wiping one side in a 1/2 in. by 2-in. area with a cotton swab followed by resuspension and dilution in vials. The results are expressed as the minimal number of bacteria per ml of solution.

Analysis of Liquid Samples

During the test period, the pH, ethanol, and acetate concentrations in each loop were measured periodically. The ethanol and acetate concentrations were measured by using HPLC. The acid producing and sulfate reducing bacterial populations were also monitored using dilution vials. The results are expressed as the minimal number of bacteria per ml of solution. The inhibitor concentration was measured at regular intervals and additional amounts of Inhibitor were added to loop D to maintain the inhibitor concentration at approximately 40 ppm. The inhibitor concentration was measured by using an inhibitor test kit. This kit uses a colometric test to determine the inhibitor concentrations. In order to avoid interference caused by the H_2S present in the test solution that will react with the reagent used in the kit, the liquid samples were purged with air for 15 minutes to remove the H_2S. The removal of the reducing H_2S could be monitored by the appearance of a light pink color due to the oxidation of the dye resazurin in the test solution. Near the end of the test period, a yellow brown coloration was detected in the inhibitor treated samples that interfered with the colometric assay.

Results

Bacterial Growth and Colonization

The liquid firewater samples from the field site were able to grow and initiate sulfate reduction when incubated in artificial firewater (Table 5) and our St. Peter artificial produced water (Table 6). This culture was easily adapted to the flow loop system with firewater and colonization, sulfate reduction, and corrosion were established. The Hemis produced water samples did not grow in our laboratory medium and reinoculation with the above active firewater samples above did not allow any growth. We believe that the high salt content in the artificial Hemis produced water (Table 5) is inhibitory and that the samples that were shipped did not survive. We suspect that the original microbial consortia growing in the field site produced water may be protected by the biofilm being attached to the pipeline surface.

Bacterial Analysis

The analysis of bacterial populations in the liquid and on metal surfaces in the test loops is described in Tables 7. After 210 hrs of incubation, all 4 loops had significant numbers (10^4-10^5/ml) of acid producing bacteria (APB) and less sulfate reducing bacteria (SRB) in the liquid cultures. The metal coupons from all loops had APB but SRB were only found in loops C and D. After 642 hours, no SRB were found in the liquid or metal surfaces of loops A and B. The Egypt Hemis produced water appears to be inhibitory to SRB. Loop D was treated with a single dose of Inhibitor (40 mM) at 793 hours and liquid samples showed a slight reduction in bacterial counts from 5 to 4 APB and 4 to 2 SRB. However, by 1,198 hours both the liquid and metal surface bacteria had regrown. A longer-term experiment with multiple additions of

Inhibitor to maintain approximately 40 mM was begun. Five injections of Inhibitor were made into loop D between 2,315 and 2,702 hours. The SRB and APB populations in the liquid samples dropped in loop D as compared to loop C during the treatment but by 2,946 hours the SRB had regrown both in the liquid and surface samples from loop D (Figure 12). The number of visible colonies on the metal surfaces were also examined during this time period (Table 8). During the Inhibitor treatments, the number of visible colonies was reduced in loop D as compared to loop C.

Coupon and Electrode Inspection

Table 8 shows the results of metal coupon surface morphology analysis for general and pitting corrosion. Coupons from loops A and B with either C1080 or Hemi steel did not have clear pitting corrosion. The surface of the Hemi steel was very rough and the detection of small pits was not possible. The overall general corrosion rate was 1.1-1.7 mpy. This result is consistent with the absence of good colonization by APB and SRB. Without the addition of Inhibitor, coupons in loop C revealed a significant amount of bacterial colonization as well as severe localized sustained pitting corrosion of the coupons (8.1-16.7 MPY max pitting rate). Coupons from the Inhibitor treated loop D showed very few bacterial colonies and did not have significant sustained localized pitting corrosion (2.9 mpy Max pitting rate). Instead, many small uniformly distributed pits were observed on the metal surface. However, from the weight loss measurements of the new coupons, the general corrosion rate was higher on the Inhibitor treated coupons of loop D as compared to loop C (5.7 versus 2.4 mpy). The higher general corrosion rate could be linked to the addition of Inhibitor in loop D. Before the addition of Inhibitor, the general corrosion rate of the coupons in loop D was lower than coupons in loop C (1.2 versus 3.0 mpy). The new coupons added during Inhibitor addition showed lower pitting corrosion rates in the loop D as compared to the loop C untreated control (2.5 versus 10.6 mpy average pitting rate). Examination of the carbon steel electrodes at the end of the experiment (Table 9) revealed that the overall general corrosion rates in loops A and B were lower than in loops C and D (0.62 and 0.83 versus 1.22 and 1.05 mpy). The only electrodes that showed pitting corrosion were the ones in the loop C positive control (3.1-3.5 mpy max pitting rate).

Electrochemical Noise Measurements

Figures 13, 14, 15, and 16 show the electrochemical noise analysis of the electrodes in loops A and B. The slope of the power spectral density (PSD) determinations are all in the range of -10 db/decade, which indicates a general corrosion mechanism. The localized index calculations are all in the range of 0.1, which also is consistent with general corrosion. Figures 17 and 18 show that the electrodes in the loop C positive control have a slope of the PSD that drops into the range of -30 db/decade when ethanol was added to trigger pitting corrosion. The localized index also was elevated into the 1.0 range. Figures 19 and 20 for loop D show the slope of the PSD initially drops but remains in the range of -10 db/decade during the addition of Inhibitor. The localized index also dropped. Figure 21 shows an analysis of the average potential noise versus a reference electrode. It can be seen that there is a potential shift in the signal when inhibitor is added to the test system. These results indicate that the addition of inhibitor has a direct effect upon the corrosion that is occurring in the test loops.

Summary

1. General corrosion rates on the coupons in the inhibitor treated loop increased as compared to the control.

2. The SRB population in the fluid of the Inhibitor treated loop decreased during treatment. The number of observable bacterial colonies and the SRB population on the metal surfaces were also significantly reduced as compared to the untreated control. However, the SRB population increased to their previous levels when the Inhibitor treatment was terminated.

3. Physical inspection of the coupons and analysis of electrochemical noise data demonstrated that when 40 ppm of inhibitor was maintained in the treated loop, the corrosion mechanism shifted from localized sustained pitting corrosion toward a more uniform general corrosion. Before Inhibitor treatment, both loops had sustained localized pitting corrosion and the metal in the control loop continued to demonstrate localized pitting corrosion.

CASE 2. THPS BIOCIDE FOR MIC CONTROL

The ECN analysis system was also used to evaluate a chemical, Tetrakishydroxymethly phosphonium sulfate (THPS), for preventing the MIC.

Experimental Setup

Three re-circulation systems that simulate pipelines with produced water simulated St. Peter water) were inoculated with sulfate-reducing bacteria (SRB) and acid-producing bacteria (APB). Four coupons and one ECN probe were inserted in each loop to monitor the corrosion activities. Two loops (B and C) were treated with the corrosion inhibitor, THPS. THPS was injected into loop B at the beginning of the test. Loop C was injected with THPS in the middle of the test (after 1,000 hours of operation). Each dosage of THPS added into the loop was 150 mg/L.

Results and Discussion

Figure 22 shows the estimated SRB population in the liquid of each loop. THPS seems to retard the SRB activities in the solution. The SRB activities in the solution of THPS-pretreated Loop B did not grow significantly during the initial 1,200 hours, while both the controlled loops A and C already showed significant SRB activities in the solution after 500 hours of test. The fluorescence analysis made at the 700 hours of test also indicated that no bacteria colonization was observed on the surface of the coupon from Loop B. On the other hand, large amounts of bacteria colonies were found on the coupons surface in the controlled loops (A and C). When the THPS were injected into the controlled loop C at 1,000 hours of test, its SRB activities in the solution was significantly reduced. However, without continuing injection of the inhibitor, the SRB activities eventually grew after some time. From the solution bacteria analysis, it was also found out that the APB activities in the solution were not influenced by the THPS.

Although the THPS can decrease the activity of SRB in the solution, the pretreated loop B appeared to develop severe sustained localized pitting (SLP) corrosion and had higher general corrosion rate (about 6 folds) than the controlled loop A. Tables 10, 11, and 12 show the corrosion rate and corrosion mechanism of the ECN probes in each loop. The morphology analysis of the ECN probes match the results measured by the on-line ENA system. Figures 23, 24, and 25 show the slope profile of power spectral density of the potential noise level (PSDPNL). The maximum SLP corrosion rate was 10 times higher than its general corrosion rate in the treated loop B.

4. Field Test of Electrochemical Noise Analysis Technique To Detect Sustained Localized Pitting Corrosion

An on-site evaluation of the novel electrochemical noise analysis system for detecting sustained localized pitting corrosion (SLP) was carried out at three locations in the Playa Del Ray gas storage facility of Southern California (SOCAL) Gas Company. The first location was the "udder" located on the intake side of V140/141, the second site was the bottom barrel of V140, and the third location was in the gas transport pipeline. Two electrochemical noise probes were inserted at each location. The electrochemical noise signals were collected for a total 1,147 hours at the first site, 1,388 hours at the second site, and 2,268 hours in the third location. The last testing site was in the Honor Rancho facility of SOCAL. In Honor Rancho, the EN probes were put into a gas storage tank with CO_2 corrosion environment.

Equipments

The electrochemical noise (ECN) probes used in the testing sites were supplied by the Rohrback Cosasco Systems (RCS) Inc.. Each ECN probe consisted a 3-electrode configuration and equipped with an 18-inch retractable probe safety clamp (RCS # 8013x-18-xxxxx-1). In each ECN probe, two C1018 carbon steel electrodes (RSC # 60814-K03005) were used as the working electrodes and one Hastalloy electrode (RCS # 60814-N-10276) was used as the reference electrode. Figure 26 shows the three-electrode configuration of the ECN probe. The current and potential noises were simultaneously measured by a computer plug-in potentiostat from Gamry Instrument Company (GI, model PCA 4/300 mA). At each testing site, two ECN probes were used to ensure the reliability of the ECN analysis results. The ECN signals of these two probes were measured in series by the potentiostat using a multiplexer as the switching device. The schematic of the setup for the ECN measurement is shown in Figure 27. The ECN measurements were continuously taken at the rate of 60 seconds per reading. The records of measurements were saved every 40 hours. At the end of the test period, the ECN probes were withdrawn from the pipe and cleaned by HCl solution mixed with antimony trioxide and stannous chloride to remove the corroded compounds. The general corrosion rate of the ECN probes was measured by the weight-loss method. An optical microscope with attachment of digital camera was used to inspect the surface morphology and measure the depth of corrosion pits on the surface of the EN probes.

Signal Acquisition and Data Interpretation

During the data acquisition, the current and potential noise signals were measured simultaneously every 0.1 seconds for a total 25 seconds. After each set of measurements (i.e., 25 seconds), the DC trends of current and potential of the 250 noise data were calculated using linear fitting method. Then, the values of current and potential level were obtained by calculating the root-mean-square of the noise data with respect to their DC trends. Finally, the two data points of current and potential noise levels were stored into the data file for later interpretation. The data collection procedure was repeated every 60 seconds until the total sampling time reached 40 hours. The ECN system created one data file for each probe every 40 hours until the end of test. In each data file, beside the values of current and potential noise level, it also contained the data of average potential and current (for the 25 seconds measurement), the standard deviation of the noise signals and the root-mean-square of the noise signals.

The collected noise data were sent back to ANL for processing. The data processing software was written in the Mathlab® script platform. The data processing program processes the noise data in the time domain as well as in the frequency domain. In time domain, it calculates the localized index (LI) that is the ratio of the standard deviation of the current noise and the average current. In frequency domain, it performs the Fourier transform to convert each noise data file (i.e., 40 hours data) into the power spectral density of the potential noise level (PSDPNL). The linear slope in the low frequency portion of PSDPNL was calculated using the linear least-square fitting method.

Some researchers claim that the localized index (LI) could be used to identify the degree of localized corrosion activity; however, they found inconsistent results. At ANL, we found that the LI cannot give a good indication of the sustained localized pitting (SLP) corrosion. However, it could be used as reference information to reveal the surface activity (e.g., the adsorption) of the EN probe. On the other hand, ANL researchers discovered that the slope of PSDPNL could effectively detect the trend of SLP corrosion development. Thus, the PSDPNL slope can be used to differentiate the SLP from the uniform corrosion.

Results and Discussion

ECN Measurements in the Playa Del Ray Facility

Figure 28 shows the slope profiles of PSDPNL of the probes at the first location. The results, see Figure 28(a), clearly show that probe #1 was under severe SLP corrosion attack during the measuring period. Near the end of the test period (i.e., 1,000 –1,200 hours), the signal indicated that the corrosion mechanism tended to develop in the mixing region of uniform and SLP corrosion. The weight loss measurements and morphology analysis of the electrodes on probe #1 indicated that the maximum localized-pitting rate was 6 times greater than the uniform-corrosion rate (i.e., 36 mpy vs. 6 mpy, as shown on Table 13). Figure 28(b) shows the slope profile of the second probe at the same location. During the initial 500 hours of measurements, the signal data were not reliable. Therefore, no interpretation of the potential noise signals was made for this period. The unreliable signal data were identified automatically using a crosschecking method written in the data-processing software. For the rest of test period, the ENA indicates that uniform corrosion and SLP corrosion were alternately controlling the overall corrosion process. However, in the final 300 hours (900-1,200 hours) of the measurement period, SLP corrosion dominated the overall corrosion process. The weight loss and morphology analysis shows that the maximum pitting rate of probe #2 was 1.7 times the uniform corrosion rate (i.e., 24 mpy vs. 14 mpy as shown in Table 14). The morphology analysis (Figures D-1 and D-2) shows that localized pitting corrosion was quite significant for all the working electrodes on both the probes. Figure 29 shows the PSDPNL slope profile for probe #1 at the second site. It indicates that uniform corrosion and localized pitting corrosion were alternating on probe #1 also at the second site. However, the corrosion mechanism was closer to the uniform corrosion region than to the SLP region. The maximum pitting rate was about the same as its uniform corrosion rate (i.e., 2.5 mpy vs. 2.45 mpy). Morphology analysis (see Figures D-3 and D-4) of the four working electrodes on the two probes at the second site revealed that only one working electrode on probe #1 developed localized pitting corrosion. The remaining working electrodes had uniform corrosion. Due to malfunction of the data acquisition software after a power failure, no data were available for probe #2 at the second location.

To verify the correlation between the PSDPNL slope and the SLP, average PSDPNL slopes measured from the 3 probes (i.e., two probes in the first location and one probe in the second location) were calculated and compared to the maximum pitting rate measured by the optical microscope. The average PSDPNL slopes for the 3 EN probes are -30.49, -28.29, and -19.89. Figure 30 shows the linear relationship between the average PSDPNL slope and the maximum pitting rate.

Most of the ECN signals measured from the third location in the Playa Del Ray were found to be useless. It was concluded that the measured average potentials and the open-circuit potentials were extremely high (more than 4.0 V, see Appendix C, Figures C5 and C6). This indicates that during the testing period, the pipeline might have limited liquid flows and the probe might have been exposed to the gas phase. Therefore, there were no ionic conductivities between the electrodes for the ECN measurement. Nevertheless, Figures. 31 (a) and (b) show the slope profiles of PSDPNL. Only 3 sets of meaningful EN signals were measured. They were measured in the time frame of 1,600 and 1,800 hours. This indicates that the environmental changes (e.g., lack of liquid) were the primary cause for unreliable and unusable EN signals. The morphology inspection (Figures D-51 and D-6) and the weight loss measurement show that uniform corrosion developed on the ECN probes (Tables 17 and 16).

ECN Measurements in the Honor Rancho Facility

Two probes were installed in the gas storage tank of the Honor Rancho facility of SOCAL. ECN signal were measured for a total of 1,400 hours. However, in the end of the measurement, all the working electrodes in both of the probes were completely destroyed by corrosion. Only the reference electrodes (i.e., the Hastalloy) left on the probes. Figures 32(a) and (b) show the PSDPNL slope profiles of the two ECN probes. Both slope profiles indicates that, after 500 hours of measurement, the ECN signals became unreliable. The average potentials of both probes [Figures C-7(b) and C-8(b)] also show that the corrosion potential of the working electrodes were more noble than the reference electrode (around 580 hours and 625 hours respectively) for probe #1 and probe #2. There are only two situations when the positive potential readings will happen. The first one is when the liquid level was so low that the probe was not in contact with the liquid. In that situation, the only conductive area to allow the potential measurement was the residual liquid on the surface of the probe holder. This would result in gradual increase of the corrosion potential in the noble direction once the residual liquid started to dry out.

The effect of residual liquid on the corrosion potential measurement is demonstrated in Figure 33 measured in the laboratory using the same field probe. Two different ECN data were measured with the ECN probe initially holding in the liquid and then in the air. When the immersed ECN probe was completely pulled out from the liquid, the corrosion potential initially increased in the noble direction (i.e., positive), and then dropped back to the previous corrosion potential level observed before the pulling the probe out of water. This dropped-back potential was due to the residual liquid on the probe holder surface that provided conductive media for the electrodes. When the residual liquid on the probe holder dried up, the corrosion potential started to increase steadily in the noble direction. To verify that the dropped-back corrosion potential was due to the residual liquid, another experiment was carried out. At the beginning of experiment, the probe was held in the air without any contact with the liquid. As expected, the potential readings were in the positive value. This “isolated” potential reading was caused by the

internal circuit arrangement. Later, the probe was halfway immersed in the liquid (i.e., the probe holder did not touch the liquid), the corrosion potential suddenly dropped to the corrosion potential of the electrodes (i.e., dropped in the negative direction). When the probe was lifted again in the air, no surface was available to hold the residual liquid; therefore, the potential immediately jumped to the previous "isolated" potential readings. The effect of the liquid levels on the corrosion potential were often seen in the probe #1 of the second location and probes #1and #2 in the third location of the Playa Del Ray facility [see Figures C-3(b), C-5(b), and C-6(b)].

Another possibility for the positive potential reading was the loss of the carbon steel electrodes during the measurement with the probes still immersed in the liquid. In this situation, the potential readings were coming from the stainless steel screw shaft on the probe holders that were used to hold the working electrodes. The corrosion potential of the screw shaft in a common tap water is about +0.1 V vs. the Hastalloy reference electrode which matches the value of the corrosion potential plateau obtained from the two probes in the Honor Rancho site [see Figures C-7(b) and C-8(b)].

Both the cases described above are likely possibilities. If the potential increase in the noble direction was due to lose contact of the liquid level, the disappearance of working electrodes must have occurred during the process of taking out the probes from the tank. Since the reference electrodes were not affected during the taking out process, it is logical to assume that both the working electrodes in all the probes must have been severely corroded. Since the weight loss measurements of the electrodes are not possible, one can utilize the EN data to give clues of the corrosion rate. The general corrosion rate of each probes were estimated on the basis of total coulomb charge of the corrosion current. The estimated general corrosion rates were 143 mpy and 204 mpy for probe #1 and #2, respectively. This corrosion rate is 7 times the maximum general corrosion measured in the probes from the Playa Del Ray. The average slopes of PSDPNL were –29.0 and –33.0 for probe #1 and #2 in Honor Rancho (see Figure 31). They are also greater than the average slopes found for the probes in the Playa Del Ray. Therefore, the general corrosion as well as the sustained localized pitting corrosion would be very severe in the Honor Rancho location according to the ENA results. This may explain the loss of working electrodes due to severe general as well as SLP corrosion attack.

Summary

The ECN analysis system was demonstrated to be able to detect the SLP corrosion on the field. The slopes of PSDPNL were correlated very well with the maximum pitting rate measured by the microscope. Both the ECN measurements and the physical examination of the probes indicate that the "udder" location of the intake side of V140/141 developed very severe SLP in the Playa del Ray facility of SOCAL. From the ECN data along indicates that the Honor Rancho location had more severe SLP corrosion attack as well as very high general corrosion rate compared with the Playa del Ray.

The interfered noise signals by the changes of environments under tested were identified and excluded during the data interpretation. The strategy of screening the interfered signal data leaned from this field test was implemented into the updated software package.

5. REFERENCES

1. Pope, D.H., “Report on Phase I Test at Southern California Gas Montebello Gas Storage Field Performed Under the Auspices of the SOCAL/ANL CRADA” (1995).
2. Monticelli, C., F. Zucchi, F. Bonollo, G. Brunoro, A. Frignani, and G. Trabanelli, *J. of Electrochem. Soc*., **142**, No. 2, 405 (1995).
3. Liu, C., D.D. Macdonald, E. Medina, J.J. Villa, and J.M. Bueno, *Corrosion Science,* **50**, No. 9, 687 (1994).
4. Cottis, R.A., and C.A. Loto, *Corrosion Science,* **46**, Vol. 1, 12, (1990).
5. Xiao, H., and F. Mansfeld, *J. of Electrochem. Soc*., **141**, Vol. 9, 2332 (1994).
6. Eden, D.A., D.G. John, and J.L. Dawson, International Patent No. 87/07022 (1987).
7. Mansfeld, F., and H. Xiao, *J. of Electrochem. Soc.,* **140**,Vol. 8, 2005 (1993).
8. Hladky, K., U.S. Patent 4,575,678 (1986).
9. Gabrielli, C., F. Huet, and M. Keddam, Electrochemical and Optical Techniques for the Study and Monitoring of Metallic Corrosion, 135, Kuiwer Academic Publishers, NATO ASI Series Vol. 203 (1991).
10. Legat, A., and V. Dolecek, *Corrosion Science*, **51**, Vol. 4, 295 (1995).
11. Bertocci, U., and F. Huet, *Corrosion Science*, **51**, Vol. 2, 131 (1995).
12. Legat, A., and V. Dolecek, *J. of Electrochem. Soc*., **142**, Vol. 6, 1851 (1995).
13. Roberge, P.R., *J. of Applied Electrochemistry*, **23,** 1223 (1993).
14. Lin, Y.P., D. Pope, J. Frank, and E. St.Martin, "In-Situ Process for the Monitoring of Localized Pitting Corrosion," U.S. Patent No. 5,888,374, 1998.
15. Lin, Y.P., E.J. St.Martin, and J.R. Frank, "Electrode Design for Corrosion Monitoring Using Electrochemical Noise Measurements, U.S. Patent No. 6,294,074, 2001.
16.

Table 1 Corrosion Rates of New Design ECN Electrodes at Chemical Corrosion Environments (RUN ECN31 and ECN32)

	initial time	final time		Initial	Final	total	Corrosion Rate		Pitting Corrosion Rate		Remark
	8/27/1999	9/3/1999		weight	weight	time					
	4:56:36 PM	9:15 am		(g)	(g)	(hours)	(g/hour)	(mpy)	(mpy)	(pitting type)	
	total time	136.3									
1	C1018	ECN31_1_W1		3.5652	3.5523	136.3	9.46E-05	8.65	N/A	uniform	mill
1	C1018	ECN31_1_C1		3.5391	3.5285	136.3	7.78E-05	7.10	N/A	uniform/LP	polished (600 grit)
1	SS316	ECN31_1_R1		3.5428	3.5406	136.3	1.61E-05	1.47	N/A	Uniform	mill
	initial time	final time		Initial	Final	total	Corrosion Rate		Pitting Corrosion Rate		Remark
	8/27/1999	9/3/1999		weight	weight	time					
	4:56:36 PM	9:15 am		(g)	(g)	(hours)	(g/hour)	(mpy)	(mpy)	(pitting type)	
	total time	136.3									
2	C1018	ECN31_1_W2		3.5807	3.5684	136.3	9.02E-05	8.24	N/A	Uniform	mill
2	C1018	ECN31_1_C2		3.5208	3.5112	136.3	7.04E-05	6.43		Localized Pitting	polished (1.0 µm)
2	SS316	ECN31_1_R2		3.5459	3.5435	136.3	1.76E-05	1.61	N/A	Uniform	mill
	initial time	final time		Initial	Final	total	Corrosion Rate		Pitting Corrosion Rate		Remark
	11/10/1999	11/18/1999		weight	weight	time					
	15:06:41	4:30 pm		(g)	(g)	(hours)	(g/hour)	(mpy)	(mpy)	(pitting type)	
	total time	193.4									
1	C1018	ECN32_1_W1		3.605	3.5521	193.4	2.74E-04	24.99	N/A	uniform corrosion	mill
1	C1018	ECN32_1_C1		3.5514	3.5414	193.4	5.17E-05	4.72	14.3	localized pitting corrosion	polished (0.3 µm)
1	SS316	ECN32_1_R1		3.6443	3.6424	193.4	9.82E-06	0.90	N/A		mill
	initial time	final time		Initial	Final	total	Corrosion Rate		Pitting Corrosion Rate		Remark
	11/10/1999	11/18/1999		weight	weight	time					
	15:06:41	4:30 pm		(g)	(g)	(hours)	(g/hour)	(mpy)	(mpy)	(pitting type)	
	total time	193.4									
2	C1018	ECN32_1_W2		3.5343	3.5136	193.4	1.07E-04	9.78	7.1	localized corrosion	polished (0.05 µm)
2	C1018	ECN32_1_C2		3.5883	3.5531	193.4	1.82E-04	16.63	N/A	uniform corrosion	mill
2	SS316	ECN32_1_R2		3.6308	3.6302	193.4	3.10E-06	0.28	N/A		mill

Table 2 Corrosion Rates of New Design ECN Electrodes at Chemical Corrosion Environments (Run ECN34)

	initial time	final time	Initial	Final	total	Corrosion Rate		Pitting Corrosion Rate		Remark
	5/12/2000	6/9/2000	weight	weight	time					
	9:51:39	9:53 AM	(g)	(g)	(hours)	(g/hour)	(mpy)	(mpy)	(pitting type)	
	total time	648.0								
1	C1018	ECN34A1W	3.5905	3.5187	648.0	1.11E-04	10.1	26.6	localized pitting corrosion	polished
1	C1018	ECN34A1C	3.5535	3.4999	648.0	8.27E-05	7.6	N/A	uniform corrosion	mill
1	SS316	ECN34A1R	3.4613	3.4597	648.0	2.47E-06	0.23	N/A	uniform corrosion	mill
2	C1018	ECN34_CPA2	3.0834	3.0301	648.0	8.22E-05	12.2	N/A	uniform corrosion	mill
3	C1018	ECN34_CPA3	2.9865	2.9320	648.0	8.41E-05	12.5	20.2	localized corrosion	polished (0.3)

	initial time	final time	Initial	Final	total	Corrosion Rate		Pitting Corrosion Rate		Remark
	5/12/2000	6/9/2000	weight	weight	time					0
	9:58:22	9:53 AM	(g)	(g)	(hours)	(g/hour)	(mpy)	(mpy)	(pitting type)	0
	total time	6.5								0
2	C1018	ECN34A2W	3.5444	3.4677	648.0	1.18E-04	10.8	N/A	uniform corrosion	mill
2	C1018	ECN34A2C	3.5586	3.4935	648.0	1.00E-04	9.2	N/A	uniform corrosion	mill
2	SS316	ECN34A2R	3.4623	3.461	648.0	2.01E-06	0.18	N/A	uniform corrosion	mill
4	C1018	ECN34_CPA4	2.742	2.6951	648.0	7.24E-05	10.7	26.1	uniform corrosion	Polished (1.0)
5	C1018	ECN34_CPA5	2.742	2.6951	648.0	7.13E-05	10.6	N/A	uniform corrosion	mill

	initial time	final time	Initial	Final	total	Corrosion Rate		Pitting Corrosion Rate		Remark
	5/12/2000	6/9/2000	weight	weight	time					
	9:56:08	9:53 AM	(g)	(g)	(hours)	(g/hour)	(mpy)	(mpy)	(pitting type)	
	total time	648.0								
1	C1018	ECN34B1W	3.5629	3.4876	648.0	1.16E-04	10.62	N/A	uniform corrosion	mill
1	C1018	ECN34B1C	3.5816	3.5193	648.0	9.61E-05	8.78	16.0	localized pitting corrosion	polished
1	SS316	ECN34B1R	3.462	3.4583	648.0	5.71E-06	0.52	N/A	uniform corrosion	mill
1	C1018	ECN34_CPB1	2.7482	2.6787	648.0	1.07E-04	15.9	9.05	uniform corrosion	polished (1.0)
4	C1018	ECN34_CPB4	2.9002	2.8529	648.04	7.3E-05	10.8	N/A	uniform corrosion	mill

	initial time	final time	Initial	Final	total	Corrosion Rate		Pitting Corrosion Rate		Remark
	5/12/2000	6/9/2000	weight	weight	time					
	9:53:53	9:53 AM	(g)	(g)	(hours)	(g/hour)	(mpy)	(mpy)	(pitting type)	
	total time	648.0								
2	C1018	ECN34B2W	3.5743	3.5014	648.0	1.12E-04	10.3	N/A	uniform corrosion	mill
2	C1018	ECN34B2C	3.5793	3.502	648.0	1.19E-04	10.9	N/A	uniform corrosion	mill
2	SS316	ECN34B2R	3.427	3.4231	648.0	6.02E-06	0.5	N/A	uniform corrosion	mill
5	C1018	ECN34_CPB5	2.8855	2.8417	648.0	6.76E-05	10.0	N/A	uniform corrosion	Mill
8	C1018	ECN34_CPB8	2.723	2.6656	648.0302	8.86E-05	13.1	12.8	uniform corrosion	polished (0.3)

Table 3 Corrosion Rates of New Design ECN Electrodes at Chemical Corrosion Environments (Run ECN35)

	initial time	final time		Initial	Final	total	Corrosion Rate		Pitting Corrosion Rate		Remark
	7/28/2000	8/18/2000		weight	weight	time					
	4:35 PM	11:59 AM		(g)	(g)	(hours)	(g/hour)	(mpy)	(mpy)	(pitting type)	
	total time	498.0									
1	C1018	ECN35A1W		3.5698	3.5675	498.0	4.62E-06	0.42	13.9	Localized corrosion	polished
1	C1018	ECN35A1C		3.5554	3.4589	498.0	1.94E-04	17.70	3.5	Localized pitting corrosion	mill
1	SS316	ECN35A1R		3.4613	3.4597	498.0	3.21E-06	0.29	-		mill
1	C1018	ECN35A_CP1		2.8373	2.8086	498.0	5.76E-05	8.5	-	uniform corrosion	half polished
	initial time	final time		Initial	Final	total	Corrosion Rate		Pitting Corrosion Rate		Remark
	7/28/2000	8/18/2000		weight	weight	time					
	4:35 PM	11:59 AM		(g)	(g)	(hours)	(g/hour)	(mpy)	(mpy)	(pitting type)	
	total time	498.0									
2	C1018	ECN35A2W		3.5609	3.5336	498.0	5.48E-05	5.01	2.1	uniform pitting corrosion	mill
2	C1018	ECN35A2C		3.5947	3.5383	498.0	1.13E-04	10.35	2.1	uniform pitting corrosion	mill
2	SS316	ECN35A2R		3.6308	3.6302	498.0	1.20E-06	0.11	-		mill
2	C1018	ECN35A_CP2		2.885	2.8558	498.0	5.86E-05	8.7	-		mill
	initial time	final time		Initial	Final	total	Corrosic		Pitting Corrosion Rate		Remark
	7/28/2000	8/18/2000		weight	weight	time					
	4:39 PM	11:59 AM		(g)	(g)	(hours)	(g/hour)	(mpy)	(mpy)	(pitting type)	
	total time	498.0									
1	C1018	ECN35B1W		3.5012	3.4714	498.0	5.98E-05	5.47	9.00	localized group pitting	polished
1	C1018	ECN35B1C		3.5423	3.4821	498.0	1.21E-04	11.04	2.08	uniform pitting corrosion	mill
1	SS316	ECN35B1R		3.4613	3.4597	498.0	3.21E-06	0.29	-		mill
1	C1018	ECN35B_CP1		2.7948	2.765	498.0	5.98E-05	8.9	-	uniform corrosion	half polished
	initial time	final time		Initial	Final	total	Corrosic		Pitting Corrosion Rate		Remark
	7/28/2000	8/18/2000		weight	weight	time					
	4:39 PM	11:59 AM		(g)	(g)	(hours)	(g/hour)	(mpy)	(mpy)	(pitting type)	
	total time	498.0									
2	C1018	ECN35B2W		3.571	3.5263	498.0	8.98E-05	8.20	-	uniform .corrosion	mill
2	C1018	ECN35B2C		3.5658	3.5337	498.0	6.45E-05	5.89	-	uniform corrosion	mill
2	SS316	ECN35B2R		3.5448	3.5428	498.0	4.02E-06	0.37	-		mill
2	C1018	ECN35B_CP2		2.8905	2.8612	498.0	5.88E-05	8.7	-		mill

Table 4 Corrosion Rates of New Design ECN Electrodes at MIC Environments (Run ECN36)

	initial time	final time		Initial	Final	total	Corrosion Rate		Pitting Corrosion Rate		Remark
	8/1/2000	8/31/2000		weight	weight	time					
	5:09 PM	11:59 AM		(g)	(g)	(hours)	(g/hour)	(mpy)	(mpy)	(pitting type)	
	total time	1220.6									
1	C1018	ECN36A1W		3.588	3.5659	1220.6	1.81E-05	1.65	6.5	Localized corrosion	polished
1	C1018	ECN36A1C		3.5601	3.5285	1220.6	2.59E-05	2.37	-	uniform corrosion	mill
1	SS316	ECN36A1R		3.6346	3.6336	1220.6	8.19E-07	0.07			mill
1	C1018	ECN36A_CP1		2.8373	2.8086	1220.6	2.35E-05	4.5		uniform corrosion	half polished
	initial time	final time		Initial	Final	total	Corrosion Rate		Pitting Corrosion Rate		Remark
	8/1/2000	8/31/2000		weight	weight	time					
	5:09 PM	11:59 AM		(g)	(g)	(hours)	(g/hour)	(mpy)	(mpy)	(pitting type)	
	total time	1220.6									
2	C1018	ECN36A2W		3.5664	3.5112	1220.6	4.52E-05	4.13	-	uniform pitting corrosion	mill
2	C1018	ECN36A2C		3.6004	3.5756	1220.6	2.03E-05	1.86	-	uniform pitting corrosion	mill
2	SS316	ECN36A2R		3.6362	3.6357	1220.6	4.10E-07	0.04			mill
2	C1018	ECN36A_CP2		2.885	2.8558	1220.6	2.39E-05	4.6			mill
	initial time	final time		Initial	Final	total	Corrosion Rate		Pitting Corrosion Rate		Remark
	8/1/2000	8/31/2000		weight	weight	time					
	5:14 PM	11:59 AM		(g)	(g)	(hours)	(g/hour)	(mpy)	(mpy)	(pitting type)	
	total time	1220.6									
1	C1018	ECN36B1W		3.5915	3.5648	1220.6	2.19E-05	2.00	13.0	Localized corrosion	polished
1	C1018	ECN36B1C		3.5699	3.5516	1220.6	1.50E-05	1.37	-	uniform corrosion	mill
1	SS316	ECN36B1R		3.6257	3.6255	1220.6	1.64E-07	0.01			mill
1	C1018	ECN36B_CP1		2.8373	2.8086	1220.6	2.35E-05	4.5		uniform corrosion	half polished
	initial time	final time		Initial	Final	total	Corrosion Rate		Pitting Corrosion Rate		Remark
	8/1/2000	8/31/2000		weight	weight	time					
	5:14 PM	11:59 AM		(g)	(g)	(hours)	(g/hour)	(mpy)	(mpy)	(pitting type)	
	total time	1220.6									
2	C1018	ECN36B2W		3.5368	3.5	1220.6	3.01E-05	2.75	-	uniform pitting corrosion	mill
2	C1018	ECN36B2C		3.5486	3.5259	1220.6	1.86E-05	1.70	-	uniform pitting corrosion	mill
2	SS316	ECN36B2R		3.6414	3.6411	1220.6	2.46E-07	0.02			mill
2	C1018	ECN36B_CP2		2.885	2.8558	1220.6	2.39E-05	4.6			mill

Table 5 Simulated Egypt Produced and Fire Water

		Inlet Hemis42"		Firewater	
	MW	g/l	20L	g/l	20L
mM					
$CaCl_2$	111	40.15	800	1.22	24
$MgCl_2$	95.2	15.2	300	5.99	120
NaCl	58.4	172.5	3450	66.6	1332
KCl	74.6	1.53	30.4	0.885	17.6
$FeCl_2$	162.2	0.531	10.6	0.016	0.32
Na_2SO_4	142	1.30	26	5.78	115.6
$(NH_2)_2SO_4$	132.1	0.05	1.0	0.05	1.0
0.38					
KH_2PO_4	136.1	0.002	0.04	0.002	0.04
0.015					
K_2HPO_4	174.2	0.002	0.04	0.002	0.04
0.012					
Na Formate	68.0	0.2	4.0	0.2	4.0
2.94					
Na Acetate	82.0	3.4	68	3.4	68
41.46					
Resazurin	0.4 ml of a 0.1% solution per Liter				
Final pH		5.6 ~15ml 10N NaOH		6.86 no additions	

Notes: All media were degassed with N2 for approximately 1 hr before inoculation and transfer into the test loops under a N2 atmosphere. Hemis medium was prepared with 1L of Hemis Egypt produced water and 10 ml of a Montana State SRB culture from Egypt inoculated into 2L of St.Peter simulated produced water and incubated for two weeks prior to loading the test loops. The firewater medium was prepared in a similar manner using 1 L of Egypt firewater as inoculum.

Table 6 Simulated St.Peter Produce Water

	MW	g/l	mM
NaCl	58.4	14.4	246.5
NaFormate	68	0.2	2.94
NaAcetate	82	3.4	41.5
$CaCl_2$	111	1.51	13.6
$MgCl_2$-$6H_20$	203.3	3.06	15.0
KH_2P0_4	136.1	0.002	0.015
K_2HP0_4	174.2	0.002	0.012
$(NH_4)_2S0_4$	132.1	0.05	0.38
$NaN0_3$	85.0	0.06	0.71
Na_2S0_4-$10H_203$	22.2	1.73	5.4
$Na_2C0_3H_20$	124	0.155	1.25
$FeS0_4$-$7H_20$	2783ml of 0.2% in 1%HCL=0.06mg/l=0.215uM		
Resazurin	0.4 ml of 0.l% solution		

pH Adjust to 5.7 with ~20 ml 1N Na0H

Table 7 Estimated Bacteria Population Analysis

Bacteria population analysis	
degree of population.	possible population (colonies/100 μm)
1	10^0 - 10^1
2	10^1 - 10^2
3	10^2 - 10^3
4	10^3 - 10^4
5	10^4 - 10^5

Sampling date :	1/22/1999		Elapsed time (hr):		210			
reading date :	2/10/1999	(1/25/99)						
elapsed days after sampling	20 days	(4 days)						
Loop	Liquid Samples				Coupon Samples			
	APB		SRB		APB		SRB	
A	4	(2)	2	(0)	1	(1)	0	(0)
B	5	(2)	2	(0)	1	(0)	0	(0)
C	5	(3)	4	(0)	4	(0)	1	(0)
D	5	(1)	2	(0)	2	(1)	1	(0)
Sampling date :	2/10/1999		Elapsed time (hr):		642			
reading date :	3/12/1999	(2/16/99)						
elapsed days after sampling	31 days	(7 days)						
Loop	Liquid Samples				Coupon Samples			
	APB		SRB		APB		SRB	
A	3	(1)	0	(0)	1	(0)	0	(0)
B	5	(1)	0	(0)	1	(1)	0	(0)
C	5	(2)	5	(2)	5	(2)	3	(2)
D	5	(5)	4	(2)	5	(5)	4	(3)
Sampling date :	2/18/1999		Elapsed time (hr):		830.0833			
reading date :	3/12/1999							
elapsed days after sampling	23 days							
Loop	Liquid Samples				Coupon Samples			
	APB		SRB		APB		SRB	
A	-		-		-		-	
B	-		-		-		-	
C	-		-		-		-	
D	4		2		-		-	
Sampling date :	3/5/1999		Elapsed time (hr):		1198.678			
reading date :	3/15/1999	(3/12/99)						
elapsed days after sampling	11 days	(8 days)						
Loop	Liquid Samples				Coupon Samples			
	APB		SRB		APB		SRB	
A	1	(0)	0	(0)	2	(0)	0	(0)
B	1	(1)	0	(0)	4	(3)	1	(1)
C	5	(5)	5	(5)	3	(3)	5	(5)
D	4	(4)	5	(5)	0	(0)	5	(3)

* - questionable result. It should have seen bacteria on the coupon surface because they were +4 in the liquid.

Table 7 Estimated Bacteria Population Analysis (continuous)

Sampling date :	4/20/1999		Elapsed time (hr):		1005.5			
reading date :	4/29/1999							
elapsed days after samplinc	10 days							
Loop	Liquid Samples				Coupon Samples			
	APB		SRB		APB		SRB	
A	-	-	-	-	-	-	-	-
B	-	-	-	-	-	-	-	-
C	2	-	5	-	-	-	-	-
D	3	-	5	-	-	-	-	-
Sampling date :	4/30/1999		Elapsed time (hr):		1225.51			
reading date :	5/6/1999	(5/3/99)						
elapsed days after samplinc	7 days	(4 days)						
Loop	Liquid Samples				Coupon Samples			
	APB		SRB		APB		SRB	
A	-	-	-	-	-	-	-	-
B	-	-	-	-	-	-	-	-
C	1	(1)	5	(2)	-	-	-	-
D	1	(1)	3	(1)	-	-	-	-
Sampling date :	5/10/1999		Elapsed time (hr):		1519.562			
reading date :	6/3/1999	(5/19/99)						
elapsed days after samplinc	25 days	(10 days)						
Loop	Liquid Samples				Coupon Samples			
	APB		SRB		APB		SRB	
A	-	-	-	-	-	-	-	-
B	-	-	-	-	-	-	-	-
C	5	(1)	5	(5)	-	-	-	-
D	0	(0)	1	(1)	-	-	-	-
Sampling date :	5/18/1999		Elapsed time (hr):		1607.891			
reading date :	6/3/1999	(5/25/99)						
elapsed days after samplinc	17 days	(8 days)						
Loop	Liquid Samples				Coupon Samples			
	APB		SRB		APB		SRB	
A	-	-	-	-	-	-	-	-
B	-	-	-	-	-	-	-	-
C	2	(2)	5	(5)	0	(0)	4	(0)
D	1	(1)	5	(5)	0	(0)	1	(1)

Table 8 Corrosion Rates of Metal Coupons in the Loops (weight-loss analysis and optical microscope inspection)

			Initial weight (g)	Final weight (g)	total time (hours)	Corrosion Rate (g/hour)	Corrosion Rate (mpy)	Pitting Corrosion Rate (mpy)	Pitting Corrosion Rate (pitting type)
	Loop A								
2	C1018	A2	12.1264	12.0901	642.0	5.65E-05	1.3	7.5	(max pit rate)
3	C1018	A3	12.1822	12.1142	1198.7	5.67E-05	1.3	2.0	(average pit rate)
4	C1018	A4	12.1946						
5	Hemi Steel	A5	10.9049	10.8699	599.6	5.84E-05	1.3	hard to determine the pitting rate	
6	Hemi Steel	A6	10.4637	10.4049	1156.3	5.09E-05	1.1	due to the surface roughness	
	Loop B								
2	C1018	B2	12.1178	12.0685	642	7.68E-05	1.7	2.7	(average pit rate)
3	C1018	B3	12.0701	12.0066	1199	5.30E-05	1.2	0.9	(average pit rate)
5	Hemi Steel	B5	10.9489	10.9163	600	5.44E-05	1.2	hard to determine the pitting rate	
6	Hemi Steel	B6	10.9782	10.8946	1156	7.23E-05	1.6	due to the surface roughness	
	Loop C								
2	C1018	C2	12.1265	12.0435	642	1.29E-04	2.9	16.7	(max pit rate)
3	C1018	C3	12.1106	11.9468	1199	1.37E-04	3.1	8.1	(max pit rate)
4	C1018	C4	12.0640	10.6715	3095	4.50E-04	10.1		
5	Fire W. S.	C5	10.8440	10.7463	642	1.52E-04	3.4	hard to determine the pitting rate	
6	Fire W. S.	C6	10.9658	10.7600	1199	1.72E-04	3.9	due to the surface roughness	
	Loop D								
2	C1018	D2	12.1726	12.1374	642	5.48E-05	1.2		
3	C1018	D3	12.2805	12.2182	1199	5.20E-05	1.2	2.9	(max pit rate)
4	C1018	D4	11.9921	10.8155	3095	3.80E-04	8.6		
5	Fire W. S.	D5	11.0948	11.0695	642	3.94E-05	0.9	hard to determine the pitting rate	
6	Fire W. S.	D6	10.6519	10.5474	1199	8.72E-05	2.0	due to the surface roughness	
8	Fire W. S.	D8	10.7717	9.3778	3119	4.47E-04	10.1		

Table 9 Corrosion rates of ECN probes in the loops

			Initial Weight (g)	Final Weight (g)	total time (hours)	Corrosion Rate (g/hour)	Corrosion Rate (mpy)	Pitting Corrosion Rate (mpy)	(pitting type)
	Loop A								
1	C1018	ECNW1	3.5874	3.56	3570	6.33E-06	0.58		Uniform corrosion
1	C1018	ECNC1	3.5814	3.56	3570	6.67E-06	0.61		Uniform corrosion
1	SS316	ECNR1	3.466	3.47	3570	5.60E-08	0.01		Uniform corrosion
2	C1018	ECNW2	3.5993	3.57	3570	7.09E-06	0.65		Uniform corrosion
2	C1018	ECNC2	3.593	3.57	3570	7.12E-06	0.65		Uniform corrosion
2	SS316	ECNR2	3.4788	3.48	3570	8.40E-08	0.01		Uniform corrosion
	Loop B								
3	C1018	ECNW3	3.6086	3.58	3570	9.41E-06	0.86		Uniform corrosion
3	C1018	ECNC3	3.5922	3.56	3570	8.43E-06	0.77		Uniform corrosion
3	SS316	ECNR3	3.4734	3.47	3570	1.12E-07	0.01		Uniform corrosion
4	C1018	ECNW4	3.5929	3.56	3570	9.41E-06	0.86		Uniform corrosion
4	C1018	ECNC4	3.6043	3.57	3570	9.36E-06	0.85		Uniform corrosion
4	SS316	ECNR4	3.4709	3.47	3570	2.80E-07	0.03		Uniform corrosion
	Loop C								
5	C1018	ECNW5	3.5940	3.54	3095	1.78E-05	1.6	3.1	
5	C1018	ECNC5	3.5669	3.53	3095	1.20E-05	1.1	3.5	(max pit rate)
5	SS316	ECNR5	3.4804	3.48	2183	1.56E-06	0.1		Uniform corrosion
6	C1018	ECNW6	3.5885	3.54	3095	1.52E-05	1.4		Uniform corrosion
6	C1018	ECNC6	3.6049	3.58	3095	8.79E-06	0.8		Uniform corrosion
6	SS316	ECNR6	3.5019	3.49	2183	4.54E-06	0.4		Uniform corrosion
	Loop D								
7	C1018	ECNW7	3.5943	3.57	3095	8.31E-06	0.8		Uniform corrosion
7	C1018	ECNC7	3.5924	3.55	3095	1.41E-05	1.3	1.1	(max pit rate)
7	SS316	ECNR7	3.4843	3.48	1608	1.37E-06	0.1		Uniform corrosion
8	C1018	ECNW8	3.6027	3.57	3095	1.06E-05	1.0		Uniform corrosion
8	C1018	ECNC8	3.6001	3.56	3095	1.16E-05	1.1		Uniform corrosion
8	SS316	ECNR8	3.5052	3.48	2183	1.14E-05	1.0		Uniform corrosion

Table 10 - Corrosion rate of the ECN probe in loop A measured by weight loss method

	initial time 11/23/1999 4:10 PM	final time 4/28/2000 3:15 pm	Initial weight (g)	Final weight (g)	total time (hours)	Corrosion Rate (g/hour)	Corrosion Rate (mpy)	Pitting Corrosion Rate (mpy)	Pitting Corrosion Rate (pitting type)	Remark
	total time	3719.1								
A	C1018	ECN33_AW	3.561	3.5237	3719.1	1.00E-05	0.92	-	uniform	
A	C1018	ECN33_AC	3.5609	3.5385	3719.1	6.02E-06	0.55	-	uniform	
A	SS316	ECN33_AR	3.6245	3.6234	3719.1	2.96E-07	0.03	-	Uniform	

Table 11 - Corrosion rate of the ECN probe in loop A measured by weight loss method

	initial time 11/23/1999 4:10 PM	final time 4/28/2000 3:15 pm	Initial weight (g)	Final weight (g)	total time (hours)	Corrosion Rate (g/hour)	Corrosion Rate (mpy)	Pitting Corrosion Rate (mpy)	Pitting Corrosion Rate (pitting type)	Remark
	total time	3719.1								
B	C1018	ECN33_BW	3.568	3.2944	3719.1	7.36E-05	6.72	47.9	SLP	80 µm
B	C1018	ECN33_BC	3.5839	3.403	3719.1	4.86E-05	4.44	59.8	SLP	100 µm
B	SS316	ECN33_BR	3.6158	3.6142	3719.1	4.30E-07	0.04	-	Uniform	

Table 12 - Corrosion rate of the ECN probe in loop A measured by weight loss method

	initial time 11/23/1999 4:10 PM	final time 4/28/2000 3:15 pm	Initial weight (g)	Final weight (g)	total time (hours)	Corrosion Rate (g/hour)	Corrosion Rate (mpy)	Pitting Corrosion Rate (mpy)	Pitting Corrosion Rate (pitting type)	Remark
	total time	3719.1								
C	C1018	ECN33_CW	3.566	3.5189	3719.1	1.27E-05	1.16	-	uniform	
C	C1018	ECN33_CC	3.5539	3.533	3719.1	5.62E-06	0.51	-	uniform	
C	SS316	ECN33_CR	3.623	3.6203	3719.1	7.26E-07	0.07	-	Uniform	

Table 13 - SOCAL 1 Probe 1 in the udder of V140

Material	Electrode	total time (hours)	Uniform Corrosion Rate (mpy)	Max. Pitting Corrosion Rate (mpy)	Corrosion type	Corrosion Type from ENA
C1018	SOCAL1_W1	1147.0	29.23	30.1	severe uniform pitting corrosion attack	SLP
C1018	SOCAL1_C1	1147.0	6.71	36.1	sustained localized pitting corrosion	
Hastalloy	SOCAL1_R1	1147.0	0.01	N/A	uniform corrosion attack	

Table 14 - SOCAL 1 Probe 2 in the udder of V140

Material	Electrode	total time (hours)	Uniform Corrosion Rate (mpy)	Max. Pitting Corrosion Rate (mpy)	Corrosion Mechanism	Corrosion Type ** from ENA
C1018	SOCAL1_W2	1147.0	14.19	24.1	severe uniform pitting corrosion attack	
C1018	SOCAL1_C2	1147.0	16.20	13.5	severe uniform pitting corrosion attack	SLP
Hastalloy	SOCAL1_R2	1147.0	0.02	N/A	uniform corrosion	

Table15 - SOCAL 2 Probe 1 in the bottom of V140

Material	Electrode	total time (hours)	Uniform Corrosion Rate (mpy)	Max. Pitting Corrosion Rate (mpy)	Corrosion Mechanism	Corrosion Type ** from ENA
C1018	SOCAL2_W1	1388.5	2.48	2.5	slight localized pitting corrosion attack	localized pitting and
C1018	SOCAL2_C1	1388.5	0.46	N/A	uniform corrosion attack	uniform corrosion mixing
Hastalloy	SOCAL2_R1	1388.5	0.02	N/A	uniform corrosion	

Table 16 - SOCAL 2 Probe 2 in the bottom of V140

Material	Electrode	total time (hours)	Uniform Corrosion Rate (mpy)	Max. Pitting Corrosion Rate (mpy)	Corrosion Mechanism	Corrosion Type ** from ENA
C1018	SOCAL2_W2	1388.5	0.43	N/A	uniform corrosion attack	N/A
C1018	SOCAL2_C2	1388.5	0.39	N/A	uniform corrosion attack	
Hastalloy	SOCAL2_R2	1388.5	0.04	N/A	uniform corrosion attack	

Table 17 - Probe 1 in the third location of SOCAL

Material	Electrode	total time (hours)	Uniform Corrosion Rate (mpy)	Pitting Corrosion Rate (mpy)	Corrosion Mechanism	Corrosion Type ** from ENA
C1018	SOCAL3_W1	2268.0	0.77	N/A	Uniform corrosion	Uniform Corrosion
C1018	SOCAL3_C1	2268.0	0.15	N/A	uniform corrosion	
Hastalloy	SOCAL3_R1	2268.0	0.01	N/A	uniform corrosion	

Table 18 - Probe 2 in the third location of SOCAL

Material	Electrode	total time (hours)	Uniform Corrosion Rate (mpy)	Pitting Corrosion Rate (mpy)	Corrosion Mechanism	Corrosion Type ** from ENA
C1018	SOCAL3_W2	2268.0	0.27	N/A	Uniform corrosion	Uniform Corrosion
C1018	SOCAL3_C2	2268.0	0.91	0.8	uniform corrosion	
Hastalloy	SOCAL3_R2	2268.0	0.01	N/A	uniform corrosion	

Table 19 - Probe 1 in the Honor Rancho location of SOCAL

Material	Electrode	total time (hours)	Uniform Corrosion Rate (mpy)	Pitting Corrosion Rate (mpy)	**Corrosion Mechanism**	Corrosion Type ** from ENA
C1018	SOCAL4_W1	1399.5	143.5*	-	SLP**	SLP
C1018	SOCAL4_C1	1399.5	143.5*	-	SLP**	
Hastalloy	SOCAL4_R1	1399.5	0.02	-	uniform corrosion	

Table 20 - Probe 2 in the Honor Rancho location of SOCAL

Material	Electrode	total time (hours)	Uniform Corrosion Rate (mpy)	Pitting Corrosion Rate (mpy)	**Corrosion Mechanism**	Corrosion Type ** from ENA
C1018	SOCAL4_W2	1399.5	204.3*	-	SLP**	SLP
C1018	SOCAL4_C2	1399.5	204.3*	-	SLP**	
Hastalloy	SOCAL4_R2	1399.5	0.02	-	uniform corrosion	

*** - the uniform corrosion rate was estimated from the total charge loss recorded by ECN**
**** - the corrosion type was revealed from the on-line ECN measurement**

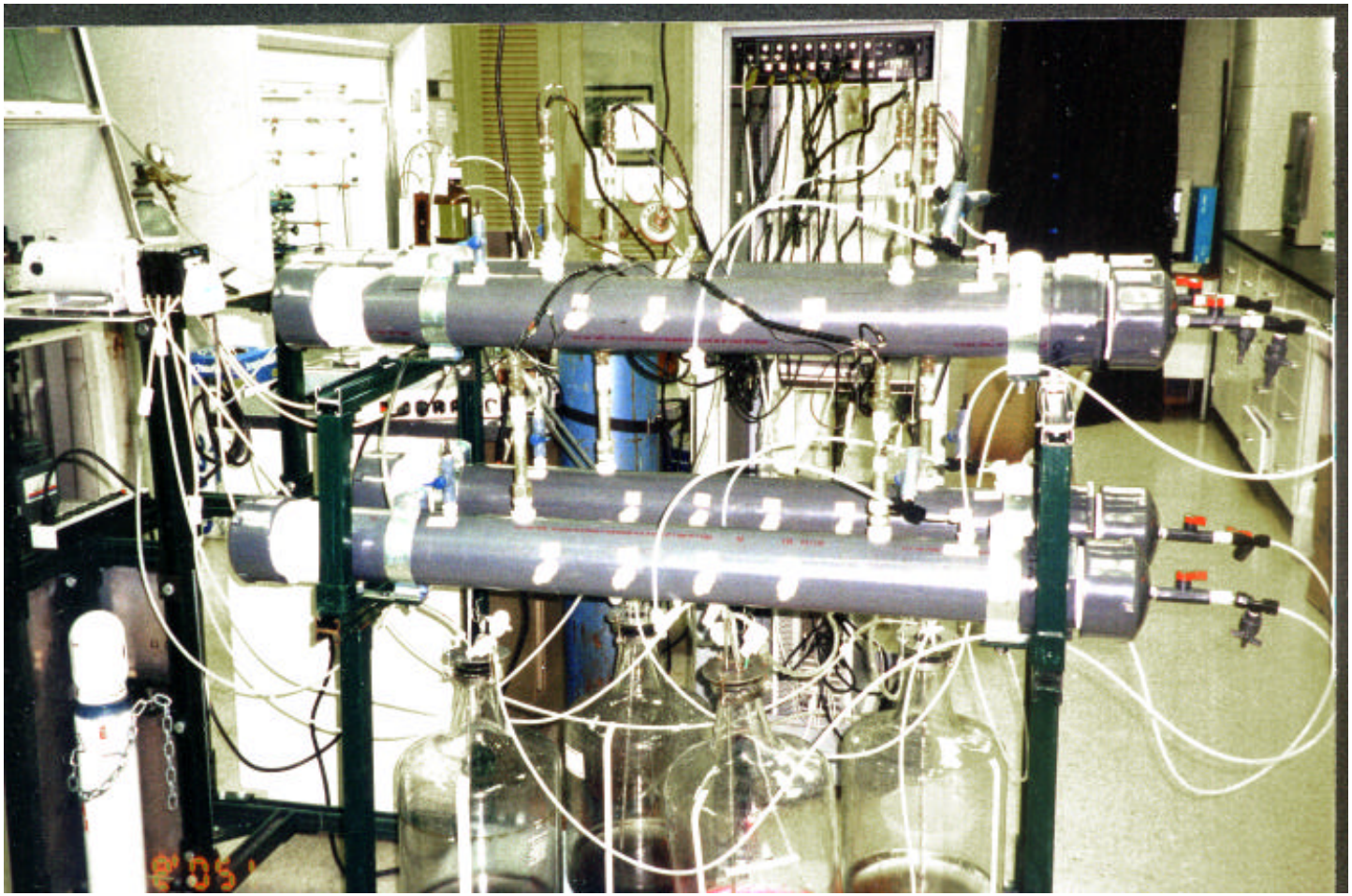

FIGURE 1: Flow loops testing facility for simulated process fluids and material corrosion process evaluation.

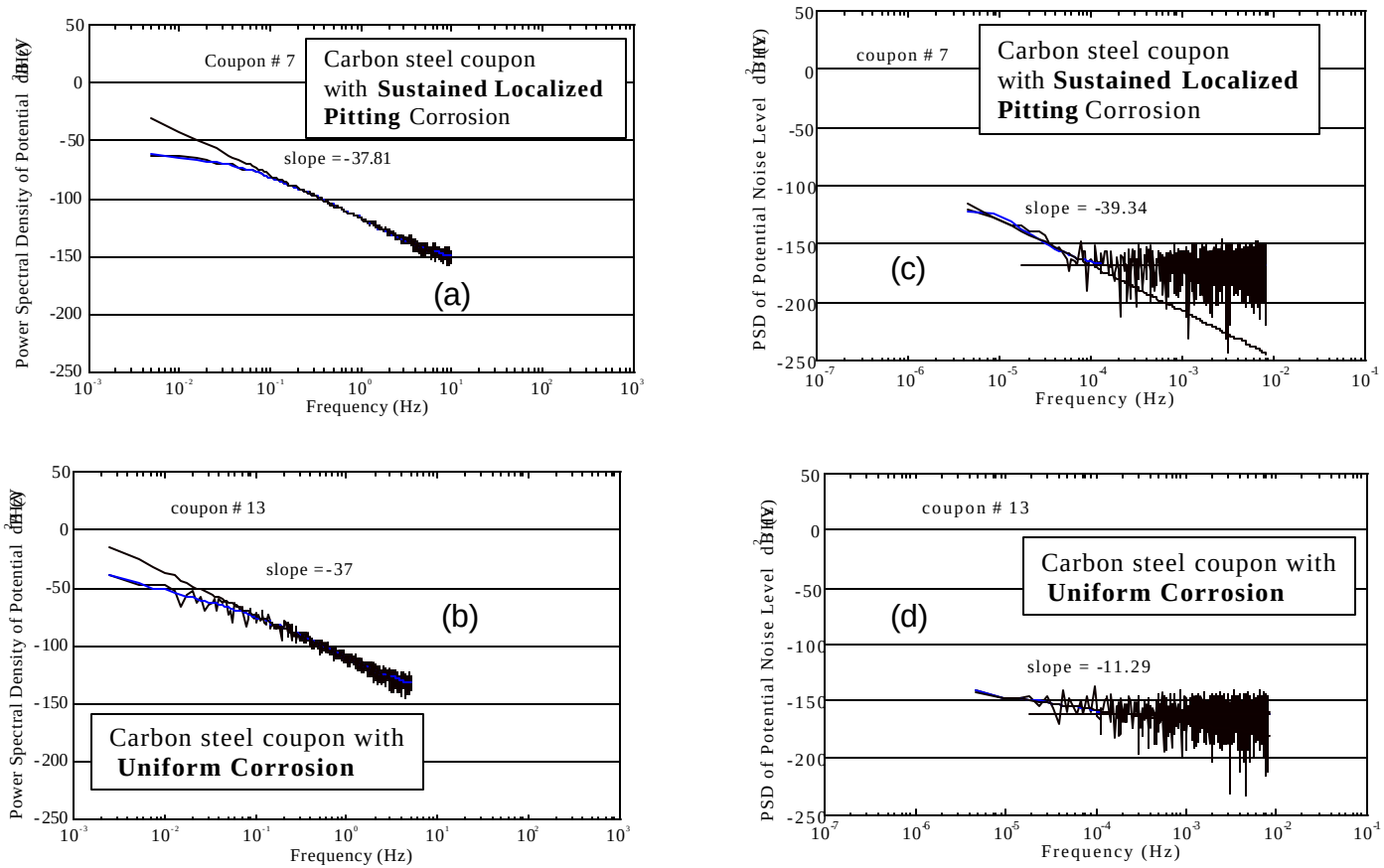

FIGURE 2: Power spectrum of electrochemical noise data acquired by zero-resistance measurement of conventional as well as Argonne's new data acquisition system.

(a) Coupon sample with pitting corrosion, by conventional data acquisition system.
(b) Coupon sample with uniform corrosion, by conventional data acquisition system.
(c) Coupon sample with pitting corrosion, by Argonne's data acquisition system.
(d) Coupon sample with uniform corrosion, by Argonne's data acquisition system.

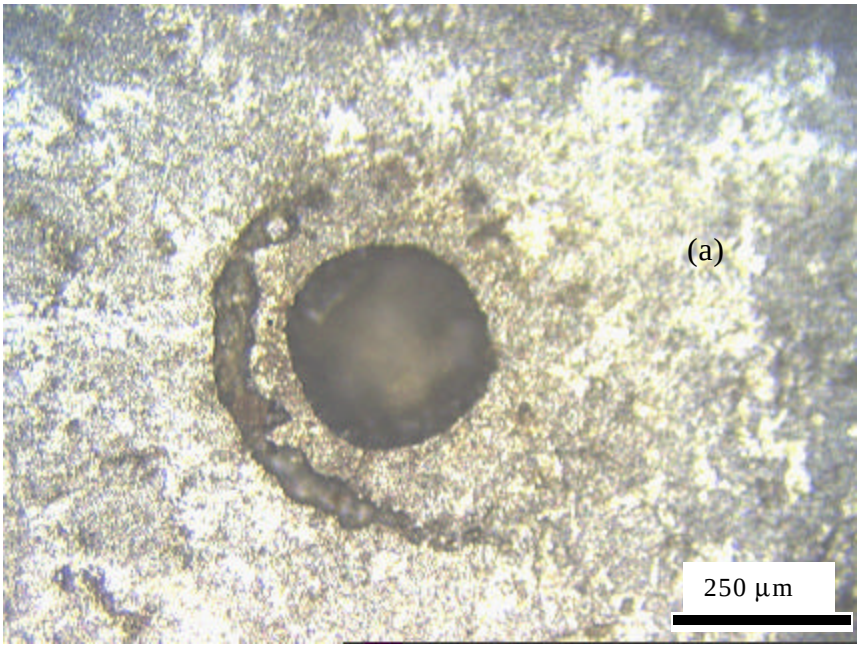

diameter : 275 µm, depth : 88 µm

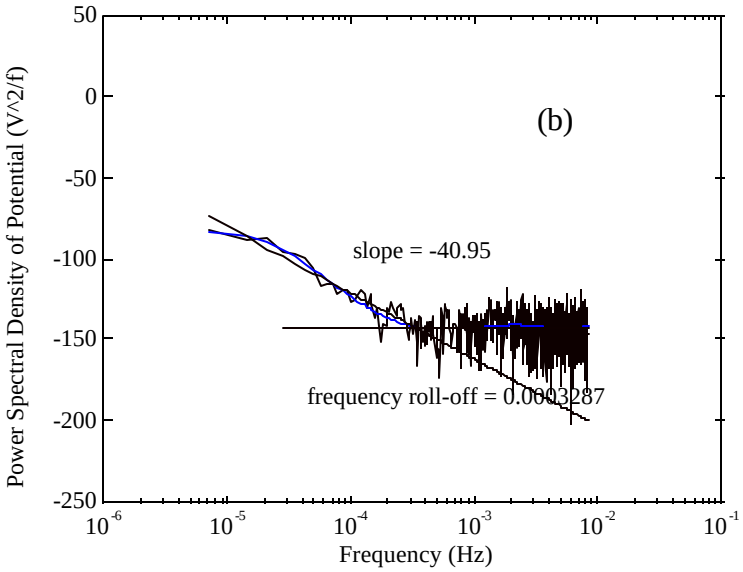

FIGURE 3: PSD of potential noise level and surface morphology of type I probe with S.S. 316 as counter electrode. The probe was immersed in water with traces of NaCl and purged with air; pH = 6.12.

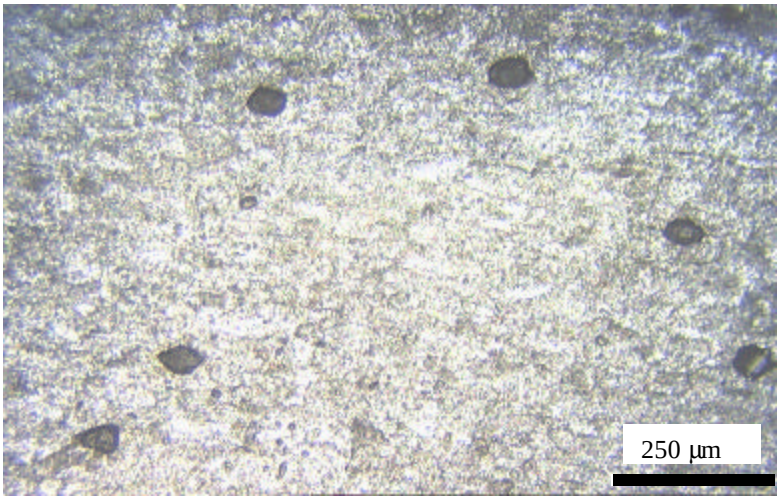

small pits uniformly distributed on the front surface
diameter: 50 µm, depth: 11 µm

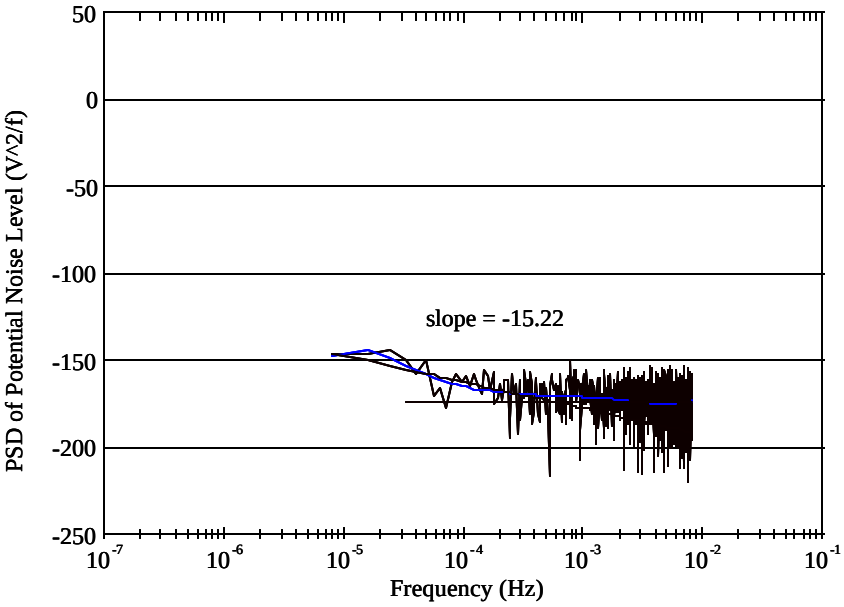

FIGURE 4: PSD of potential noise level and surface morphology of type I probe with S.S. 316 as counter electrode. The probe was immersed in water and purged with air; pH = 6.97.

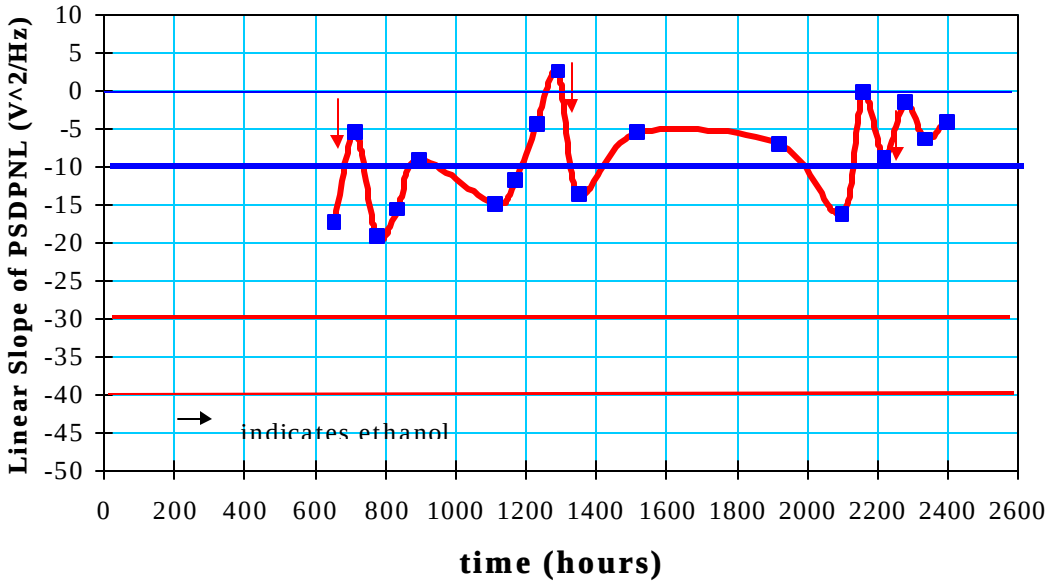

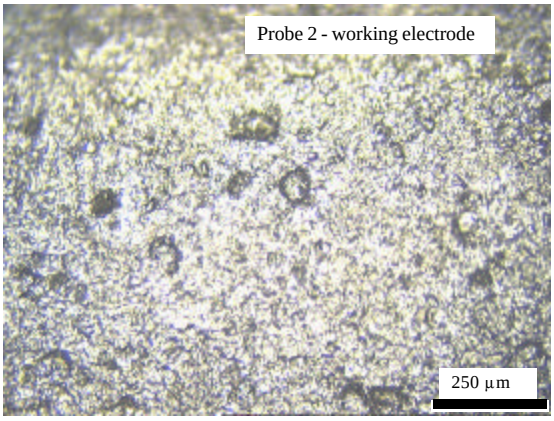

diameter ≈ 30-50 µm; depth ≈ 10-12µm; surface roughness ≈ 3 µm

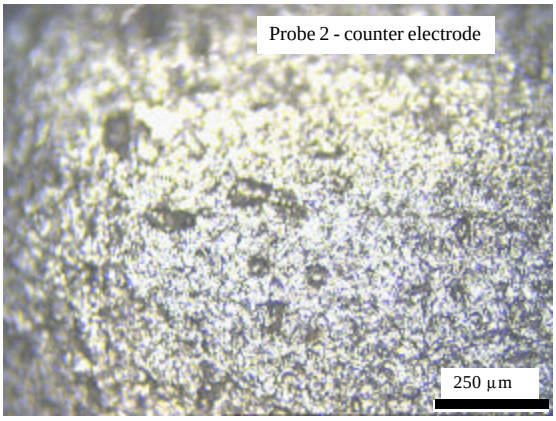

diameter ≈ 40 µm; depth ≈ 10 µm; surface roughness ≈ 3 µm

FIGURE 5: Change profile of PSDPNL and morphology of probe 2 from flow loop A.

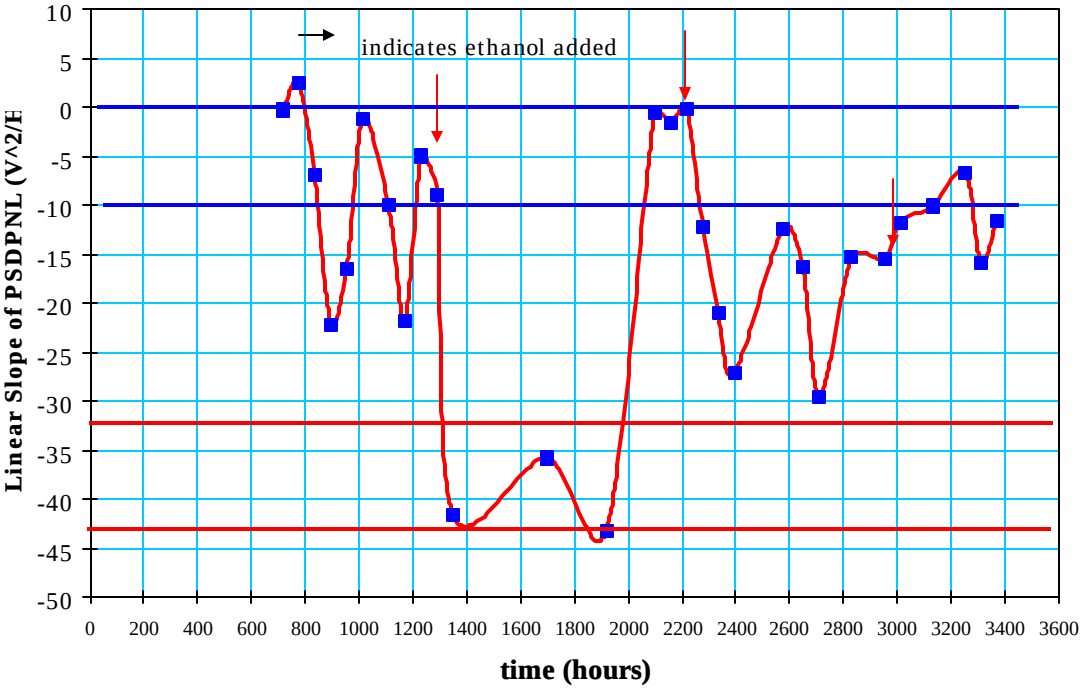

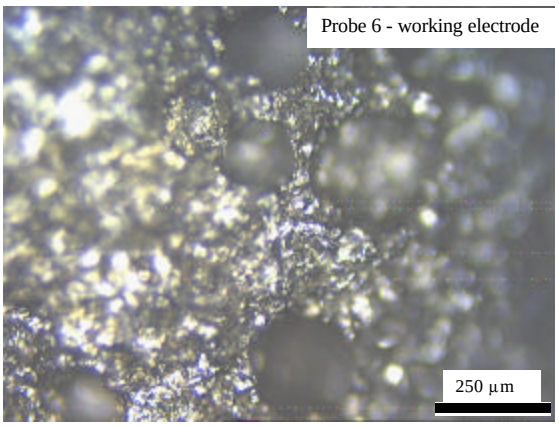

diameter ≈ 125 µm; depth ≈ 80 µm; surface roughness ≈ 3 µm

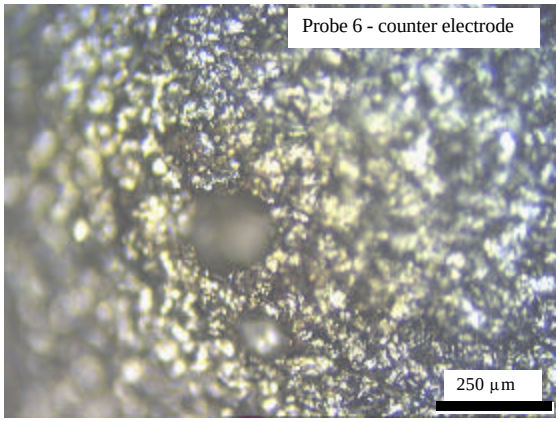

diameter ≈ 120 µm; depth ≈ 37 µm; surface roughness ≈ 3 µm

FIGURE 6: Change profile of PSDPNL and morphology of probe 6 from flow loop.

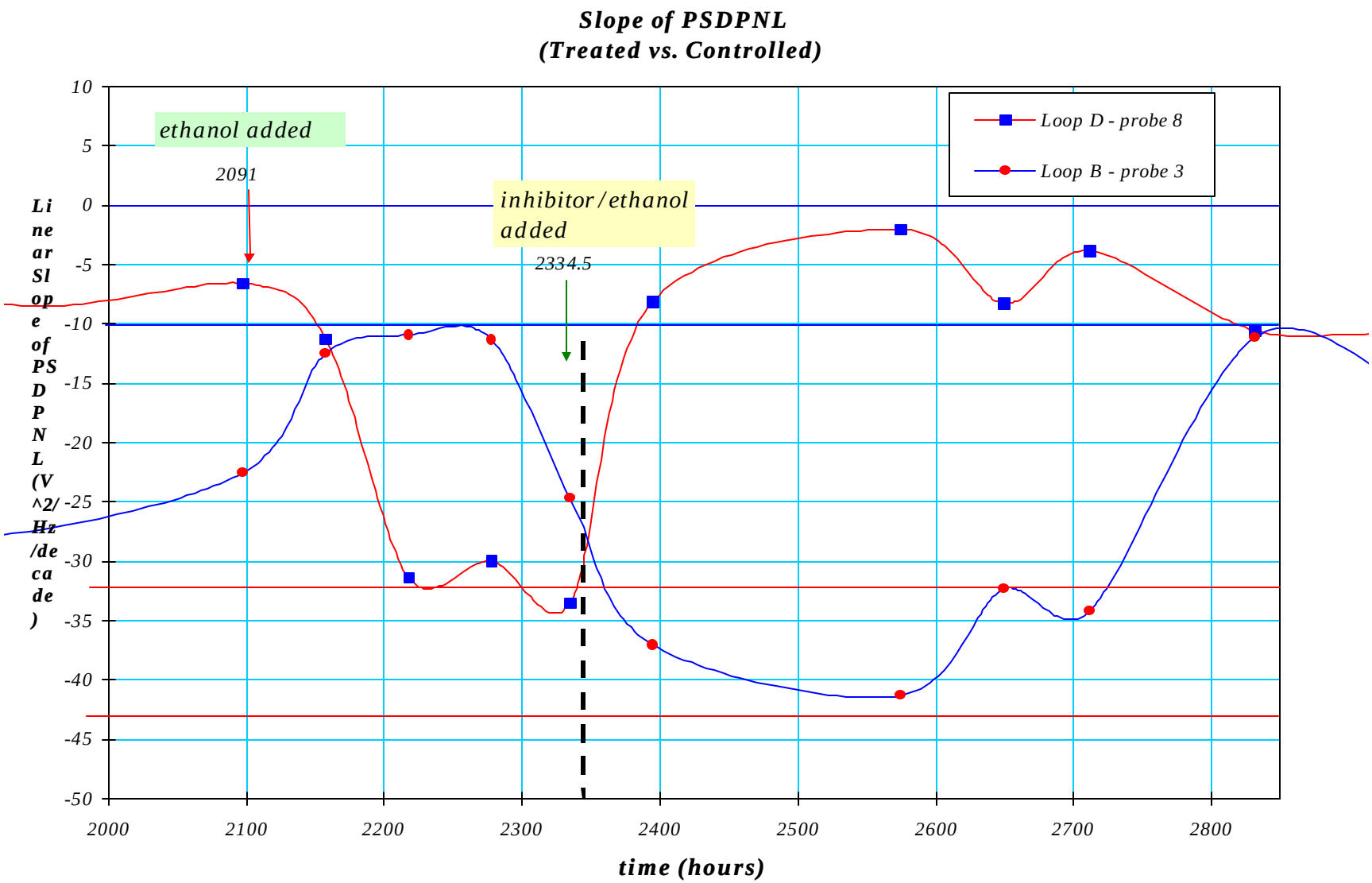

FIGURE 7: Change profile of PSDPNL's linear slope in different corrosion environments

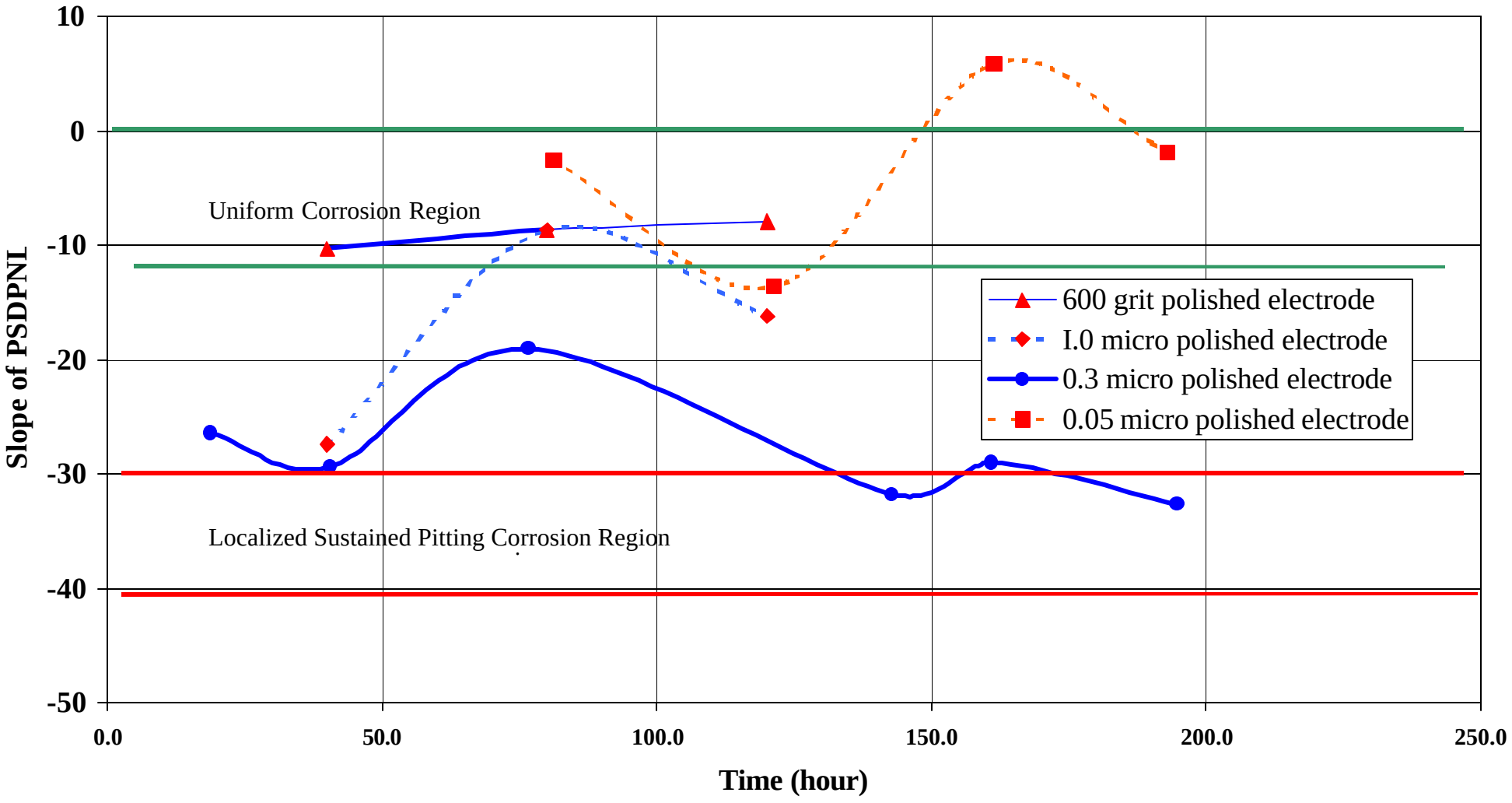

Figure 8 Slope profile of new ECN probes with SMEs.

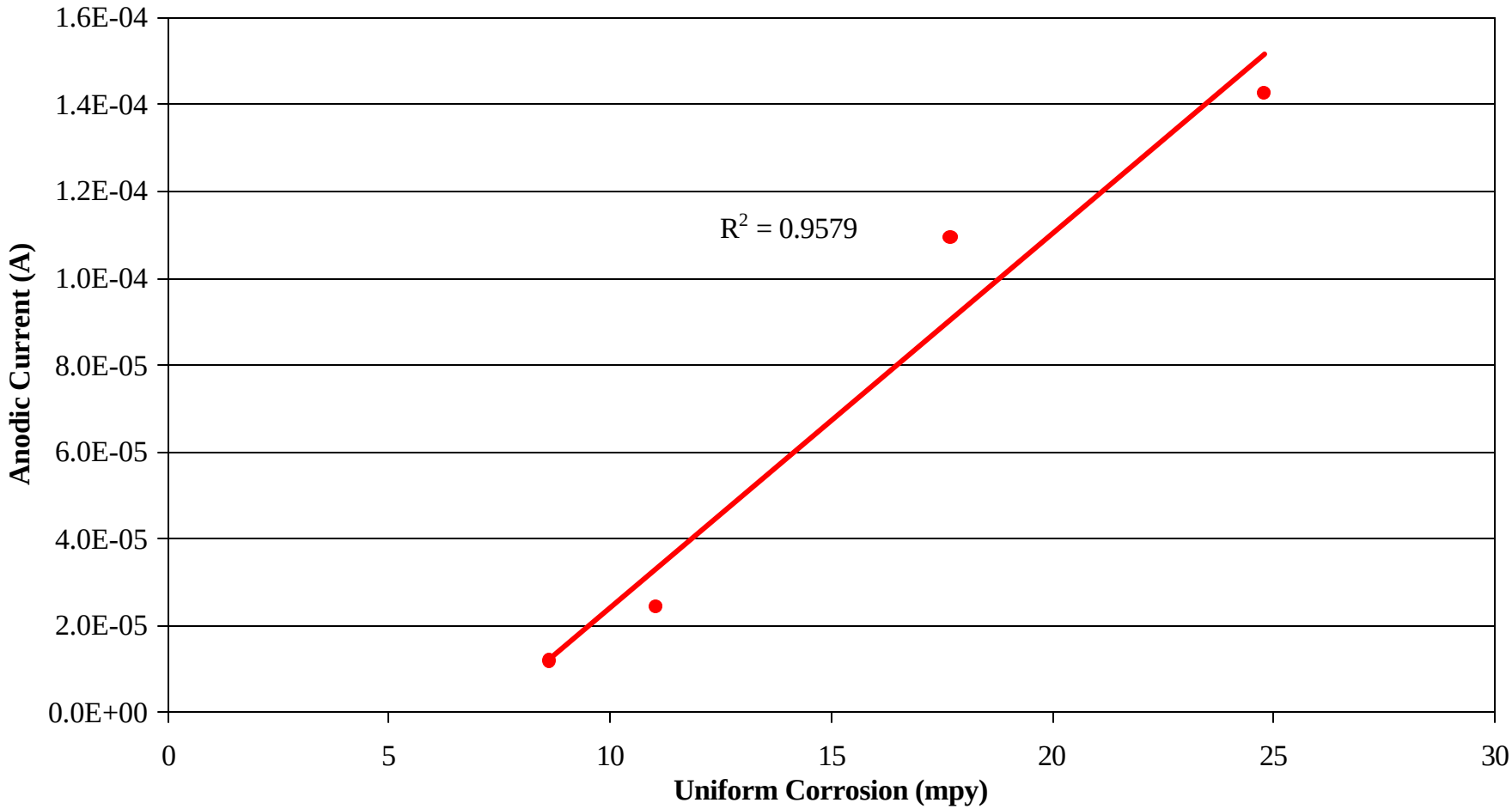

Figure 9 Correlation of average anodic current and the uniform corrosion rate in chemical corrosion environments

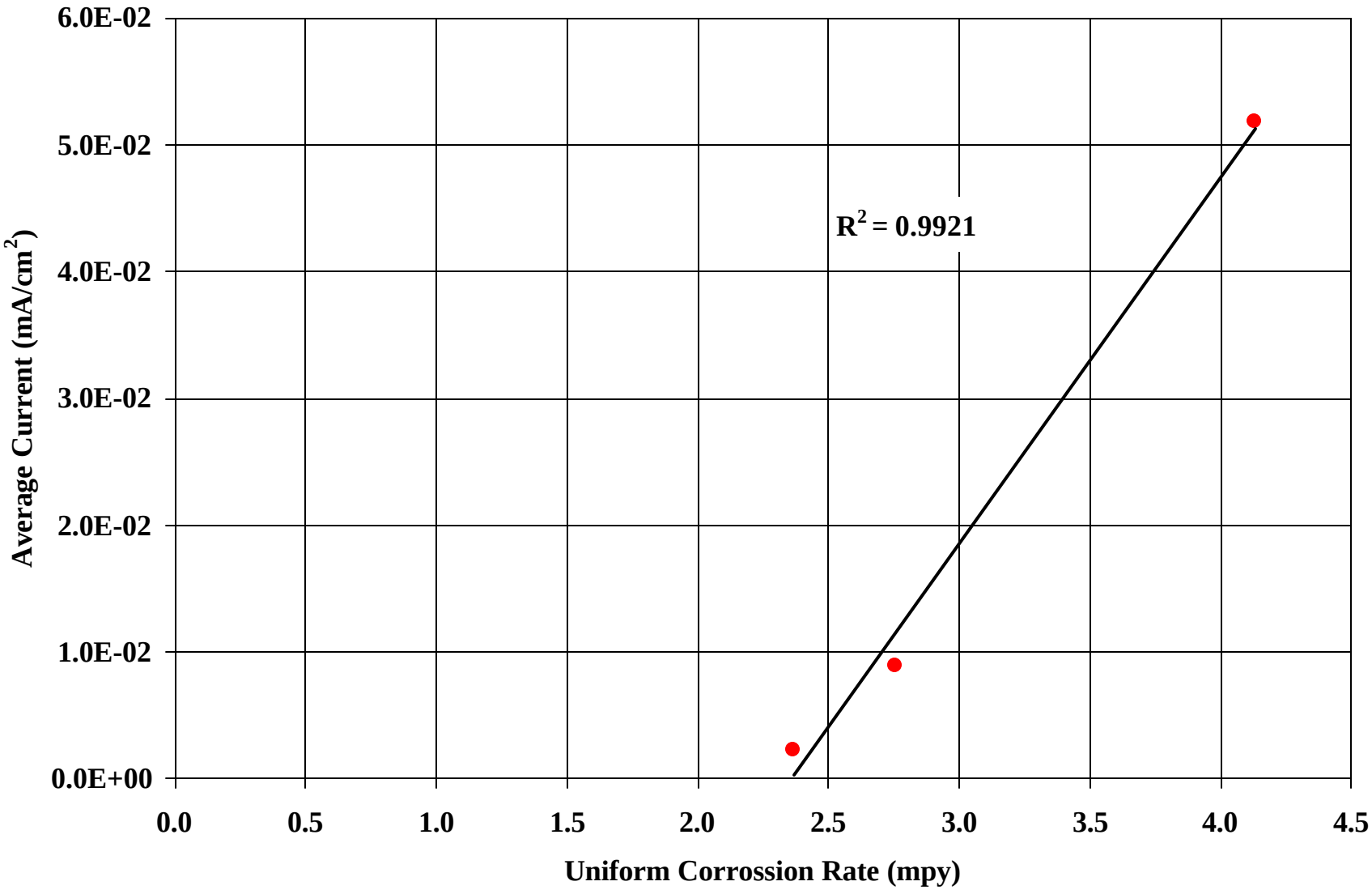

Figure 10 Correlation of average anodic current and the uniform corrosion rate in MIC environments

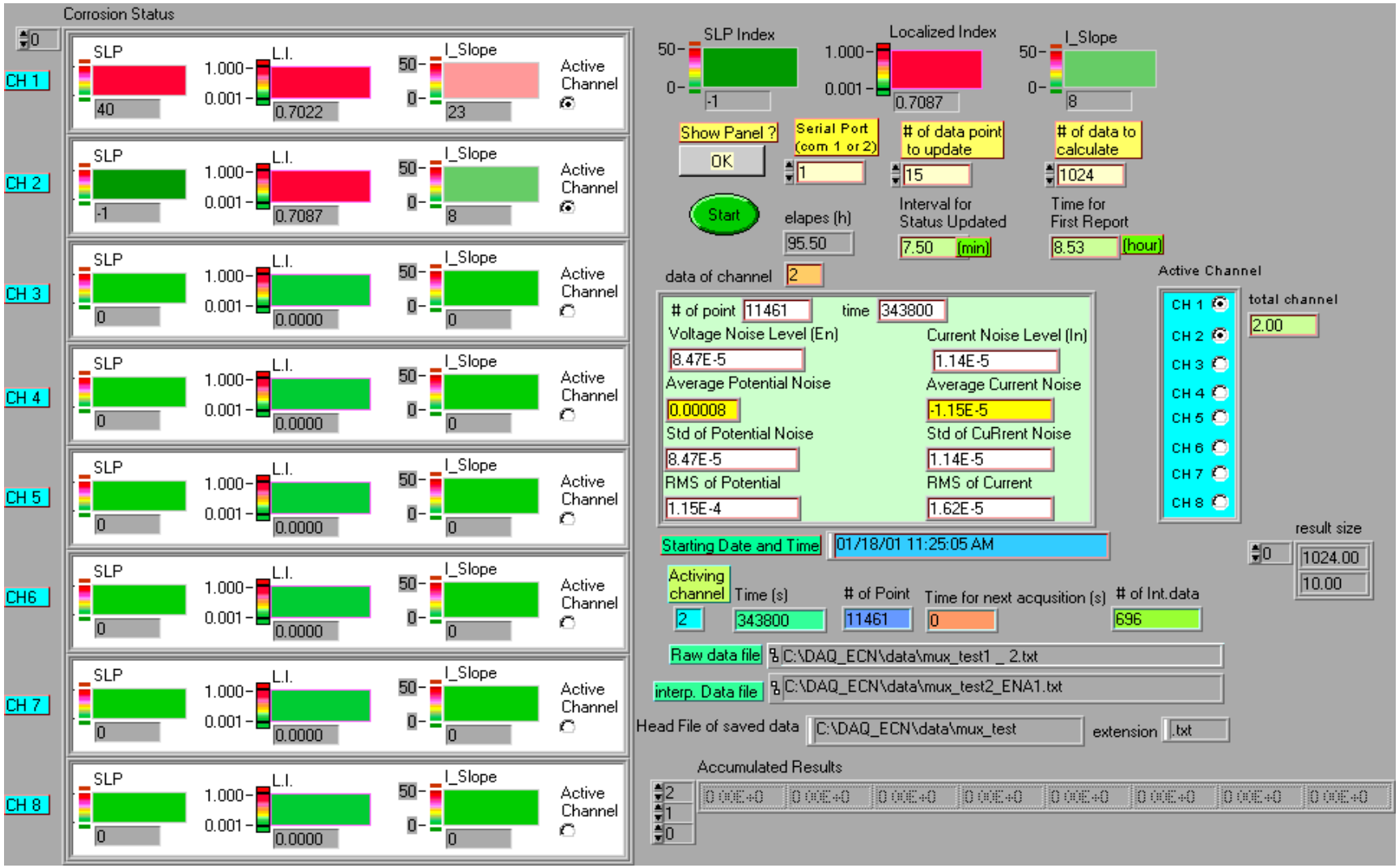

Figure 11 Display Screen of the Automatic ECN analysis System

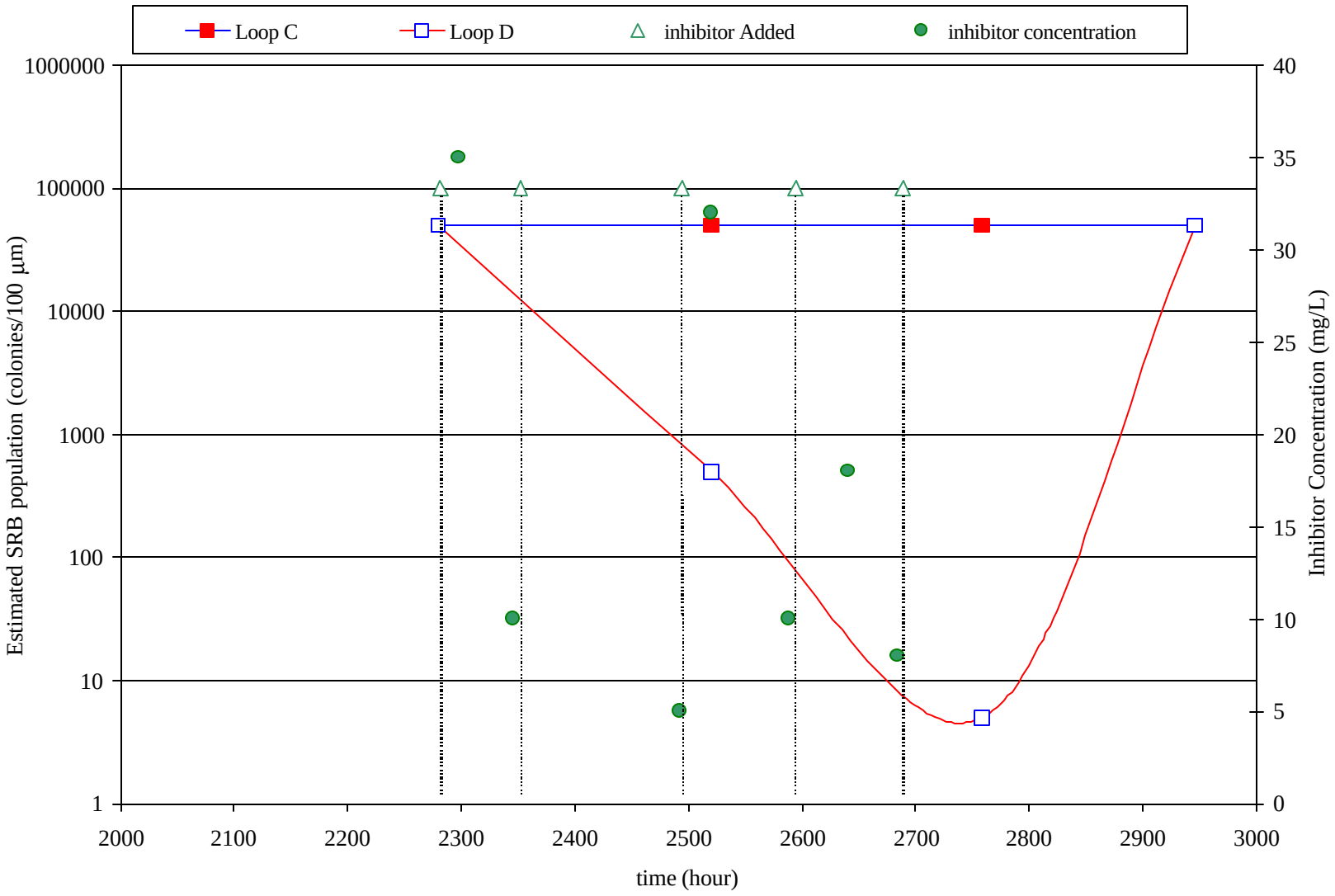

Figure 12 Comparison of SRB and APB population in Loop C and D

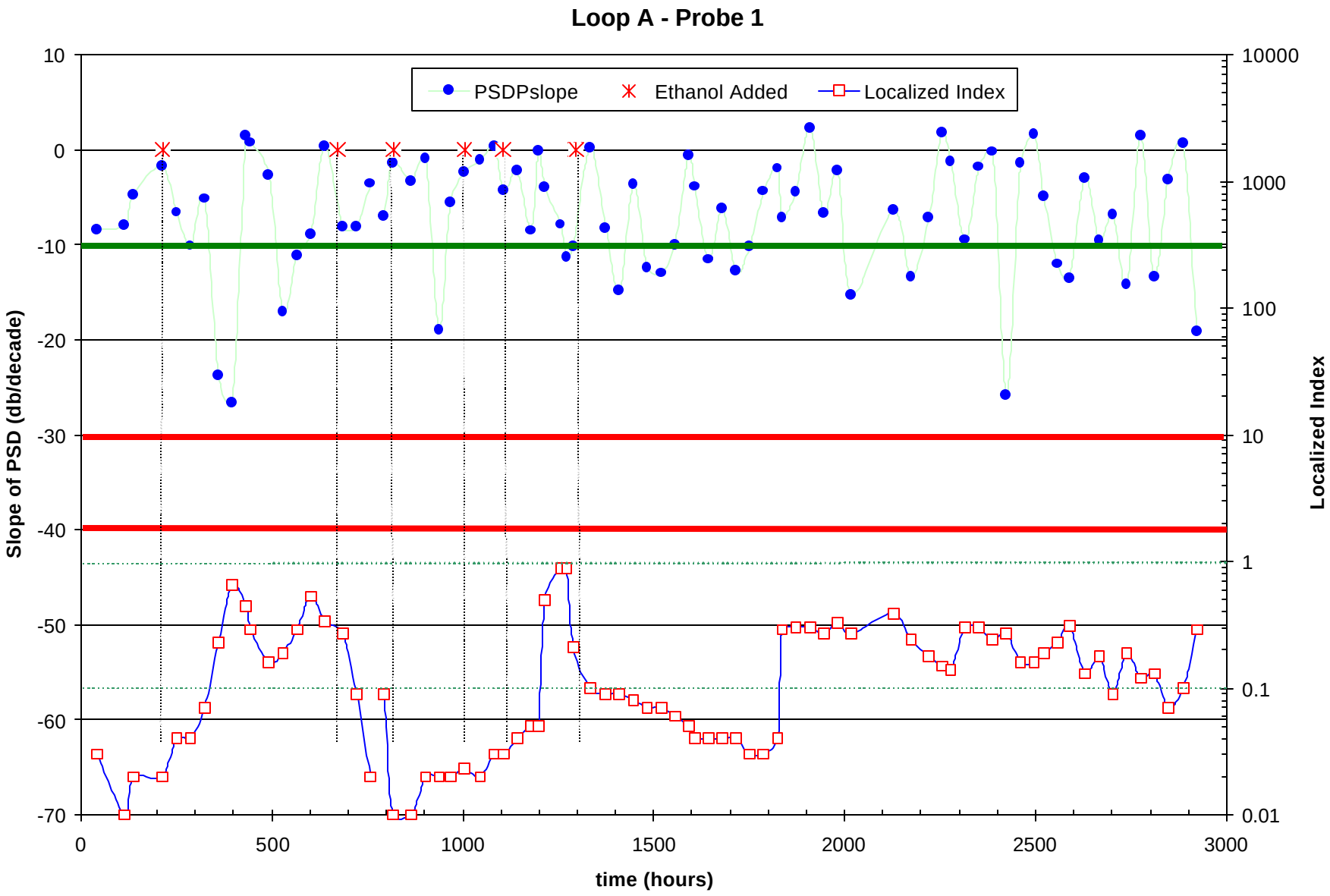

Figure 13 Slope profiles of potential noise level of probe 1 in Loop A

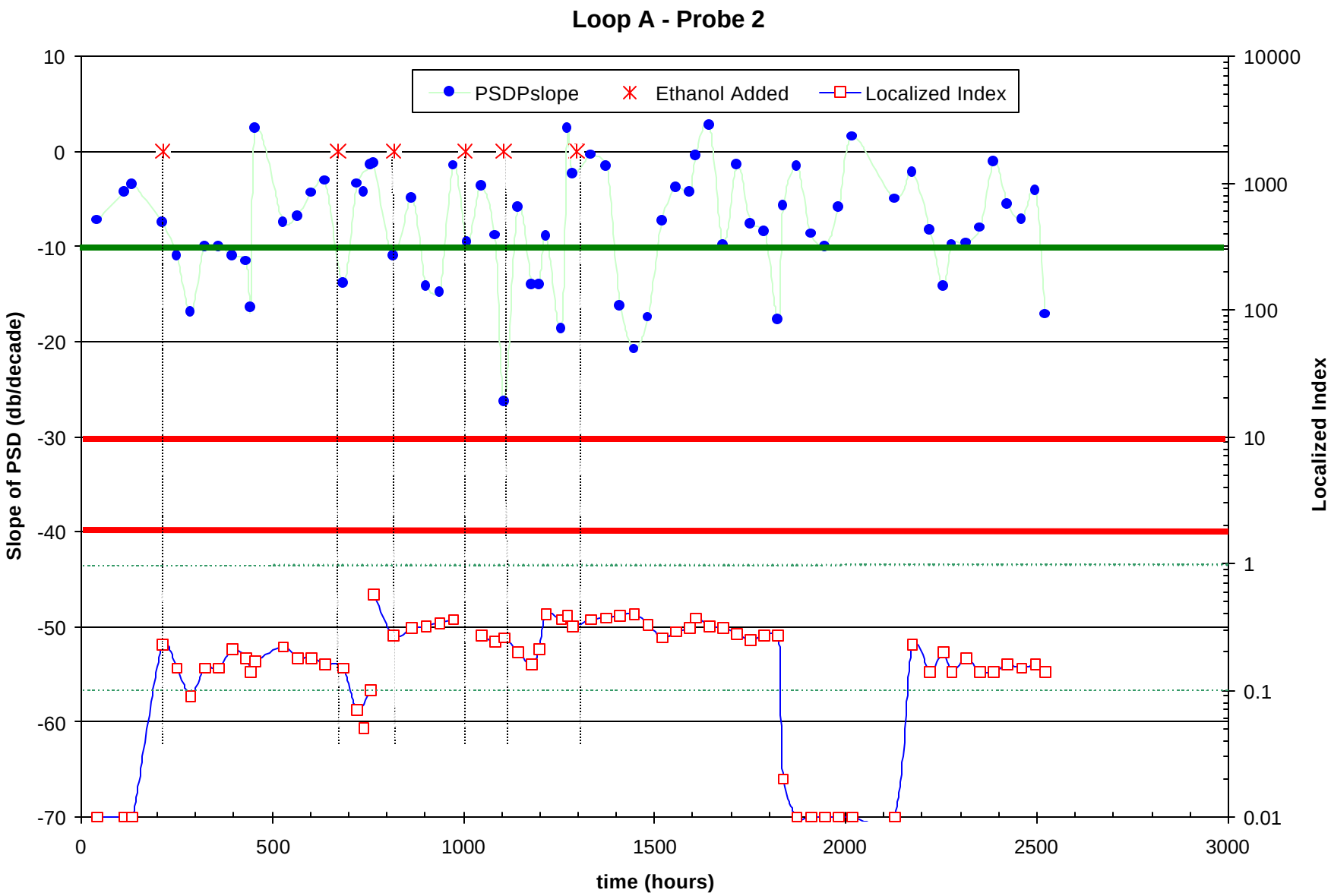

Figure 14 Slope profiles of potential noise level of probe 2 in Loop A

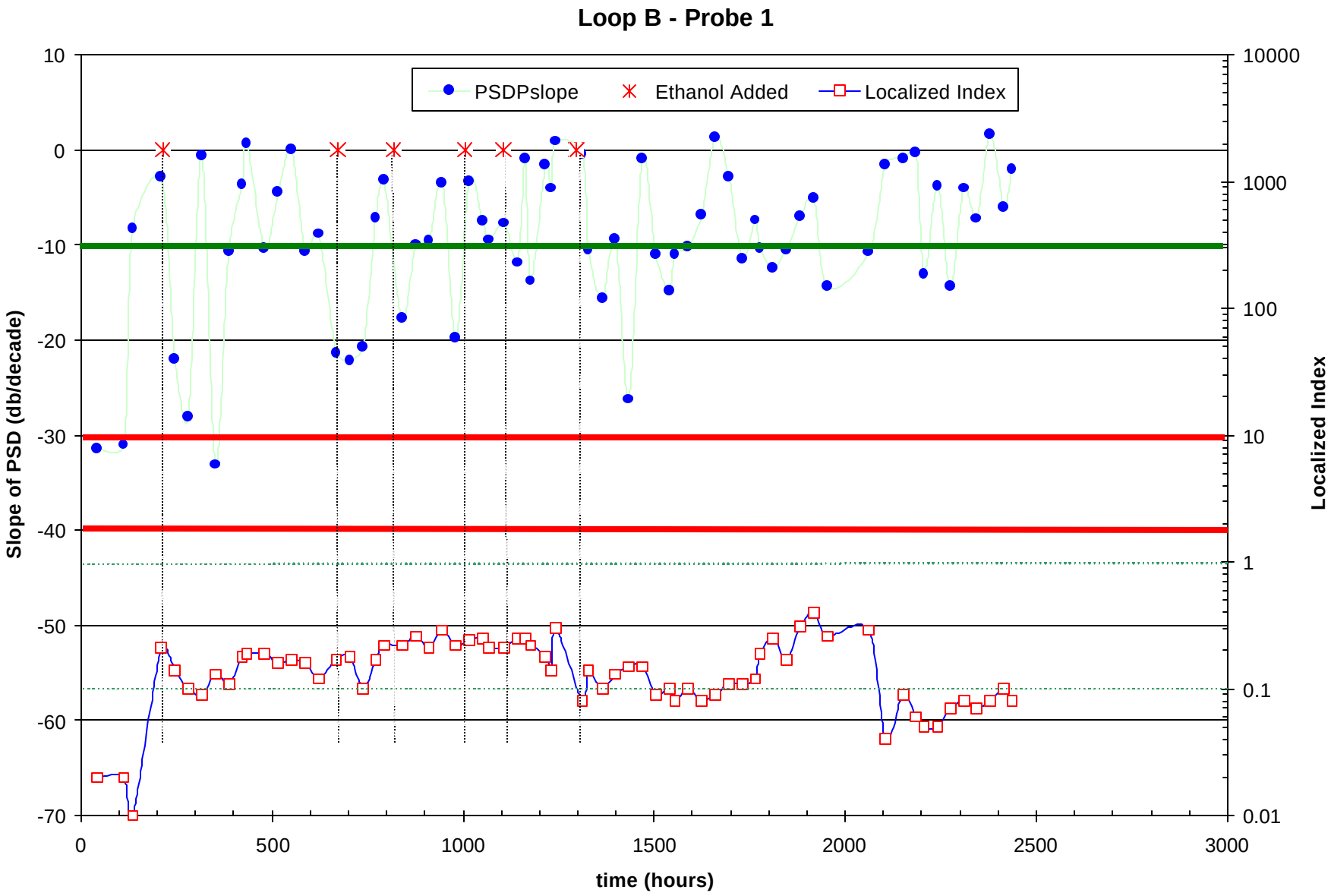

Figure 15 Slope profiles of potential noise level of probe 1 in Loop B

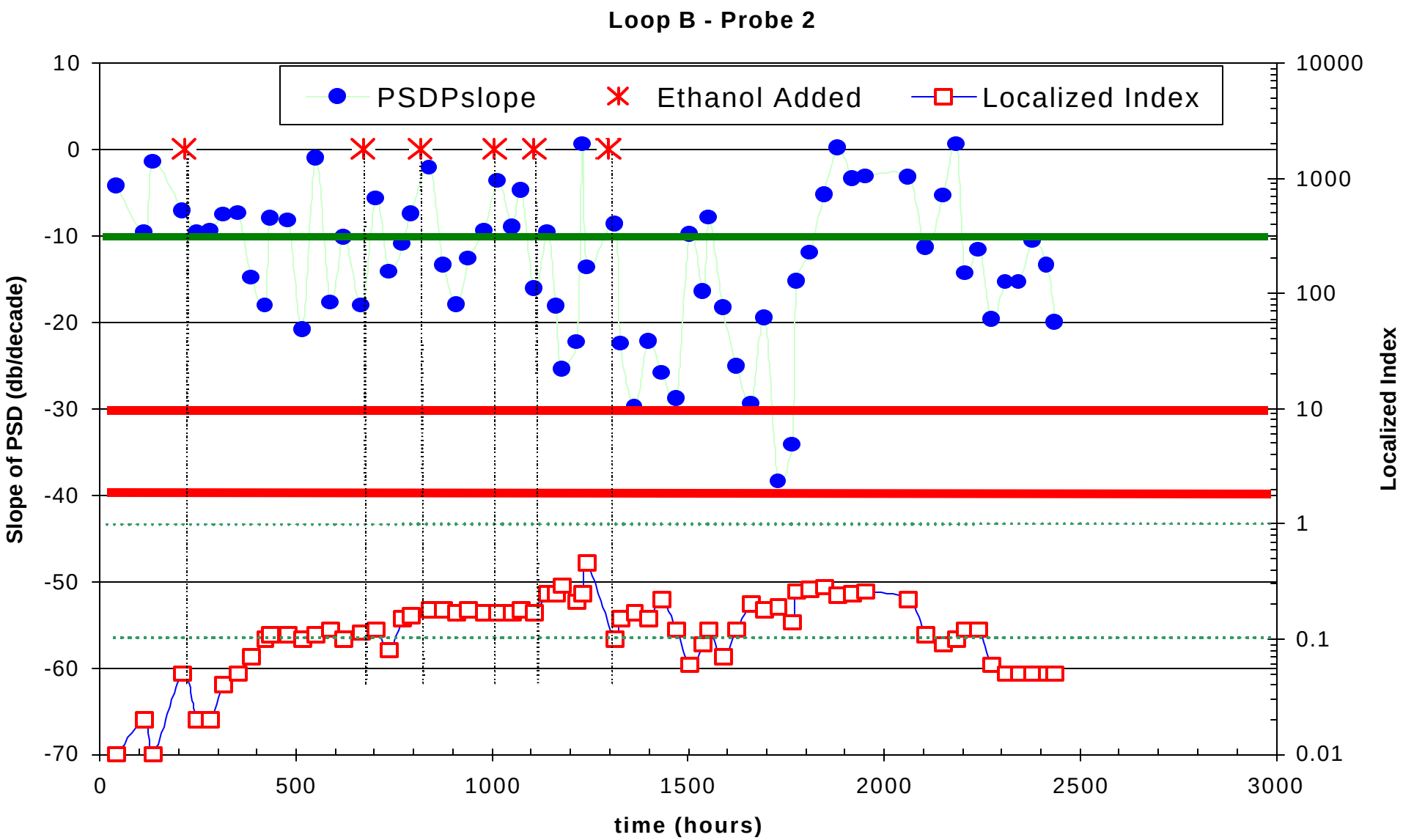

Figure 16 Slope profiles of potential noise level of probe 2 in Loop B

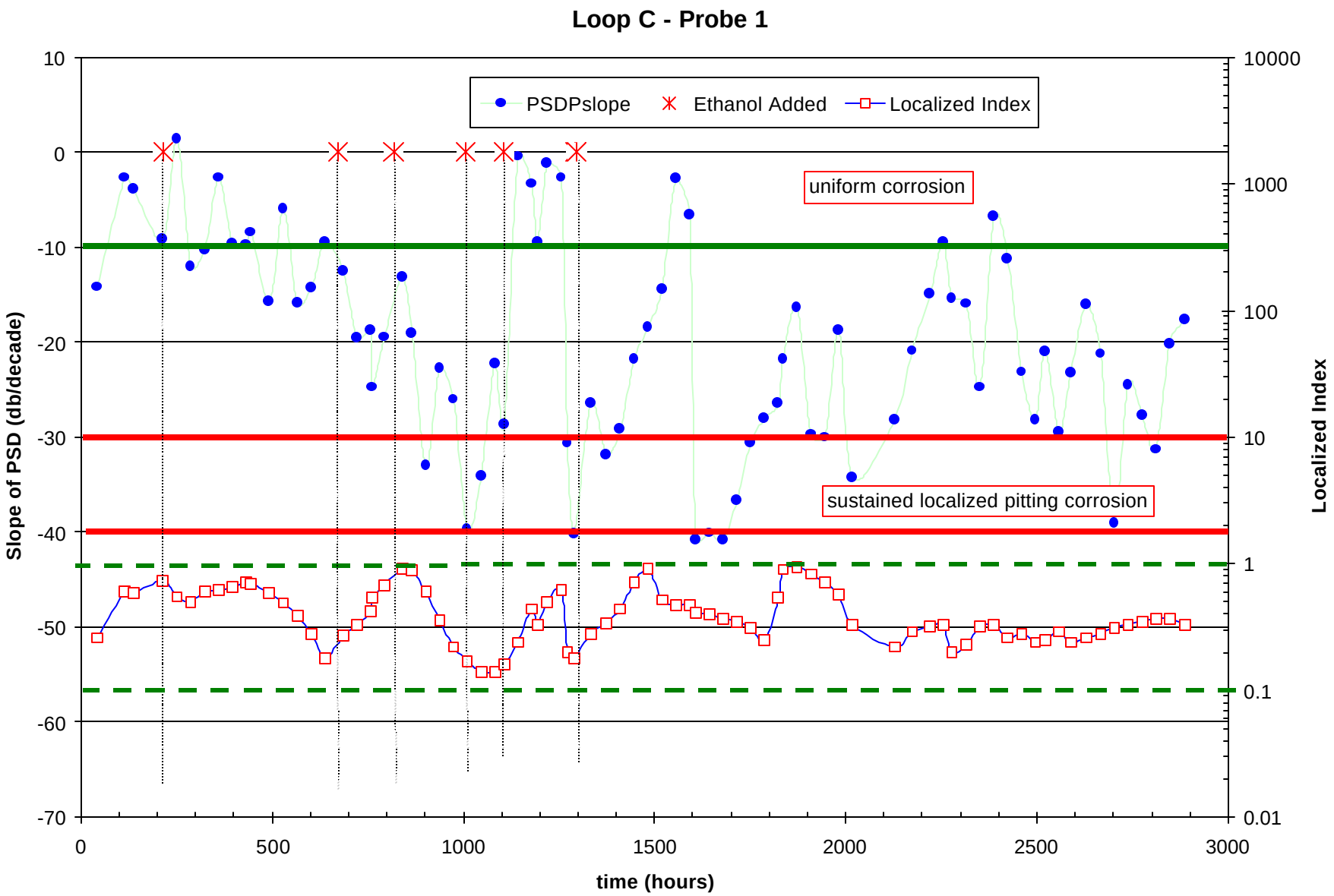

Figure 17 Slope profiles of potential noise level of probe 1 in Loop C

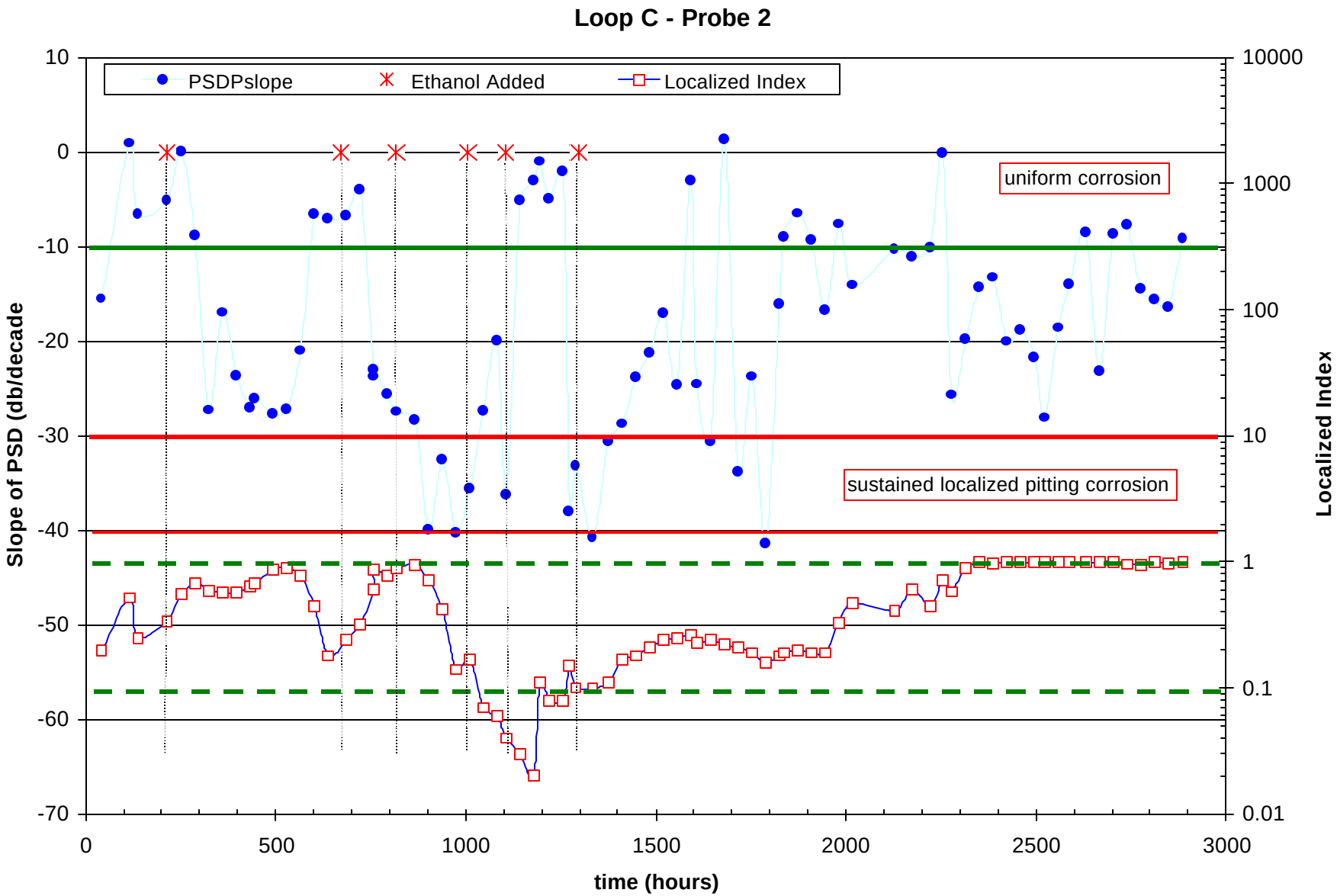

Figure 18 Slope profiles of potential noise level of probe 2 in Loop C

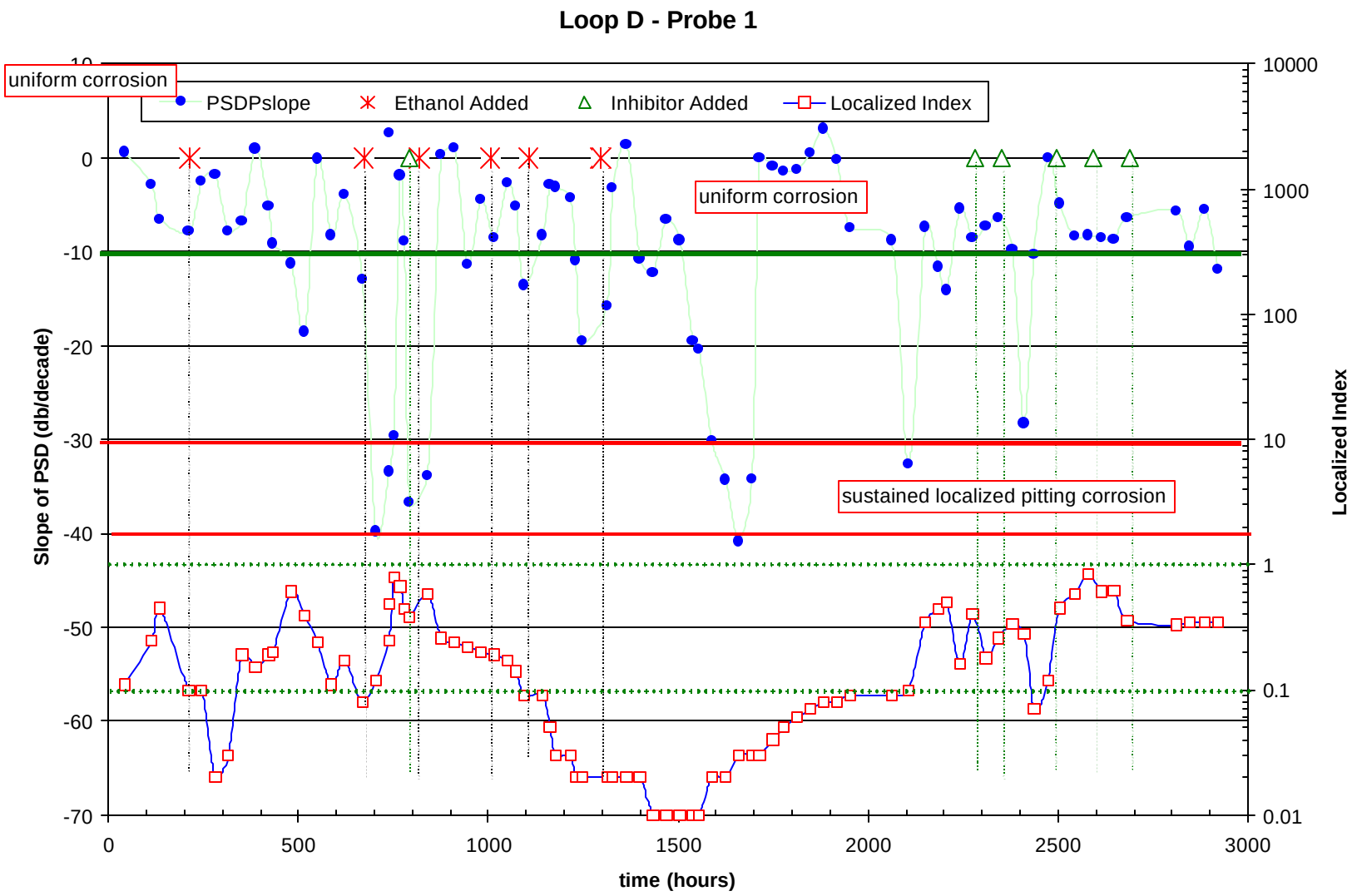

Figure 19 Slope profiles of potential noise level of probe 1 in Loop D

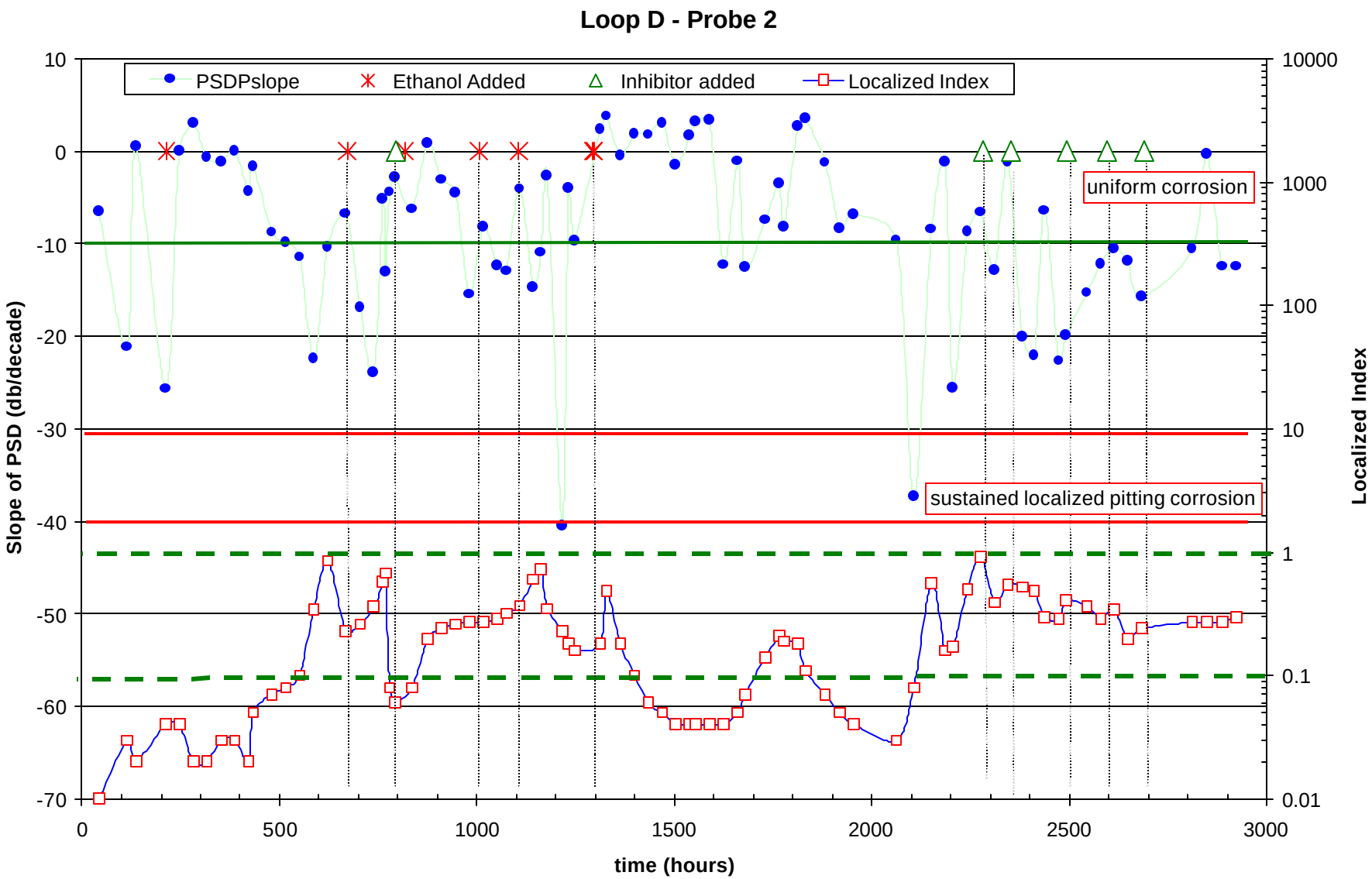

Figure 20 Slope profiles of potential noise level of probe 1 in Loop D

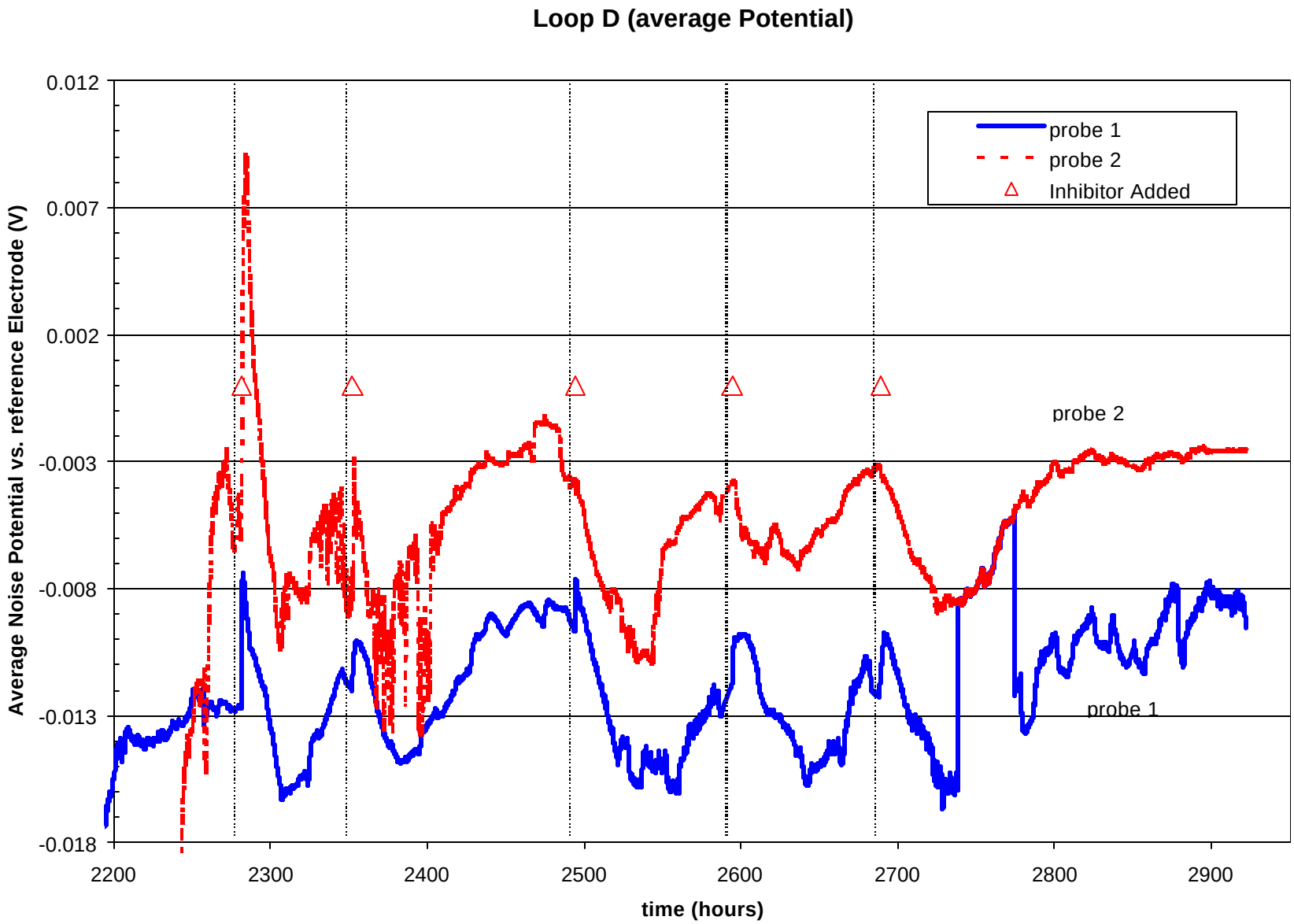

Figure 21 Average potentials of ECN probe

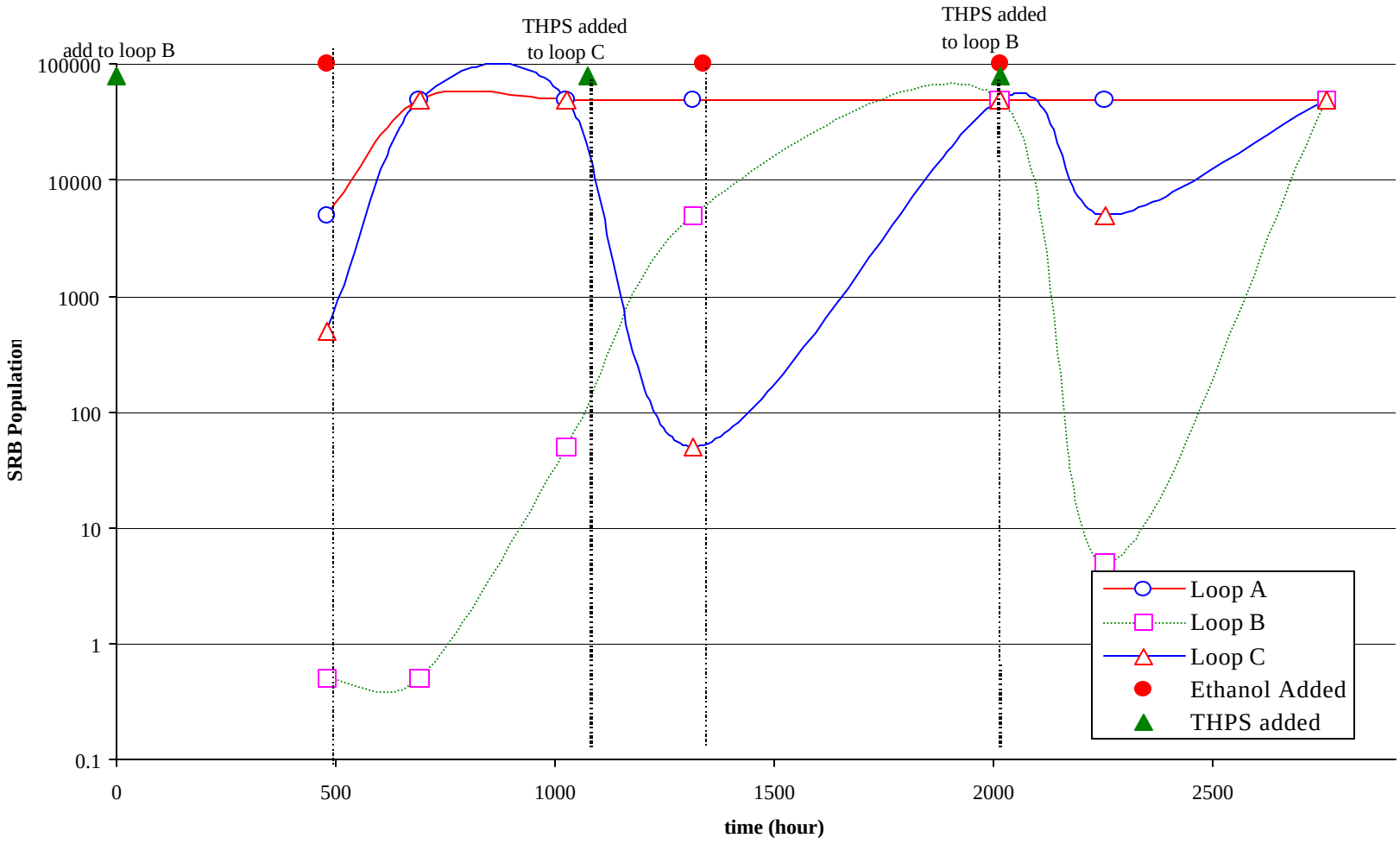

Figure 22 The population of SRB in the liquid of each loops

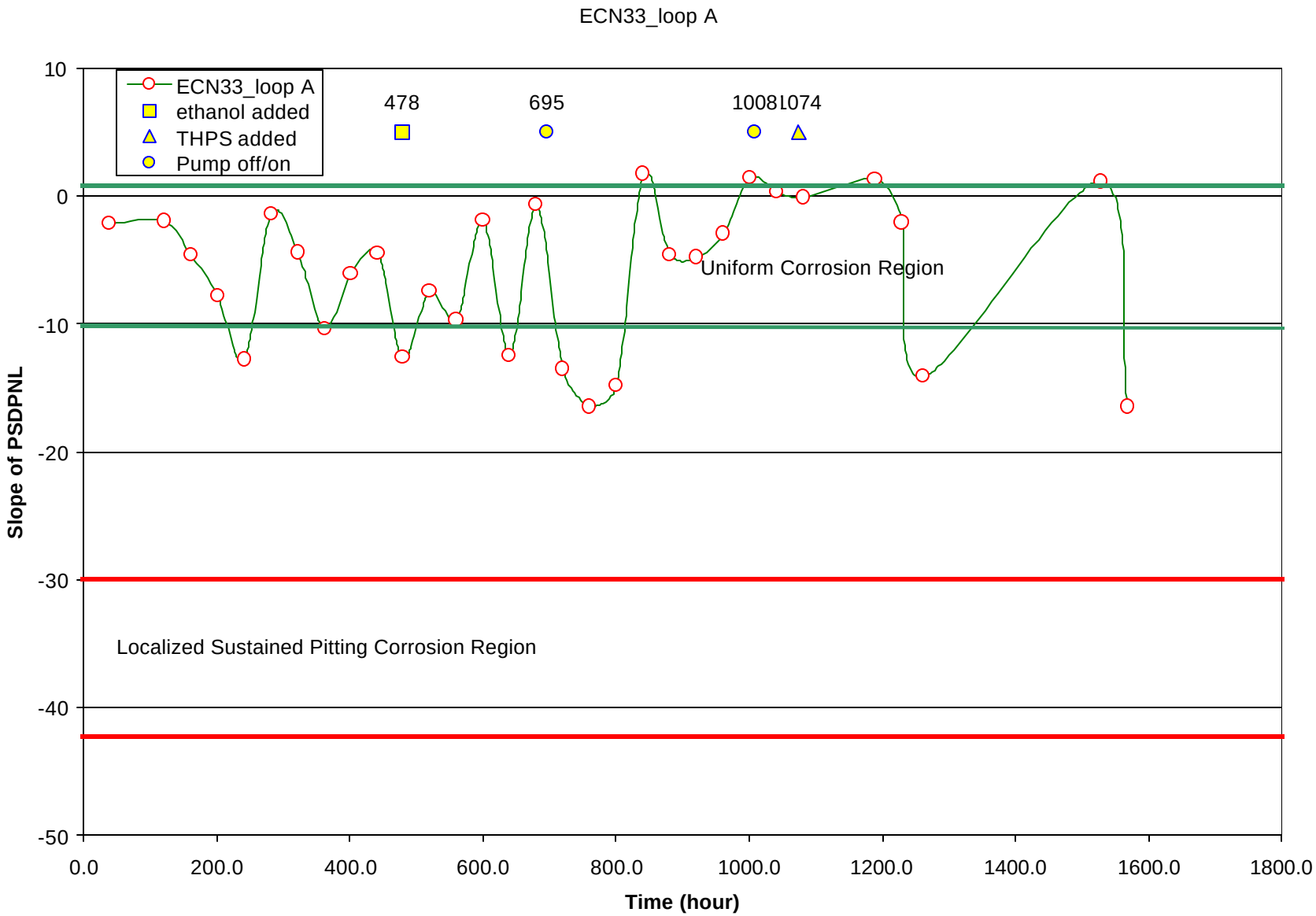

Figure 23 The slope profile of the PSDPNL of ECN probe in Loop A

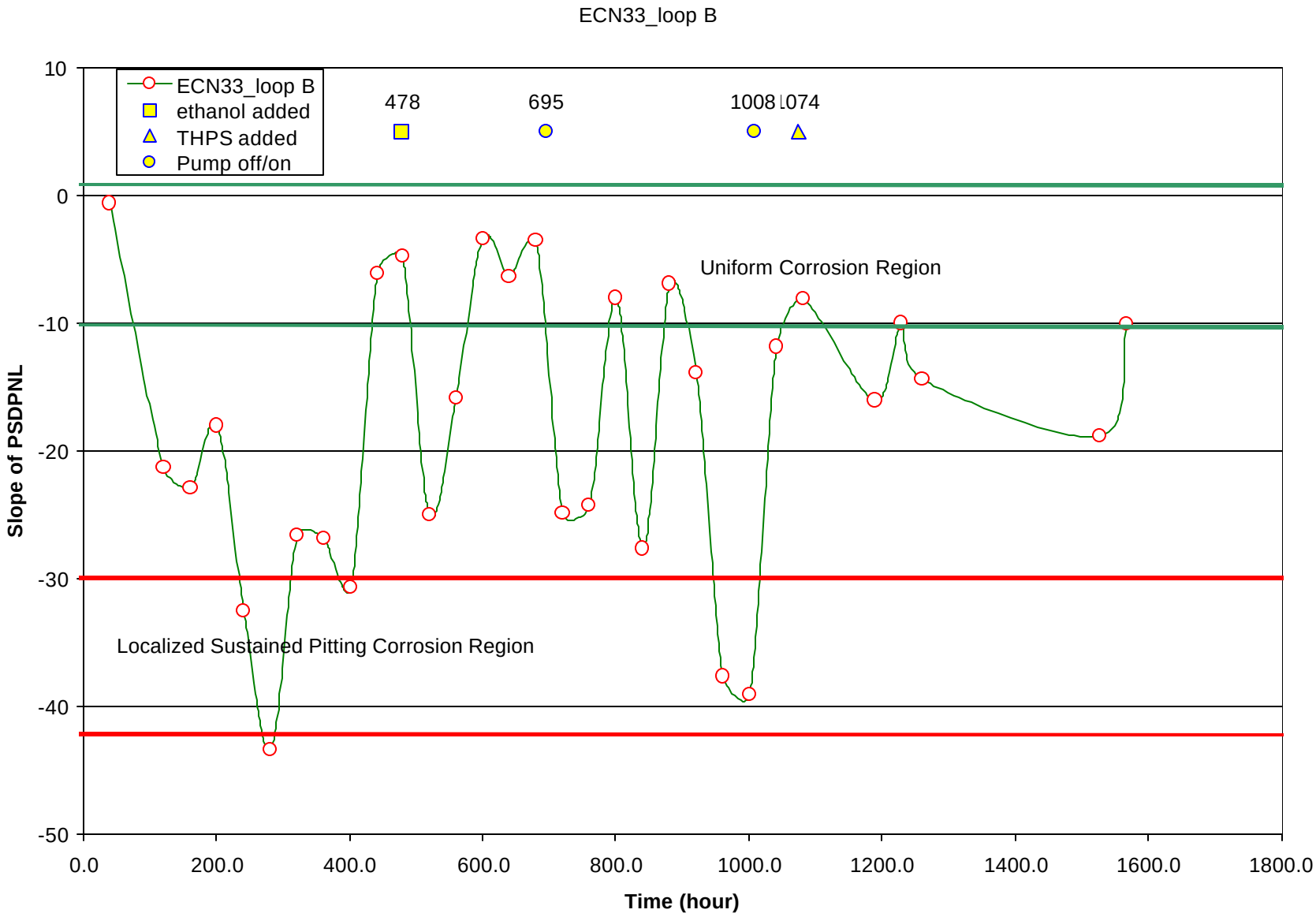

Figure 24 The slope profile of the PSDPNL of ECN probe in Loop B

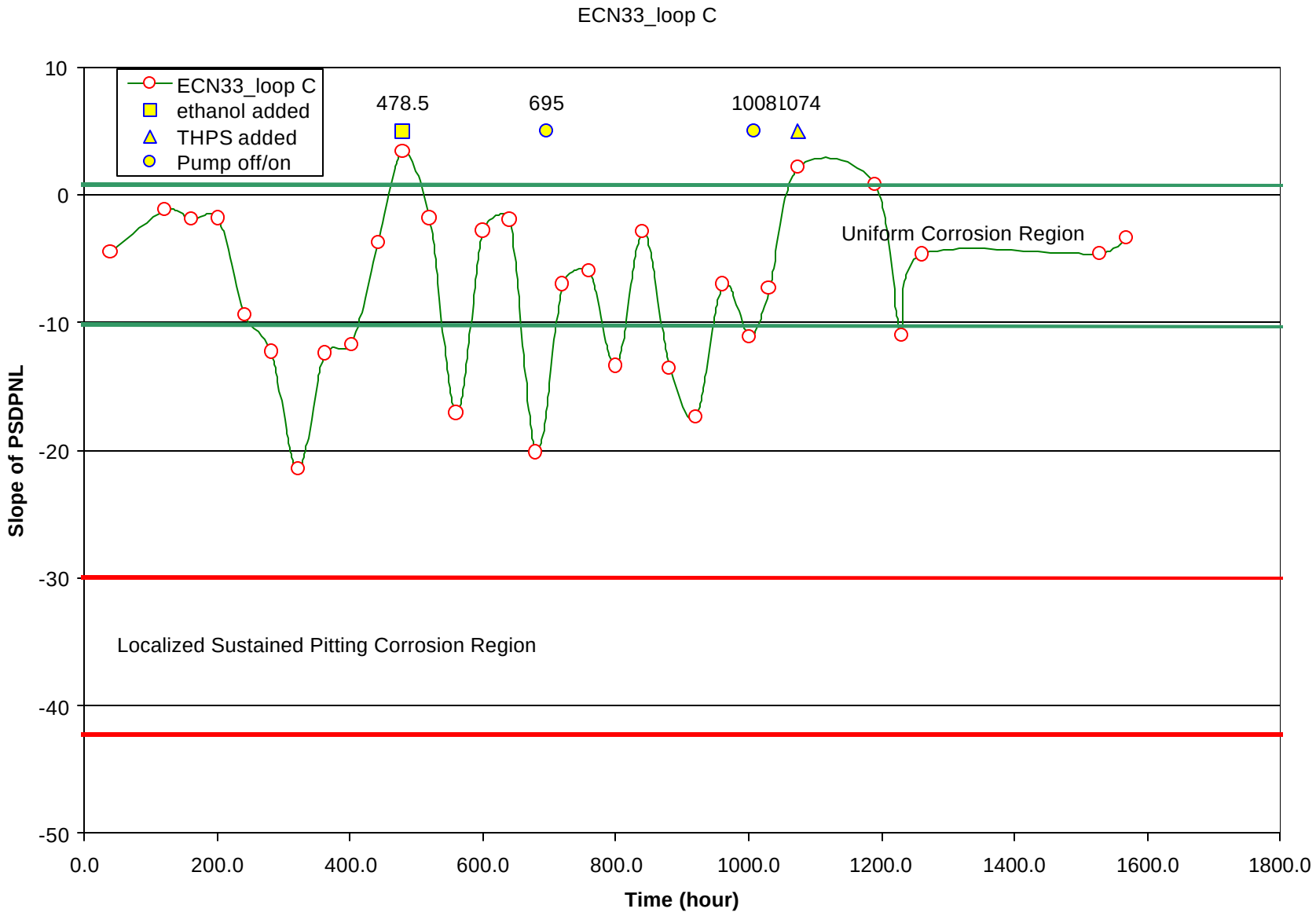

Figure 25 The slope profile of the PSDPNL of ECN probe in Loop C

ECN probe used in the field test

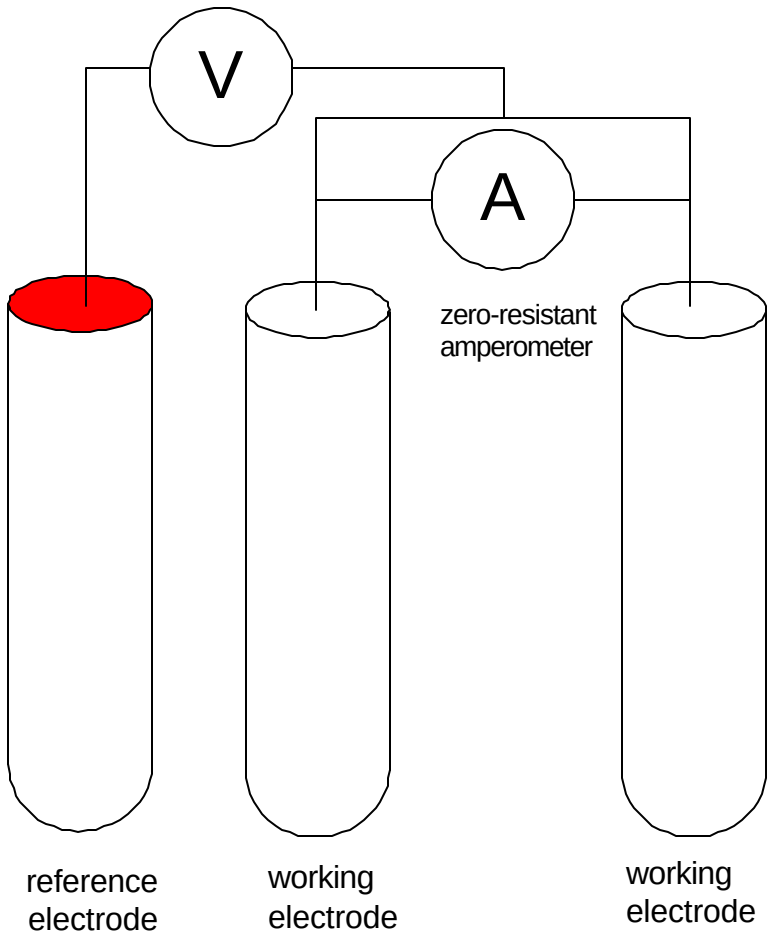

Figure 26 Three electrodes system with zero-resistant ampermetor (a computer plug-in potentiostat). Carbon steel was used in the two working electrodes and the reference electrode was a Hastalloy

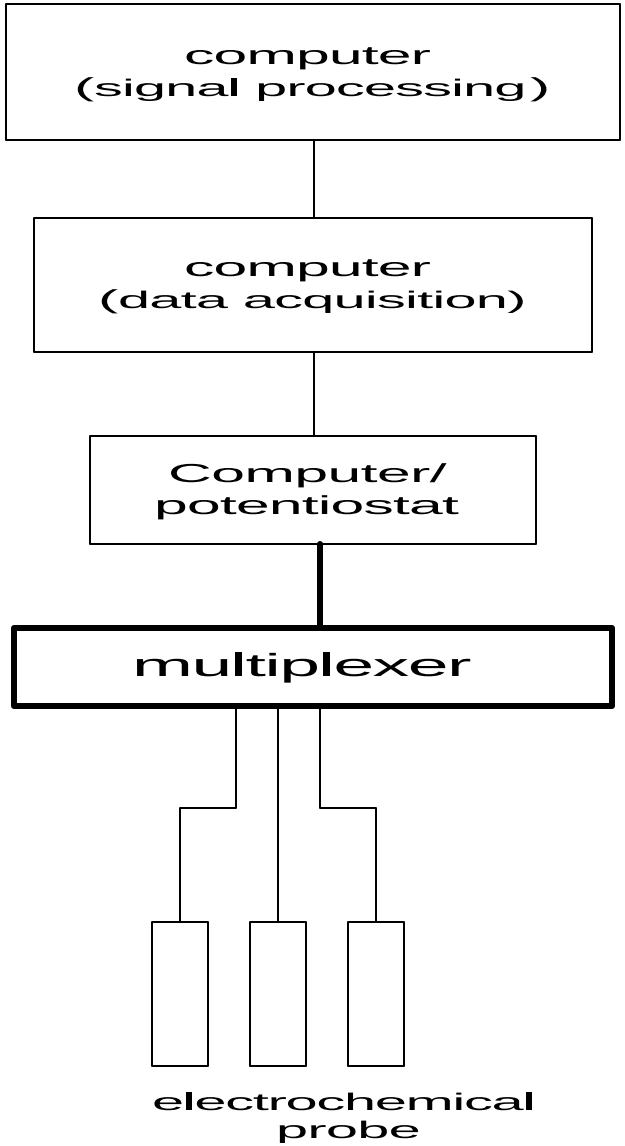

Figure 27 Schematic of the field unit for ECN measurement

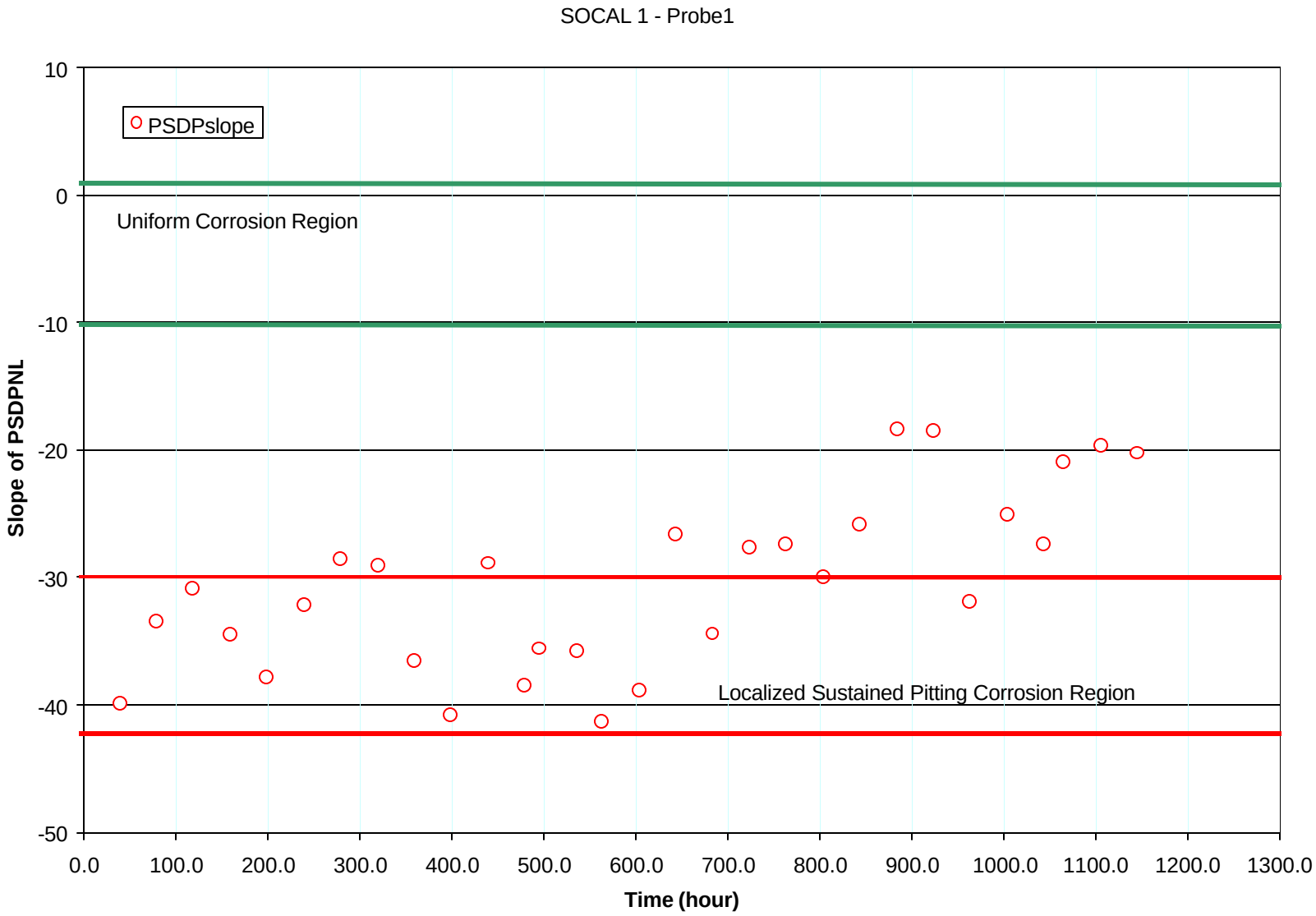

Figure 28 (a) Slope Profile of PSDPNL of Probe 1 from the First Location

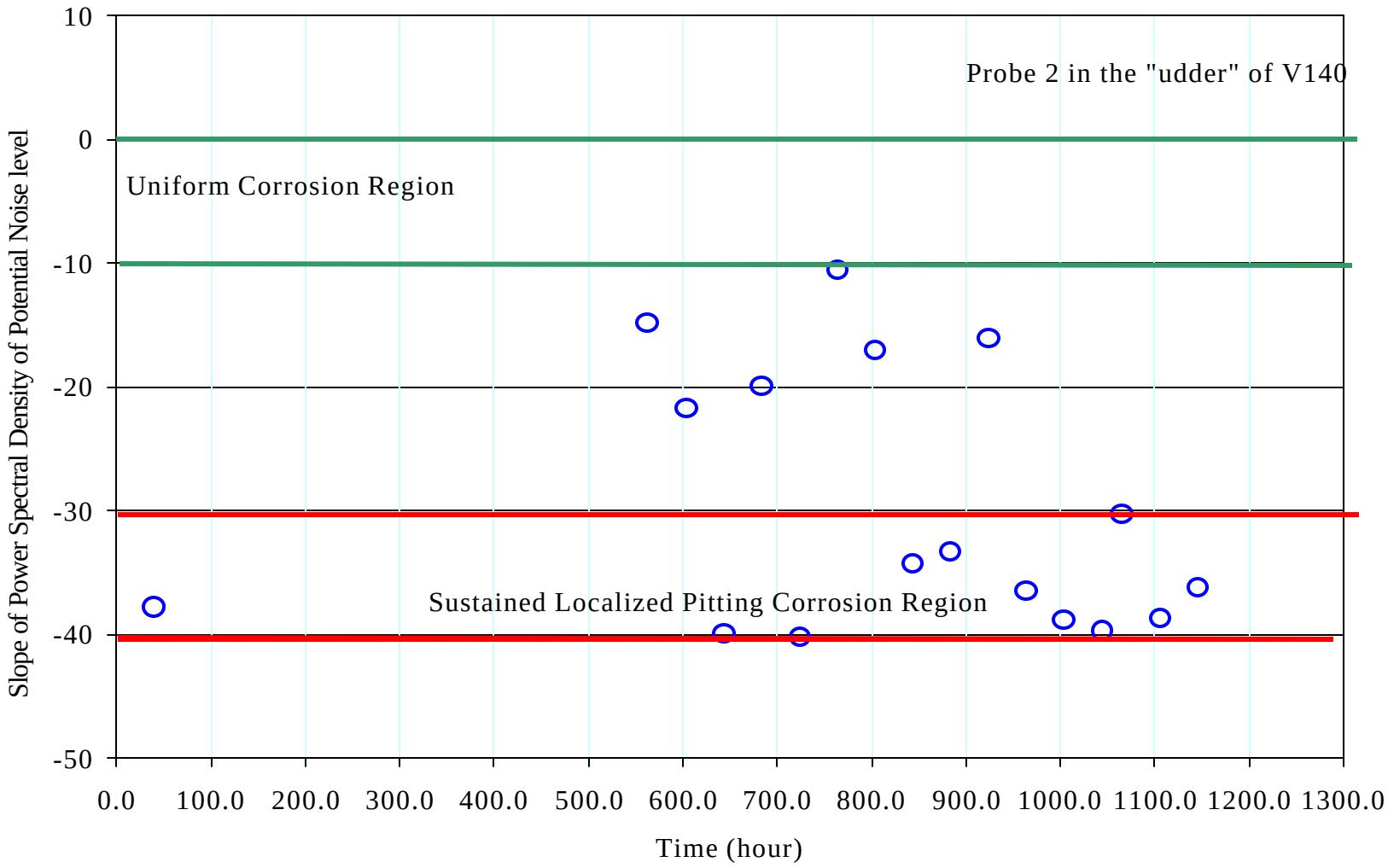

Figure 28(b) Slope Profile of PSDPNL of Probe 2 from the First Location

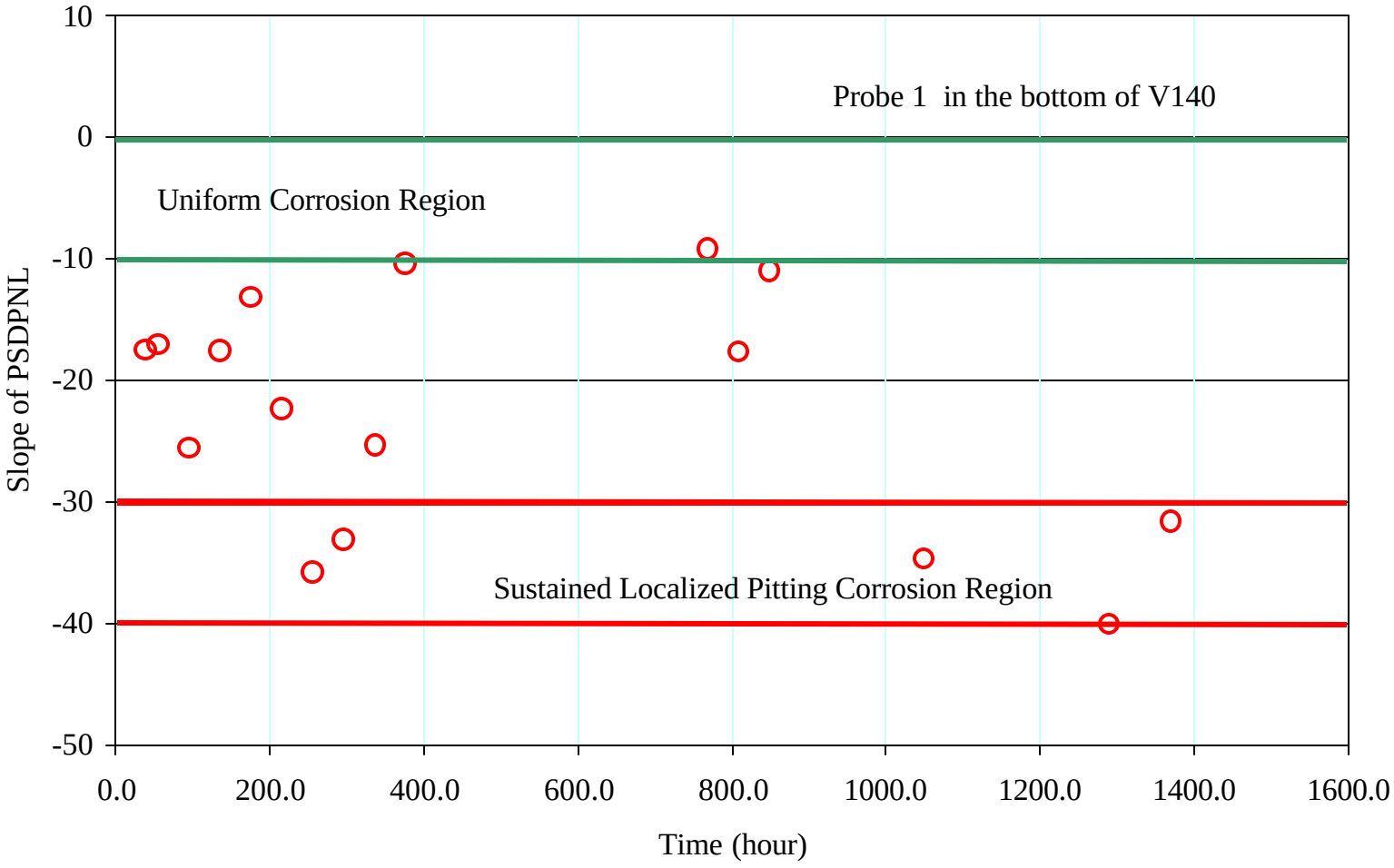

Figure 29 Slope Profile of PSDPNL of Probe #1 from the Second Location

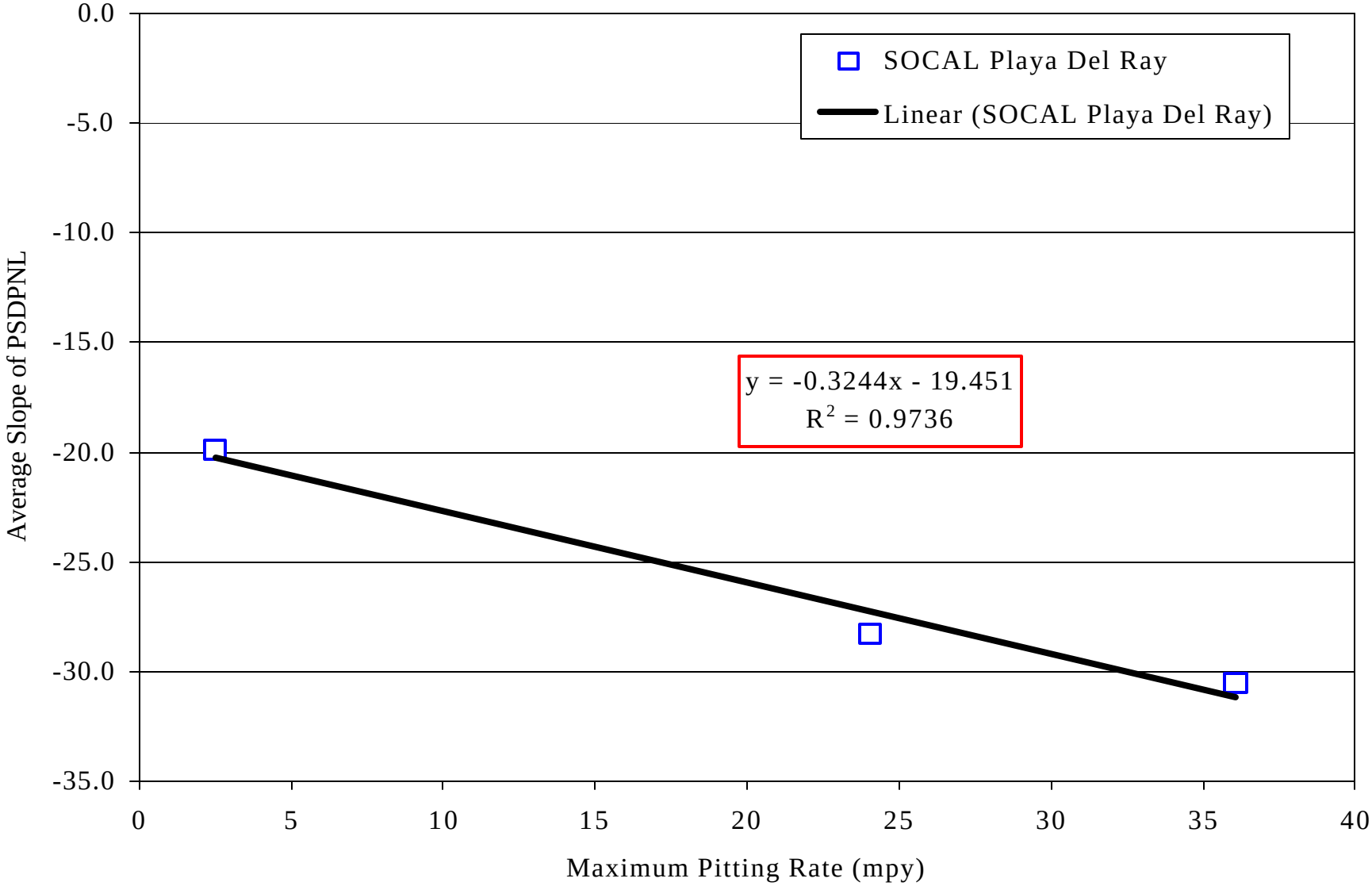

Figure 30 Correlations of the Average Slopes of PSDPNL and the Maximum Pitting Rate.

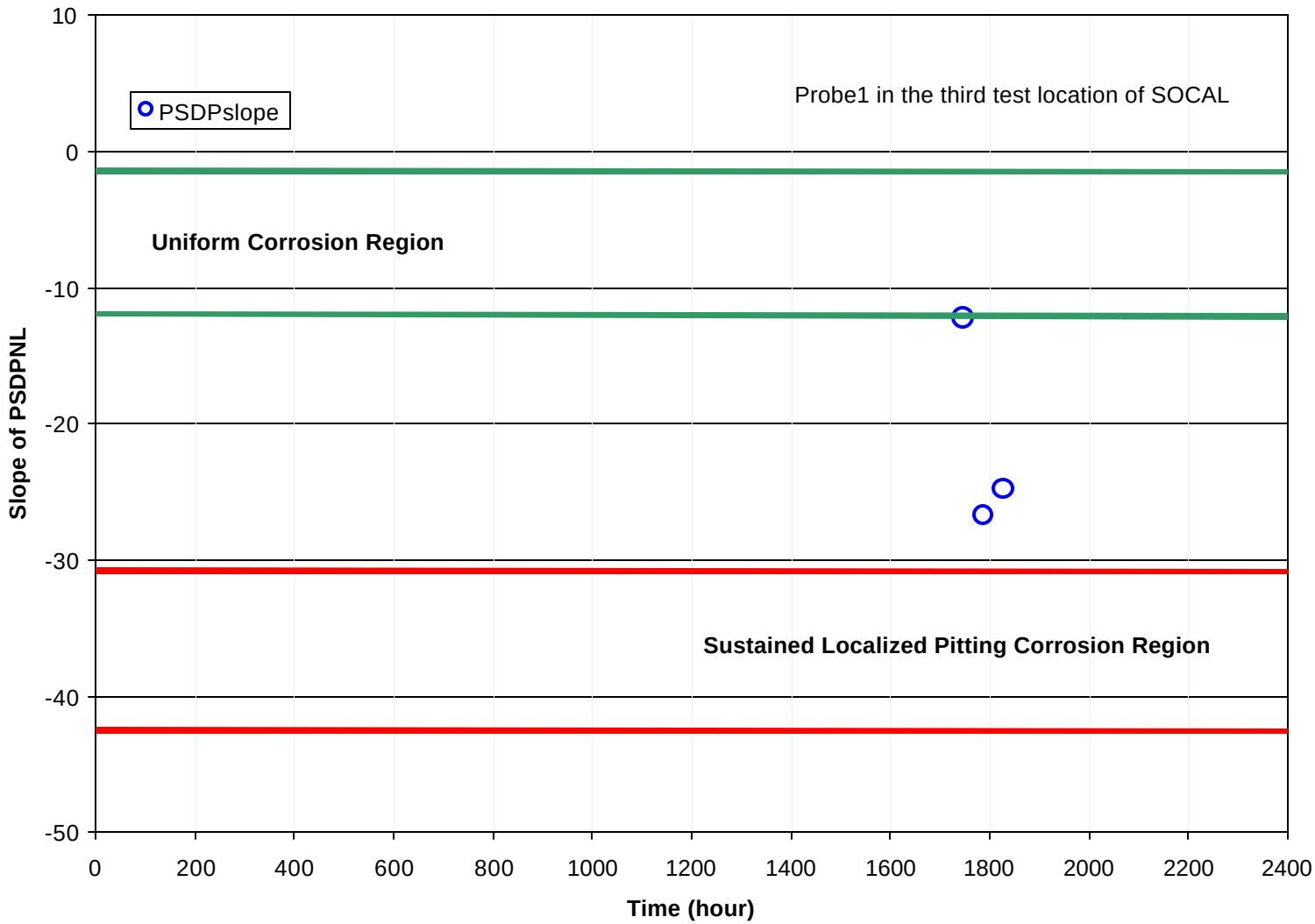

Figure 31 (a) Slope Profile of PSDPNL of Probe #1 from the Third Location

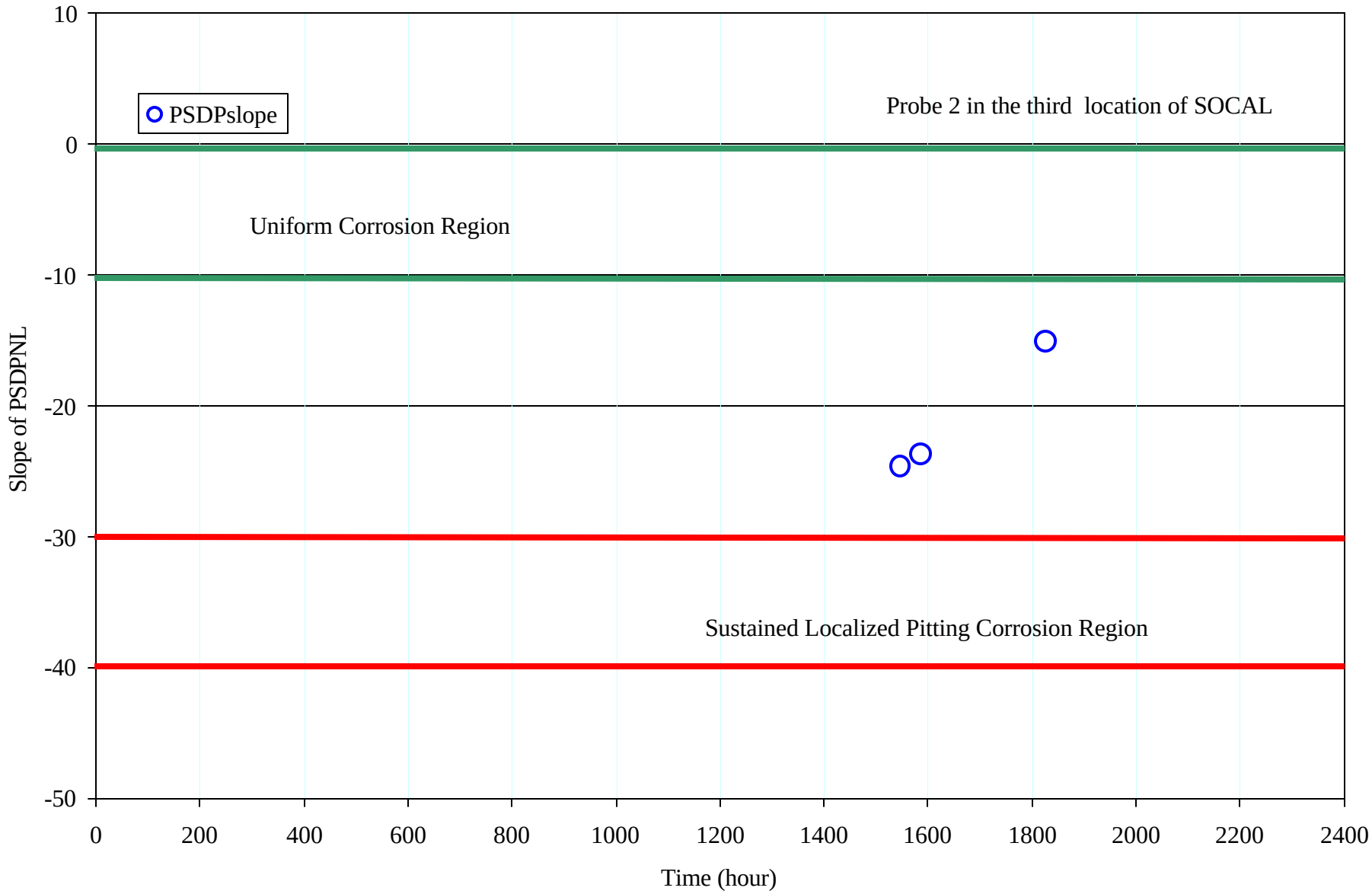

Figure 31(b) Slope Profile of PSDPNL of Probe #2 from the Third Location

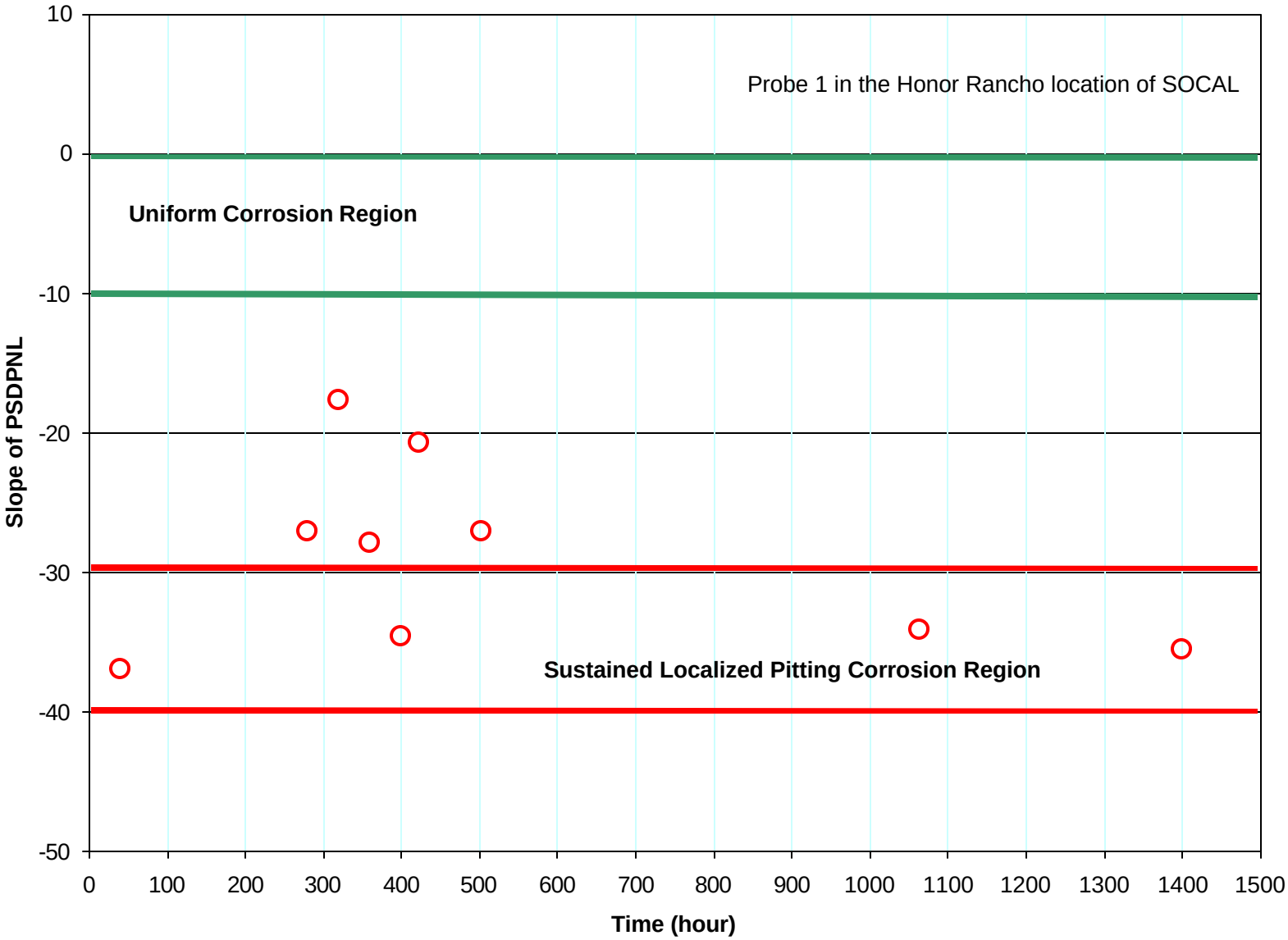

Figure 32(a) Slope Profile of PSDPNL of Probe #1 from the Honor Rancho Location

Figure 32(b) Slope Profile of PSDPNL of Probe #2 from the Honor Rancho Location

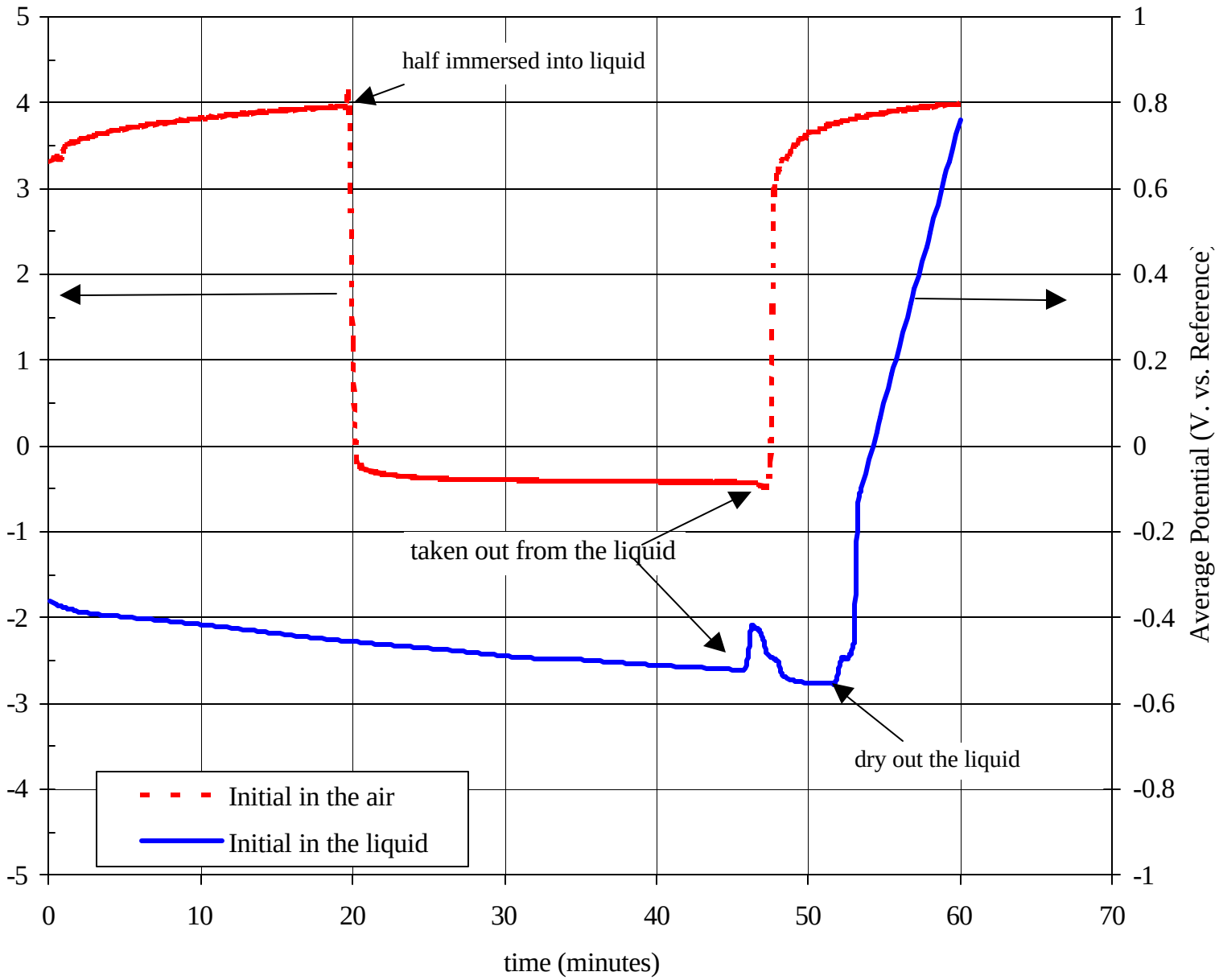

Figure 33 Effects of Liquid Levels on the Potential Readings

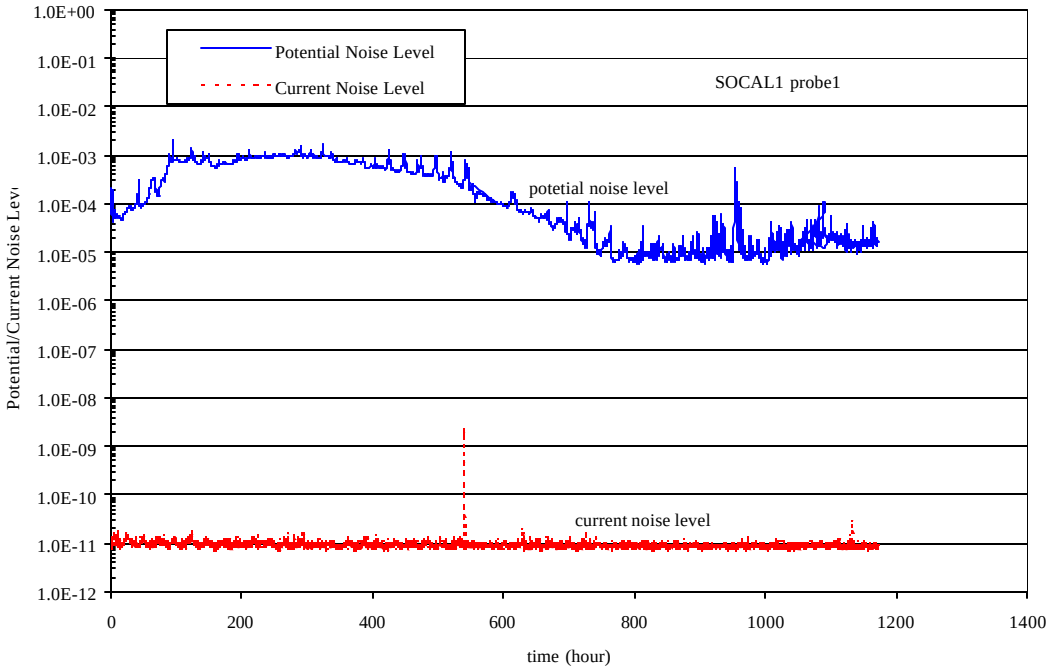

Figure C-1 (a) Potential and current noise level of probe #1 in the bottom of V140

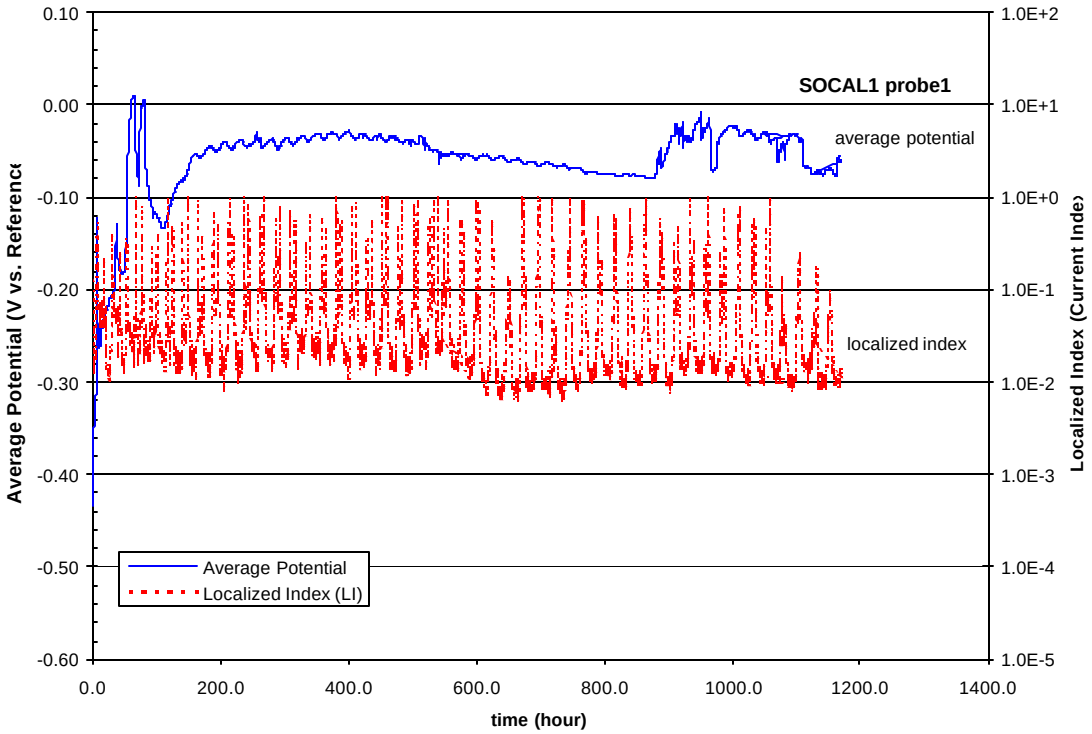

Figure C-1 (b) Average potential and localized index of probe #1 in the bottom of V140

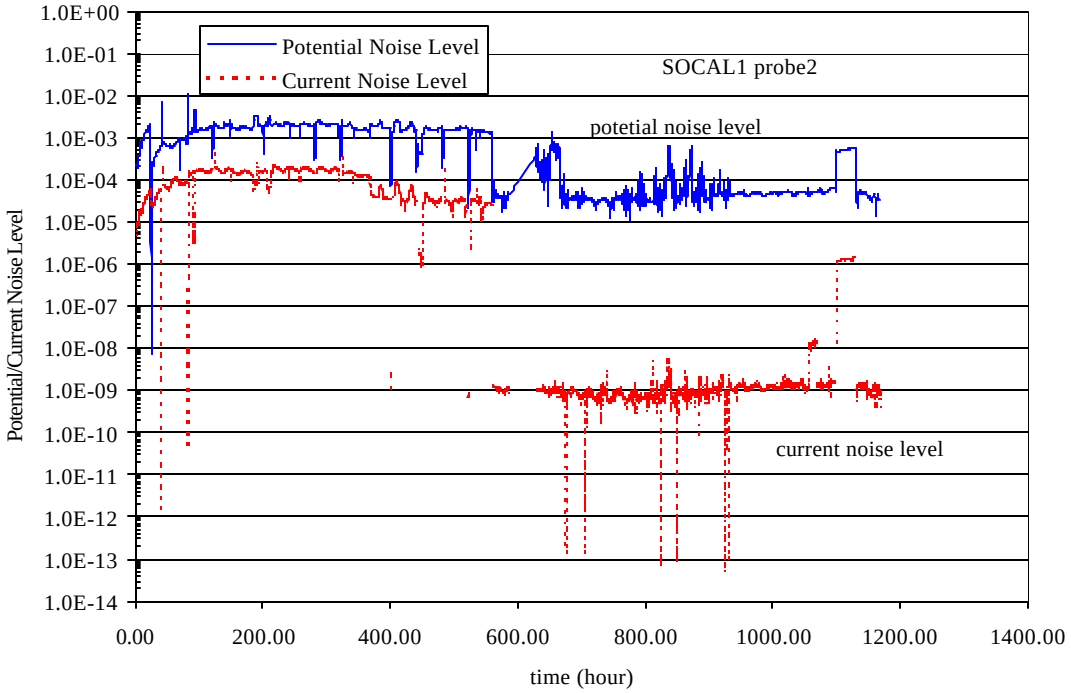

Figure C-2 (a) Potential and current noise level of probe #2 in the bottom of V140

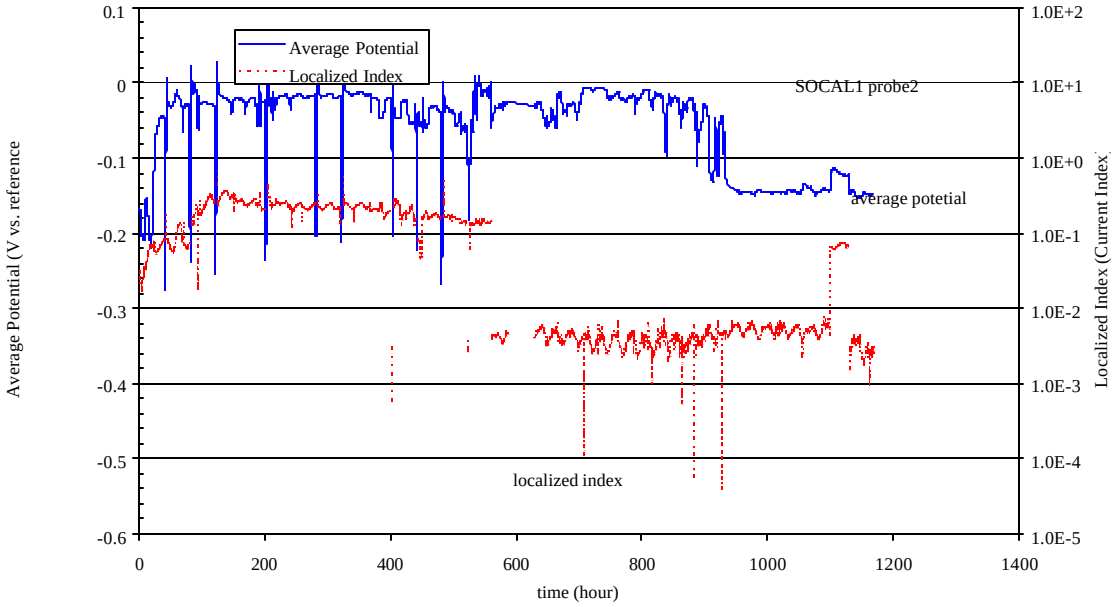

Figure C-2 (b) Average potential and localized index of probe #2 in the bottom of V140

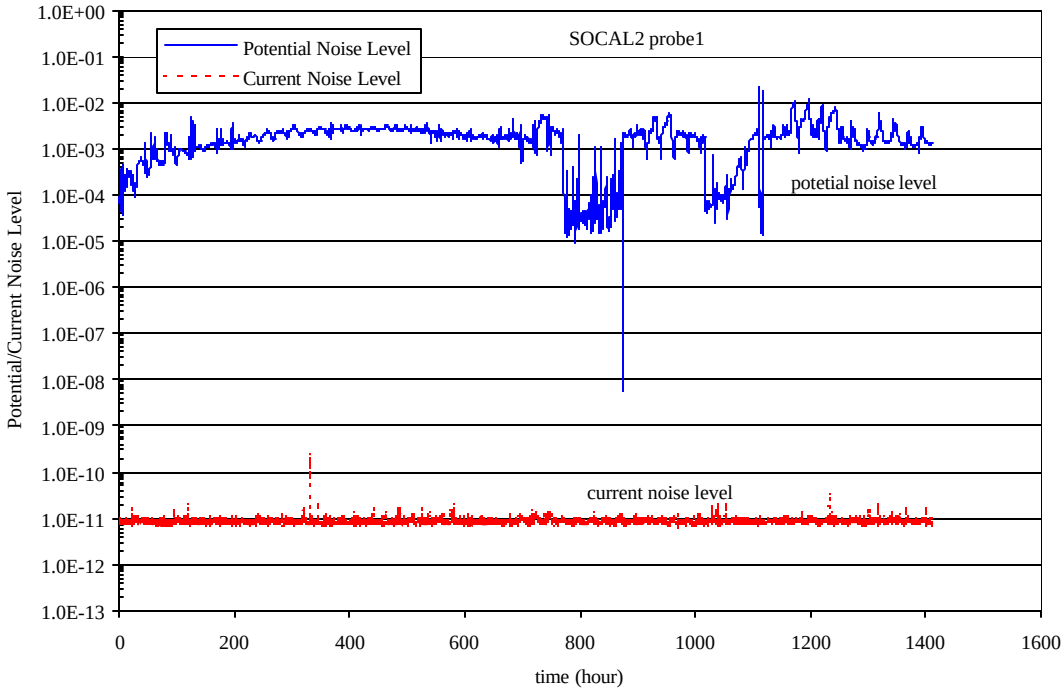

Figure C-3 (a) Potential and current noise level of probe #1 in the Udder of V140

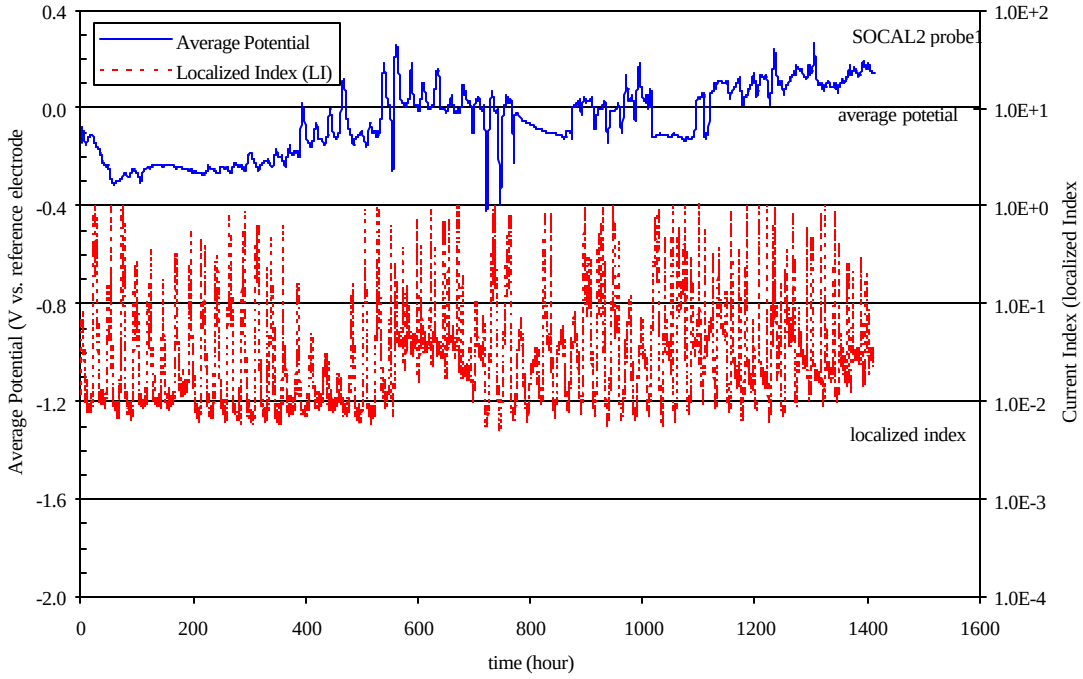

Figure C-3 (b) Average potential and localized index of probe #1 in the Udder of V140

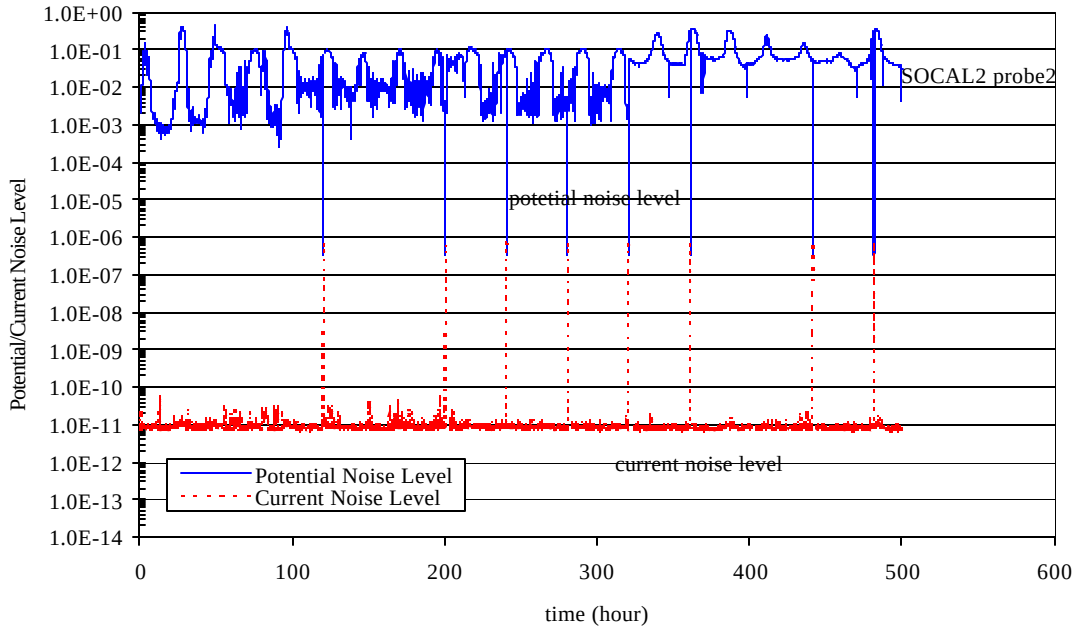

Figure C-4 (a) Potential and current noise level of probe #2 in the Udder of V140

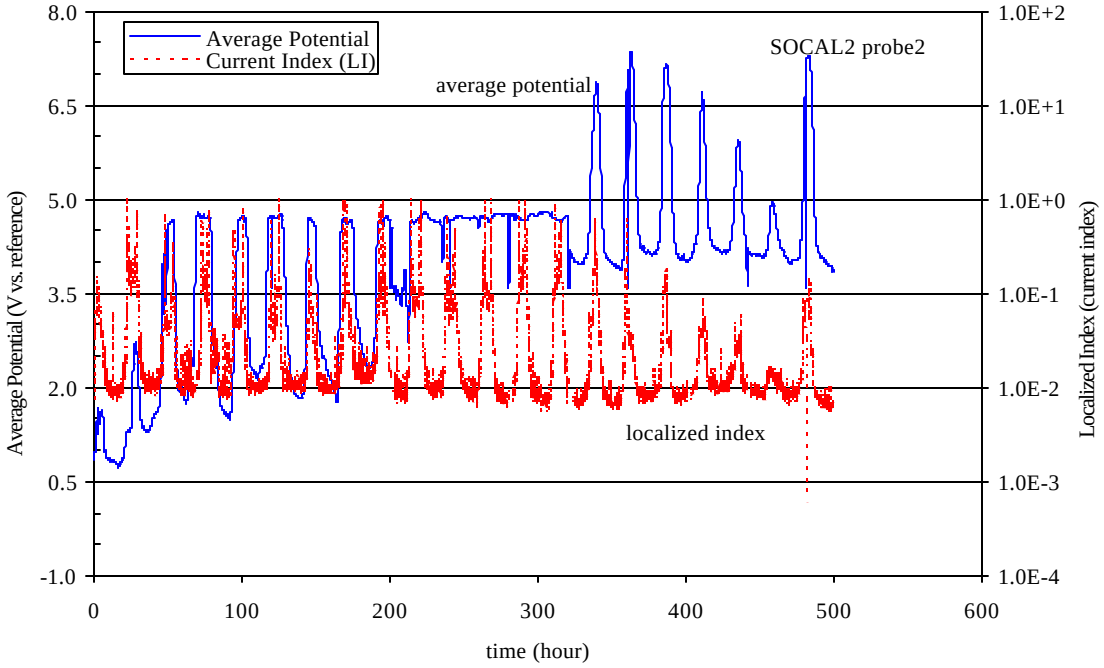

Figure C-4 (b) Average potential and localized index of probe #2 in the Udder of V140

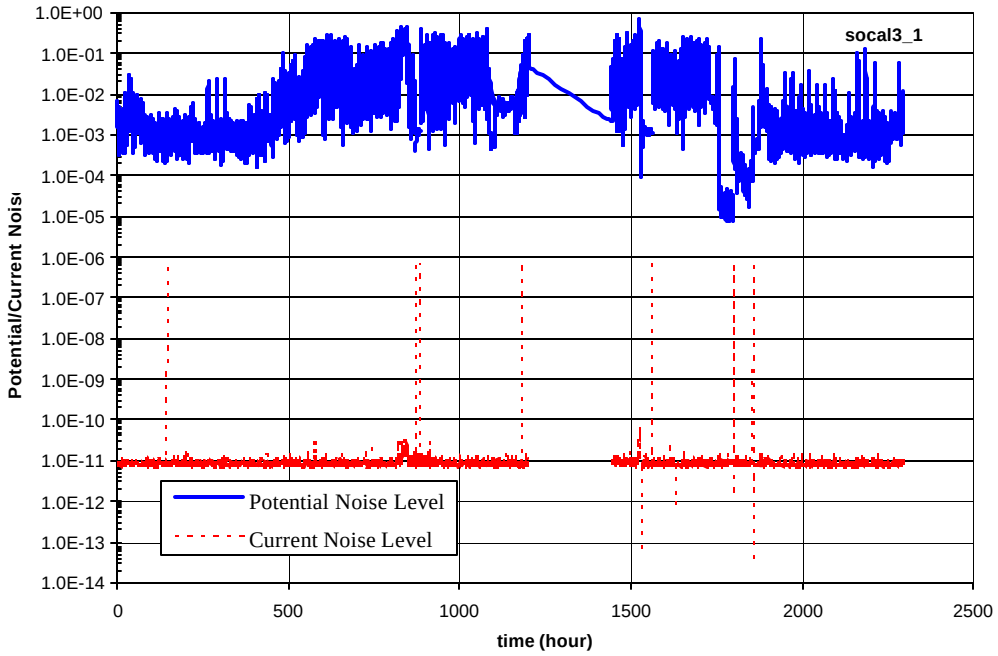

Figure C-5 (a) Potential and current noise level of probe #1 in the third location

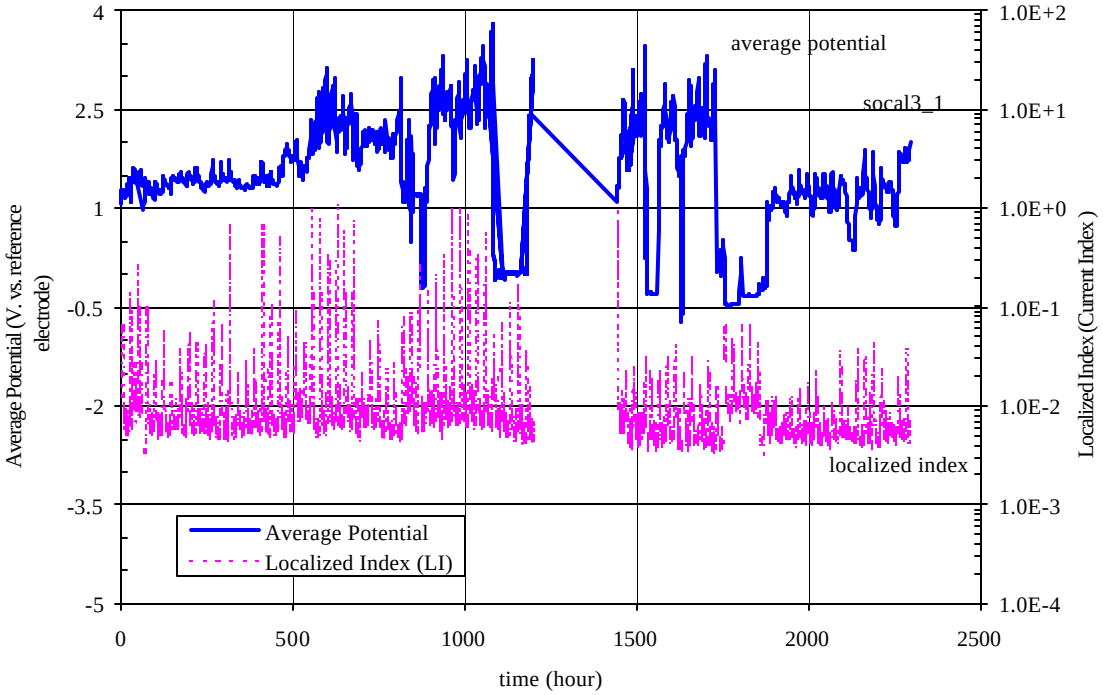

Figure C-5 (b) Average potential and localized index of probe #1 in the third location

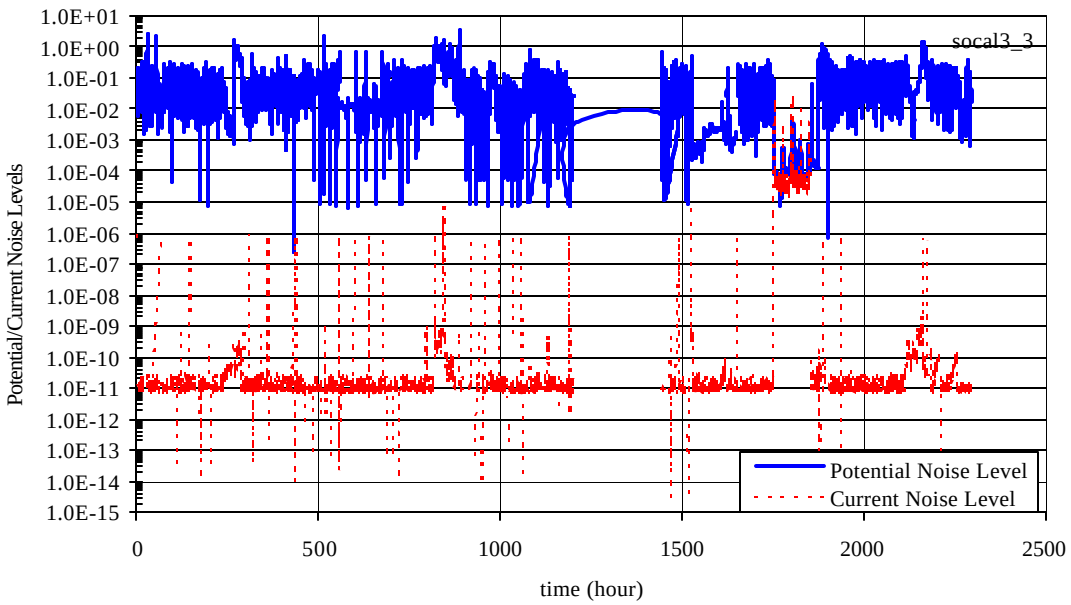

Figure C-6 (a) Potential and current noise level of probe #2 in the third location

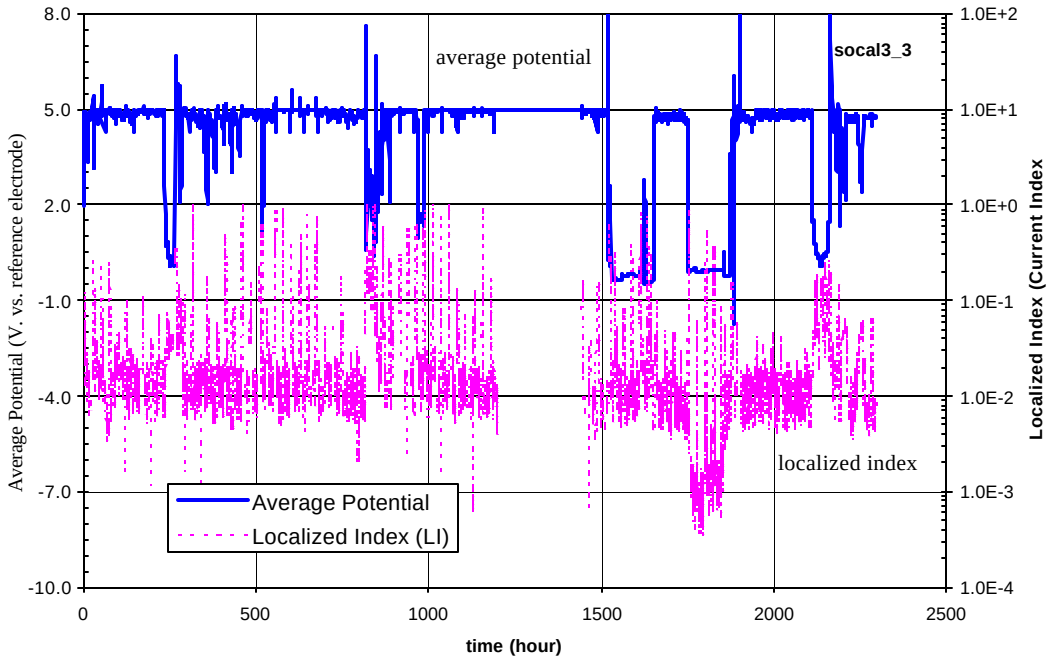

Figure C-6 (b) Average potential and localized index of probe #2 in the third location

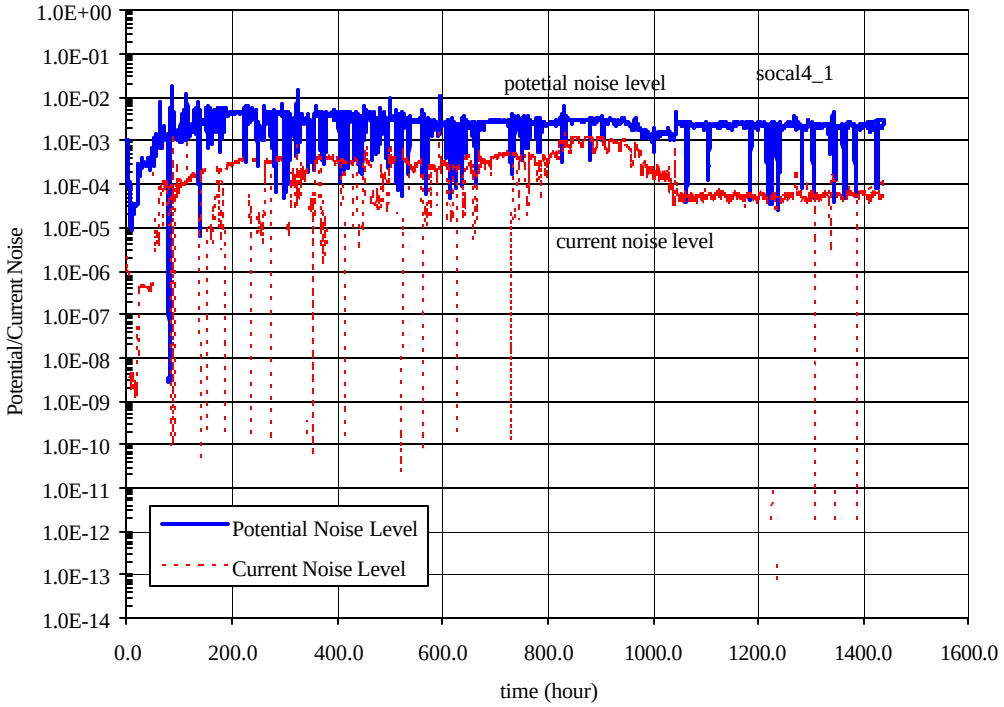

Figure C-7 (a) Potential and current noise level of probe #1 in Honor Rancho

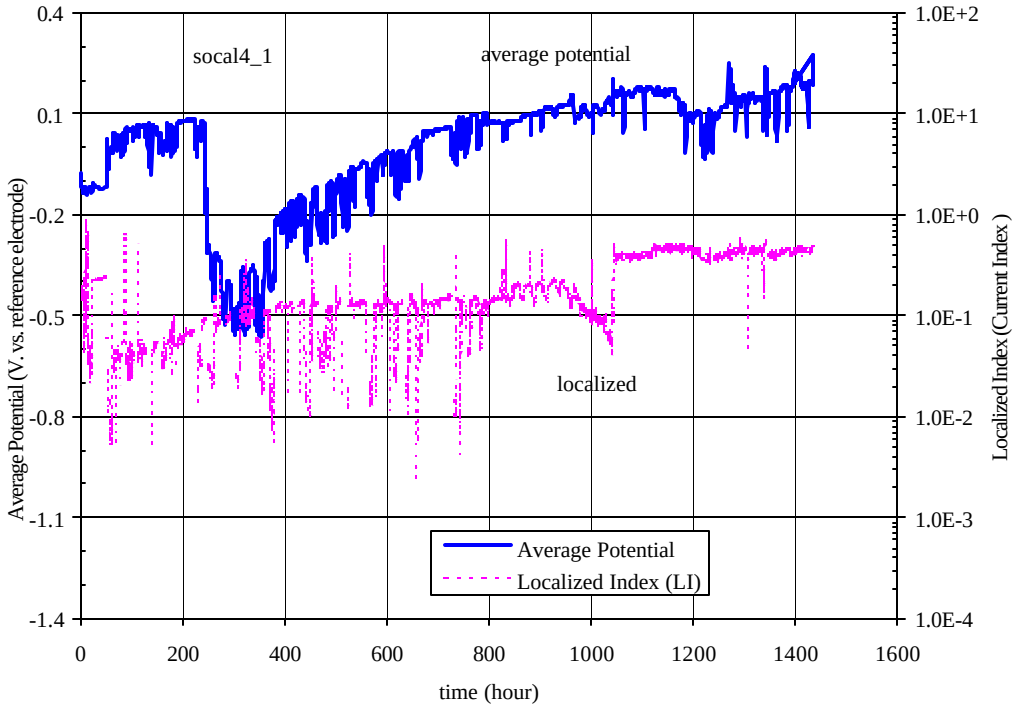

Figure C-7 (b) Average potential and localized index of probe #1 in Honor Rancho

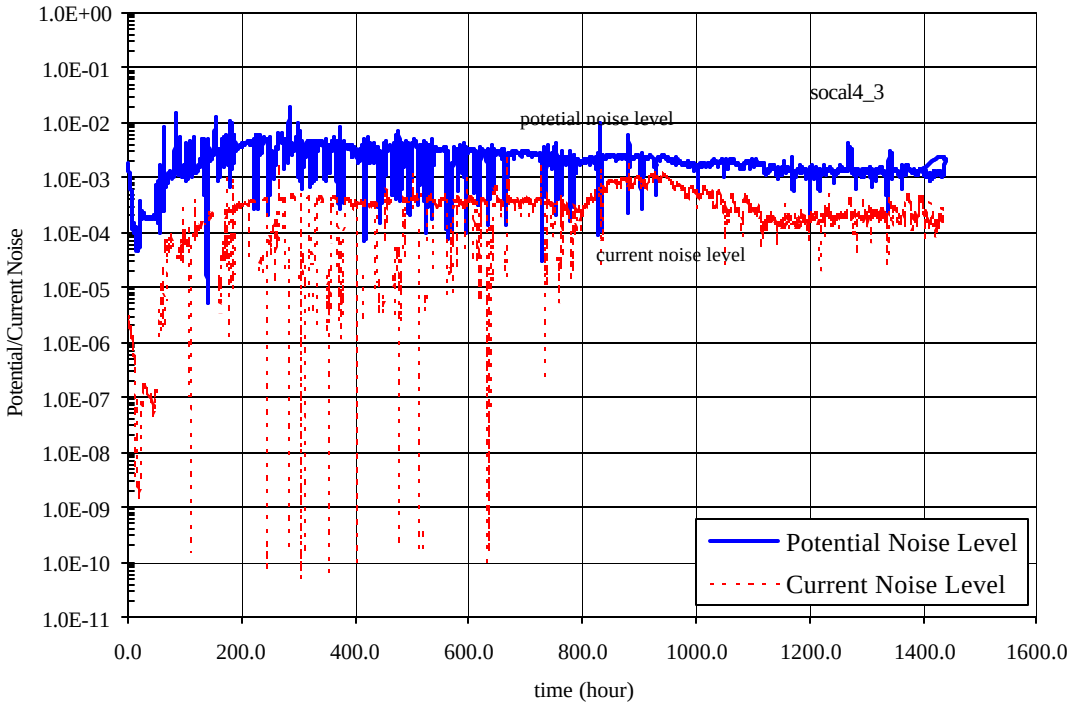

Figure C-8 (a) Potential and current noise level of probe #2 in Honor Rancho

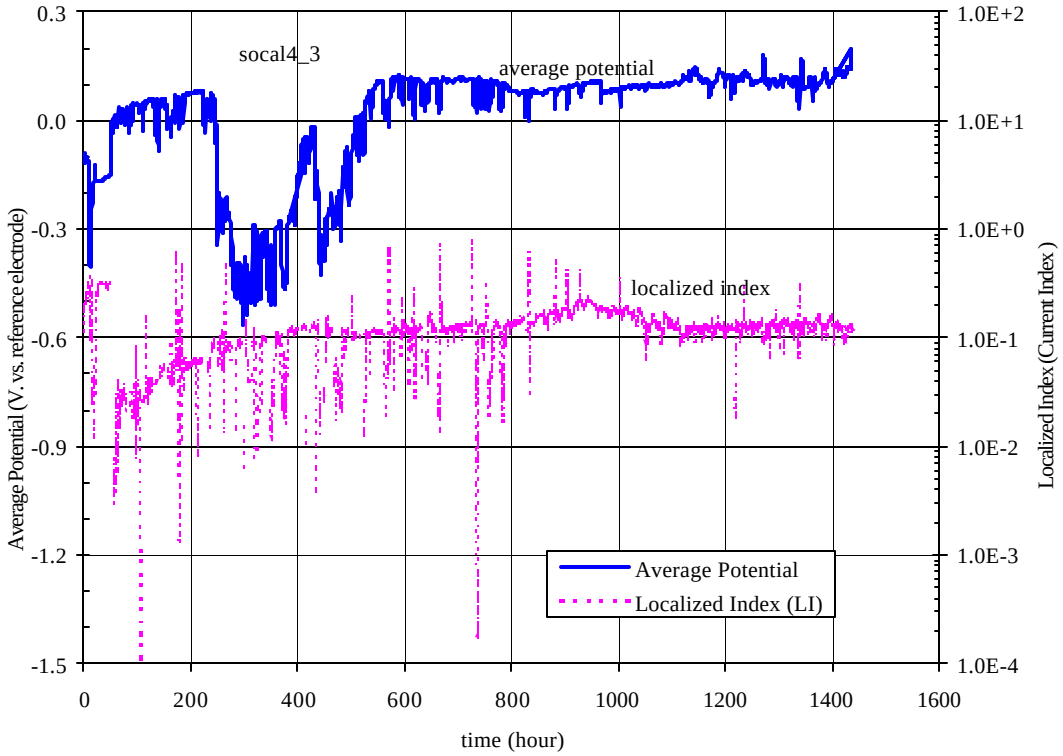

Figure C-8 (b) Average potential and localized index of probe #2 in Honor Rancho

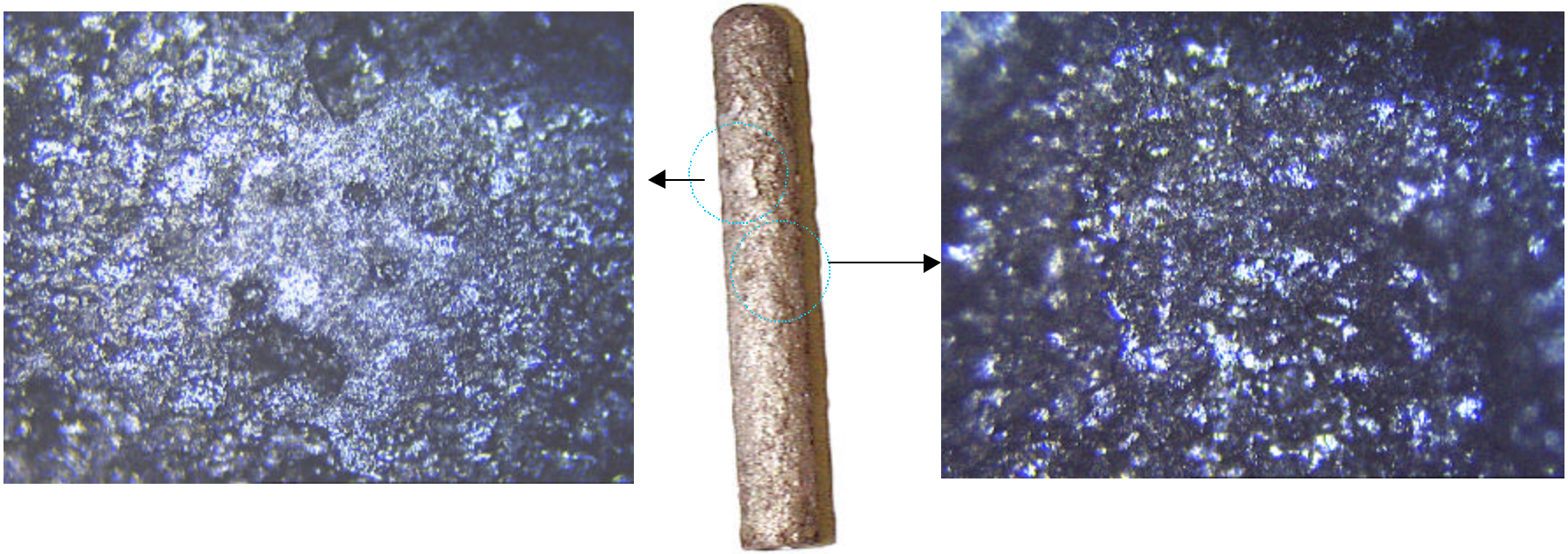

working electrode I of Probe 1 in the “udder” of V140 (SOCAL1_W1)
severe uniform pitting corrosion -
Max Pitting Rate ~ 30 mpy
Uniform Corrosion rate ~ 29 mpy

Figure D-1 (a) Morphologies of working electrode I of probe #1 in the “udder” of V140

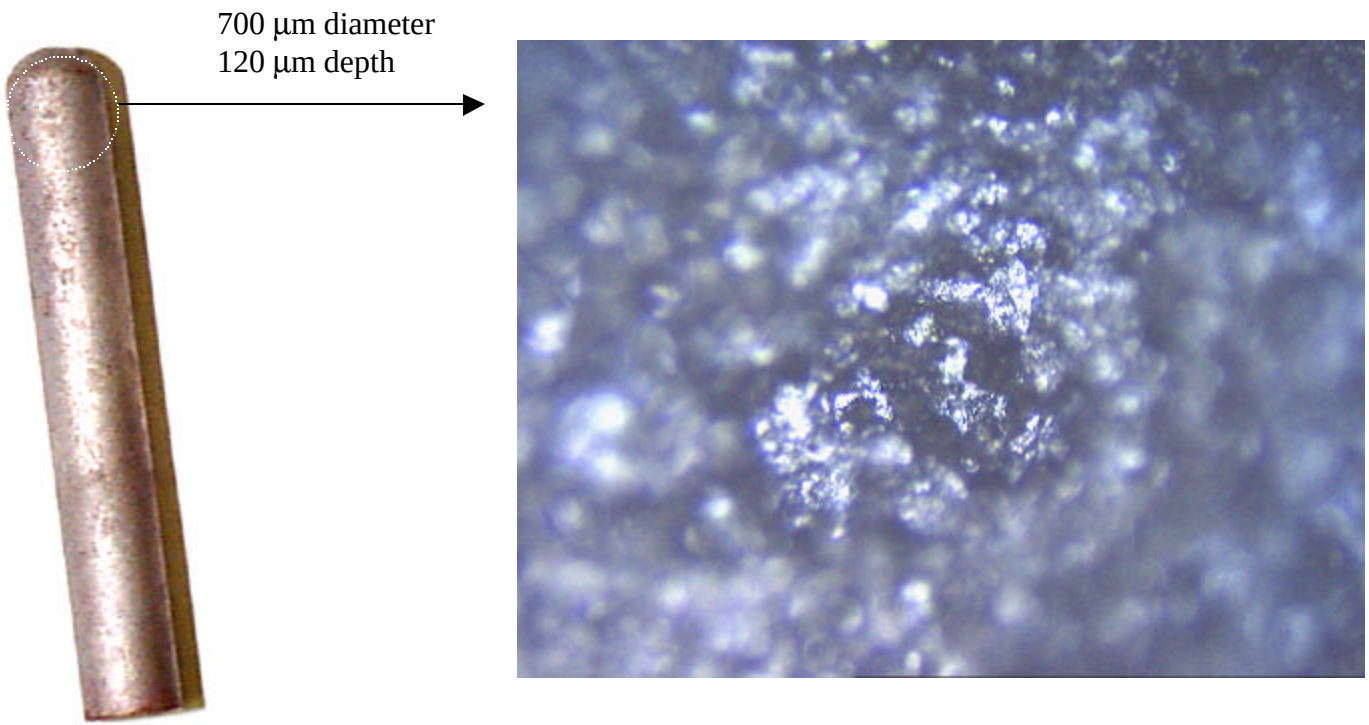

working electrode II of Probe 1 in the "udder" of V140 (SOCAL1_C1)
sustained localized pitting corrosion -

Max Pitting Rate ~ 36 mpy
Uniform Corrosion rate ~ 7 mpy

Figure D-1 (b) Morphologies of working electrode II of probe #1 in the "udder" of V140

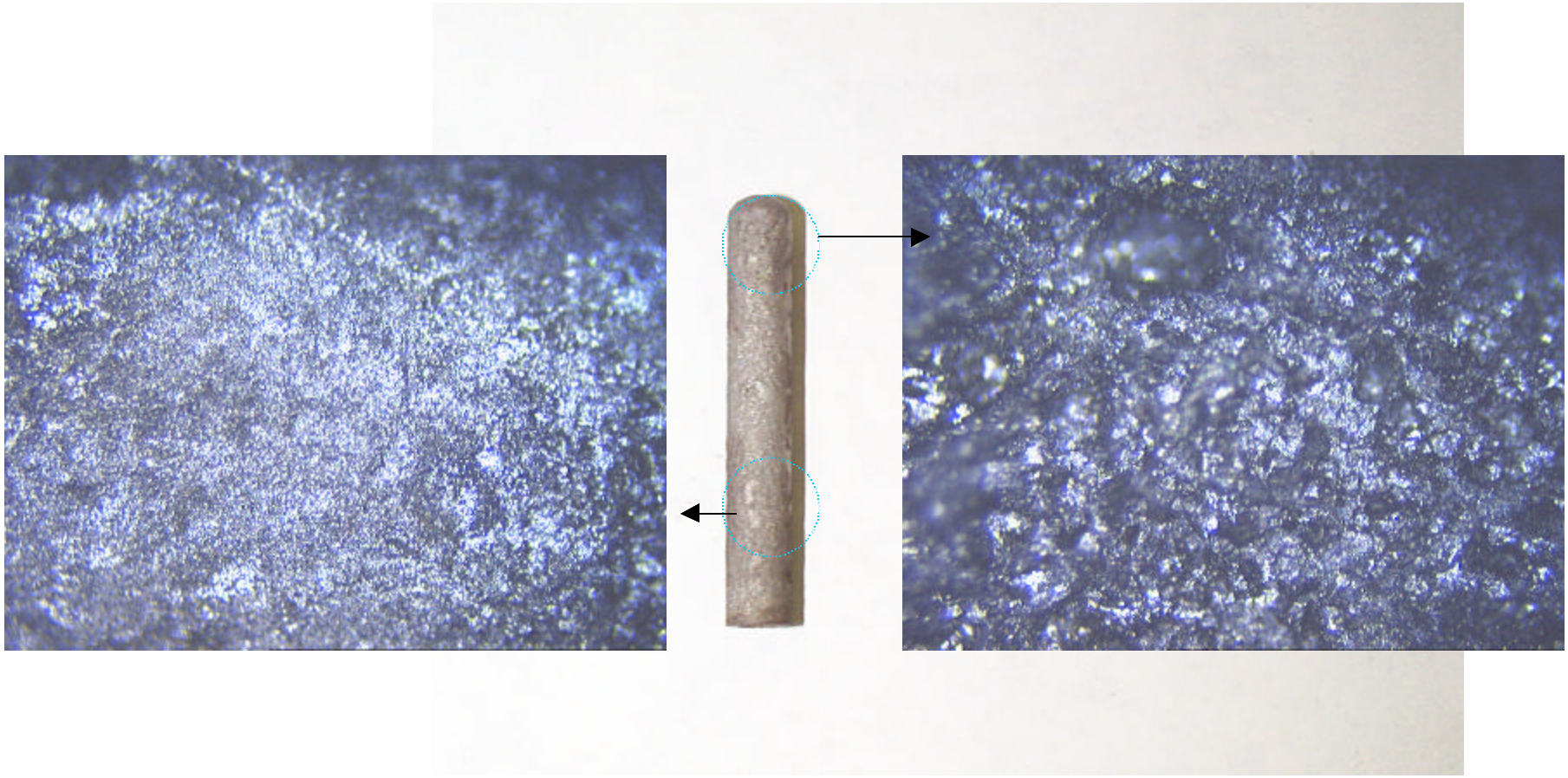

working electrode I of Probe 2 in the “udder” of V140 (SOCAL1_W1)
severe pitting corrosion -
Max Pitting Rate ~ 24 mpy
Uniform Corrosion rate ~ 14 mpy

Figure D-2 (a) Morphologies of working electrode I of probe #2 in the “udder” of V140

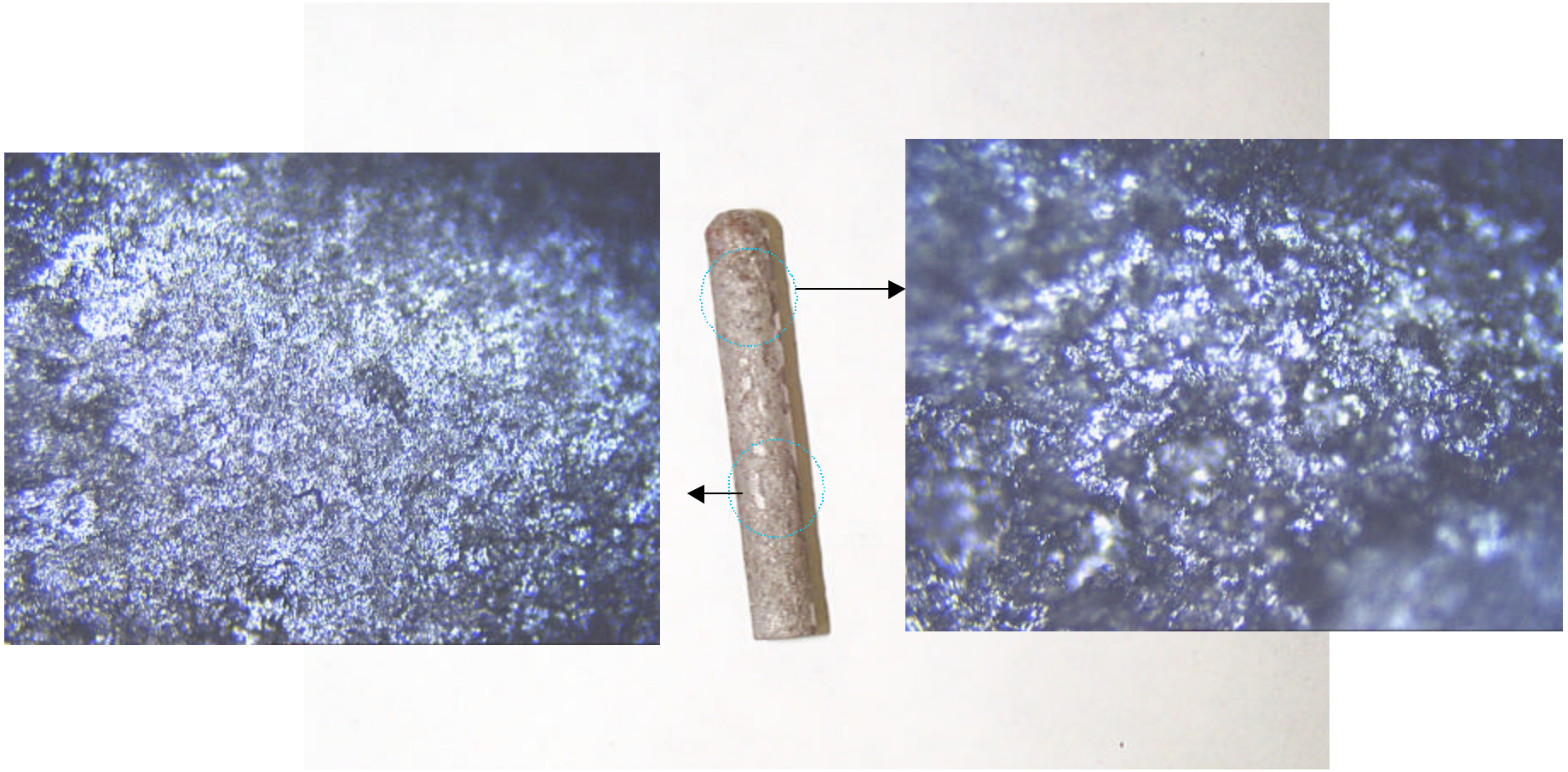

working electrode II of Probe 2 in the “udder” of V140 (SOCAL1_C2)
severe pitting corrosion -

Max Pitting Rate ~ 14 mpy
Uniform Corrosion rate ~ 16 mpy

Figure D-2 (b) Morphologies of working electrode II of probe #2 in the “udder” of V140

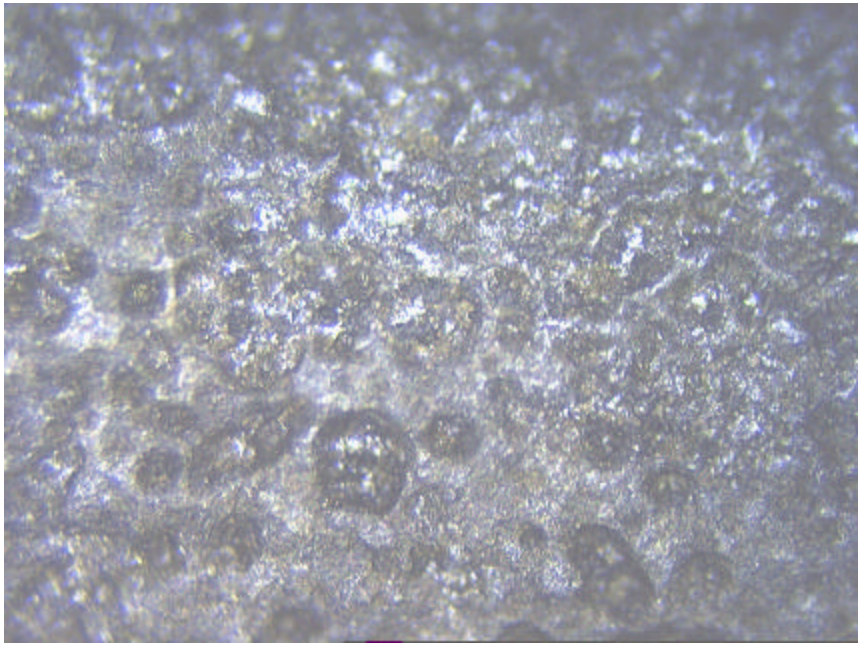

working electrode I of Probe 1 in the “bottom” of V140 (SOCAL2_W1)
localized pitting corrosion -
Max Pitting Rate ~ 3.7 mpy
Uniform Corrosion rate ~ 2.48 mpy

Figure D-3 (a) Morphologies of working electrode I of probe #1 in the “bottom” of V140

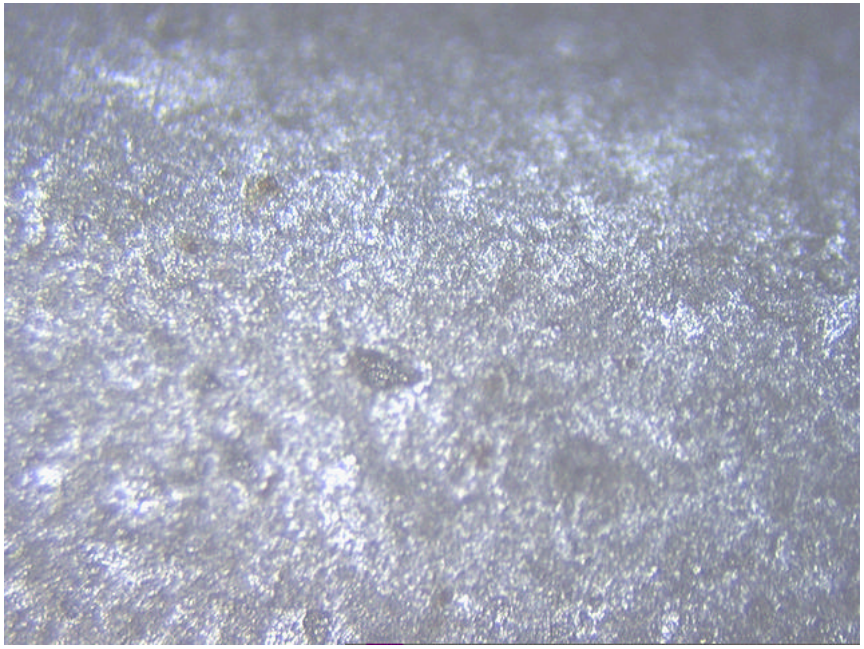

working electrode II of Probe 1 in the “bottom” of V140 (SOCAL2_C1)
uniform corrosion –

Uniform Corrosion rate ~ 0.46 mpy

Figure D-3 (b) Morphologies of working electrode II of probe #1 in the “bottom” of V140

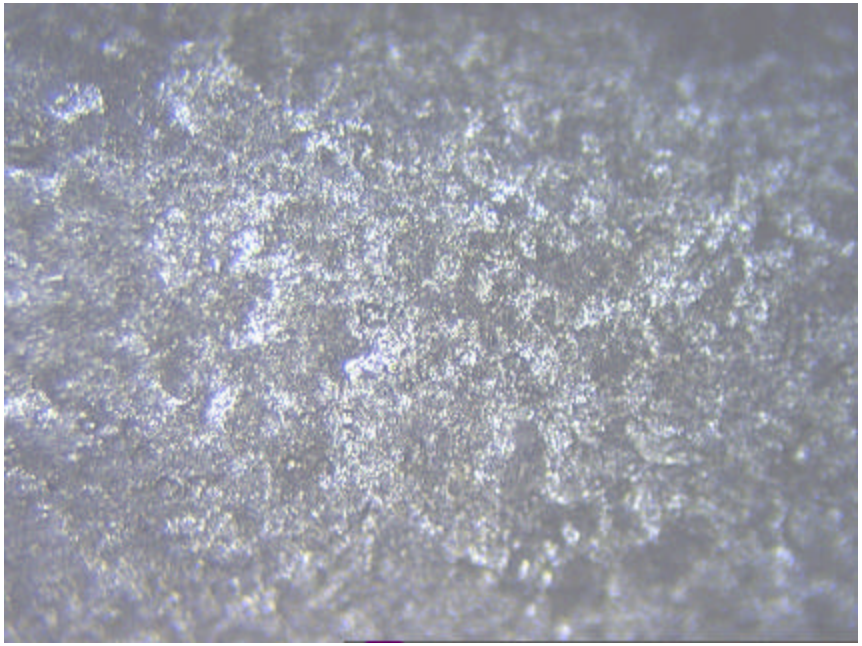

working electrode I of Probe 2 in the “bottom” of V140 (SOCAL2_W2)
uniform corrosion –

Uniform Corrosion rate ~ 0.43 mpy

Figure D-4 (a) Morphologies of working electrode I of probe #2 in the “bottom” of V140

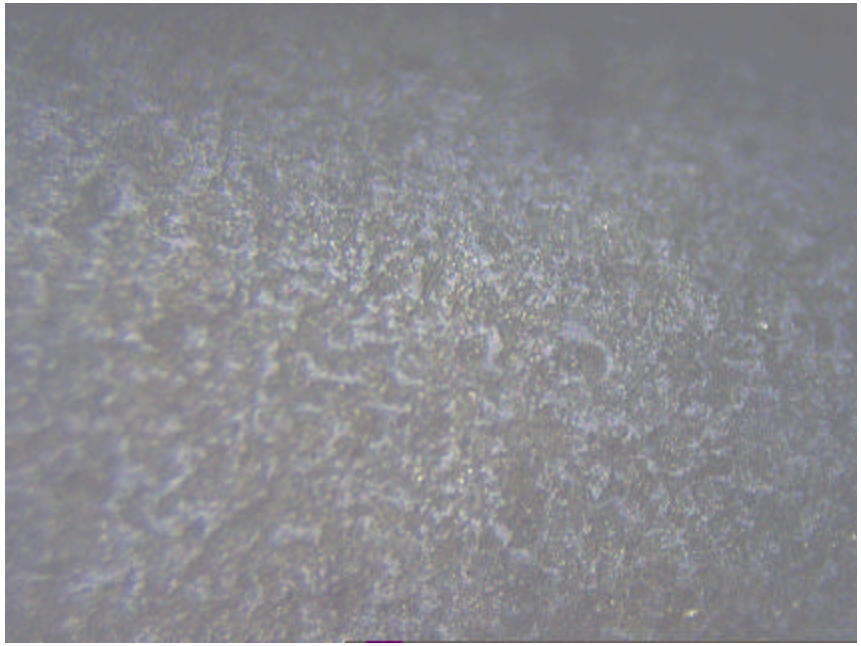

working electrode II of Probe 2 in the “bottom” of V140 (SOCAL2_C2)
uniform corrosion –

Uniform Corrosion rate ~ 0.39 mpy

Figure D-4 (b) Morphologies of working electrode II of probe #2 in the “bottom” of V140

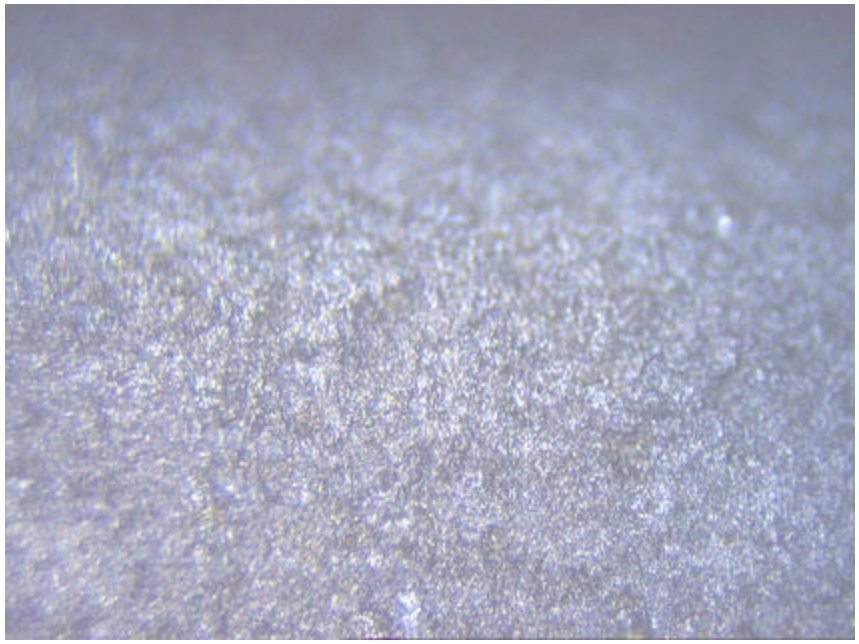

working electrode I of Probe 1 in the third location of SOCAL (SOCAL3_W1)
uniform corrosion –
Uniform Corrosion rate ~ 0.77 mpy

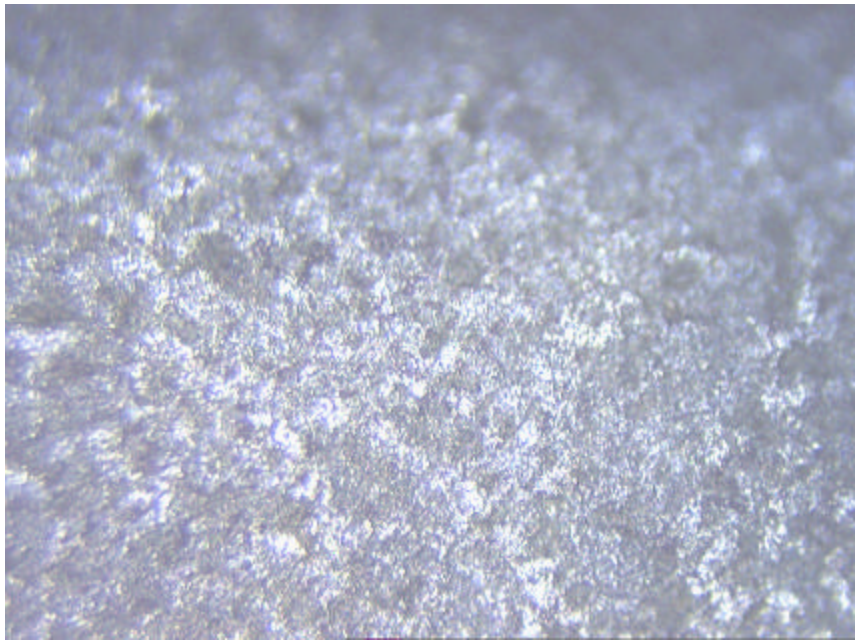

working electrode II of Probe 1 in the third location of SOCAL (SOCAL3_C1)
uniform corrosion –
Uniform Corrosion rate ~ 0.15 mpy

Figure D-5 Morphologies of the working electrodes of probe #1 in the third location of SOCAL

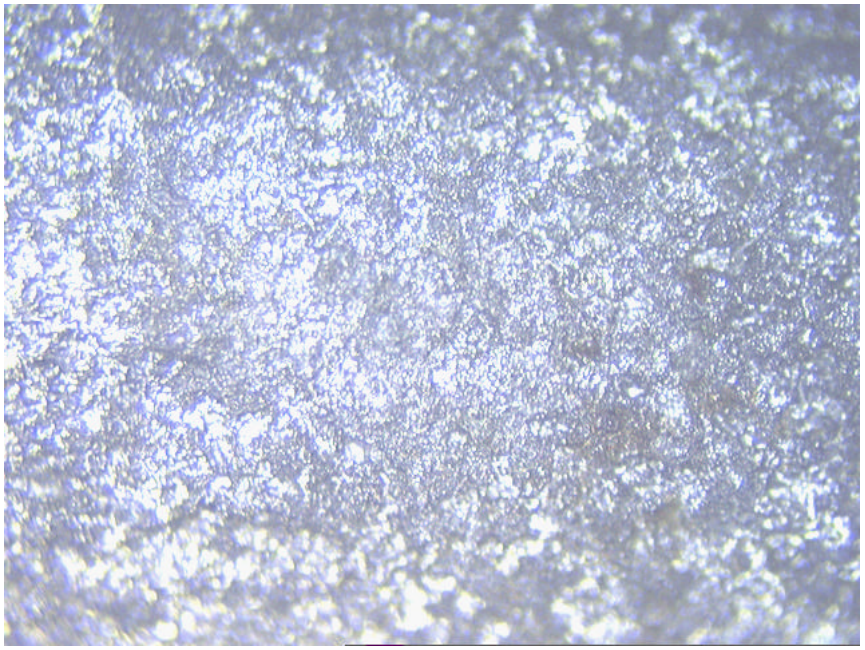

working electrode I of Probe 1 in the third location of SOCAL (SOCAL3_W2)
uniform corrosion –
Uniform Corrosion rate ~ 0.27 mpy

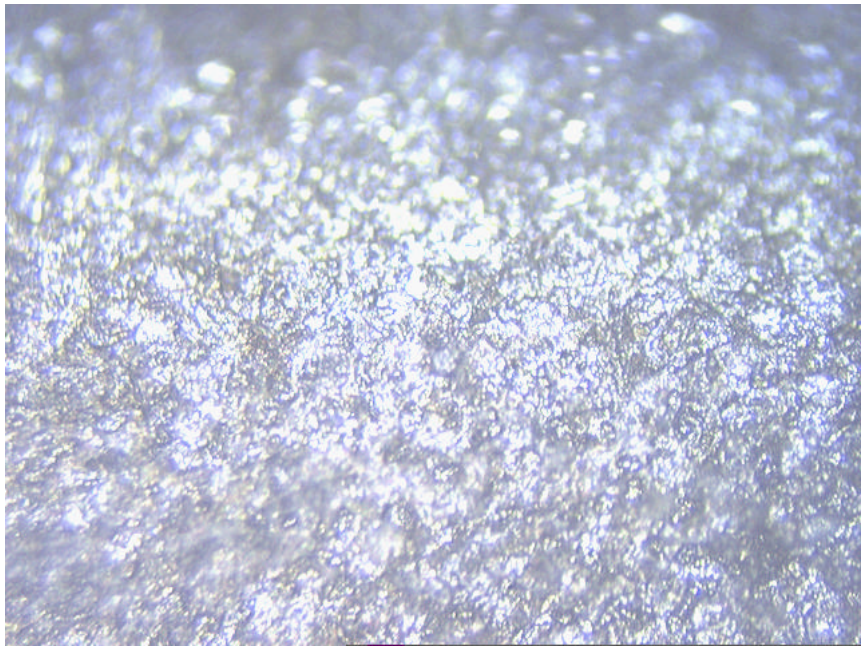

working electrode II of Probe 1 in the third location of SOCAL (SOCAL3_C2)
uniform corrosion –
Uniform Corrosion rate ~ 0.91 mpy

Figure D-6 Morphologies of the working electrodes of probe #2 in the third location of SOCAL